MISSOURI COOPERATIVE HIGHWAY RESEARCH PROGRAM
FINAL REPORT 90-5

DETERMINATION OF AASHTO LAYER COEFFICIENTS

Volume II

UNBOUND GRANULAR BASES AND CEMENT TREATED BASES

MISSOURI HIGHWAY AND TRANSPORTATION DEPARTMENT
FEDERAL HIGHWAY ADMINISTRATION

DETERMINATION OF AASHTO LAYER COEFFICIENTS

VOLUME II:
UNBOUND GRANULAR BASES AND
CEMENT TREATED BASES
STUDY 90-5

Prepared for

MISSOURI HIGHWAY AND TRANSPORTATION DEPARTMENT

by
DAVID N. RICHARDSON
PAUL A. KREMER

DEPARTMENT OF CIVIL ENGINEERING
UNIVERSITY OF MISSOURI - ROLLA
ROLLA, MISSOURI

in cooperation with
U.S. DEPARTMENT OF TRANSPORTATION
FEDERAL HIGHWAY ADMINISTRATION

December 1994

EXECUTIVE SUMMARY

The purpose of this study was to determine the layer (a) coefficients for several commonly specified materials used in MHTD designed pavements for use in the 1986 AASHTO Guide pavement design method. The project entailed a review and compilation of published literature, laboratory testing, analysis of results, and preparation of this report. The study was divided into two parts. Volume I presented the determination of layer coefficients for several Type C and I-C asphalt surface mixes and plant mix bituminous bases. This Volume II presents the layer coefficients determined for granular and soil-cement materials. Layer coefficients were shown to be a function of the resilient or static modulus for each material.

Resilient moduli were determined for four sources of the unbound granular Types 1 and 2 base material (two crushed stones, two gravels). In addition, static compressive chord moduli were determined for two cement-treated soils. Additional tests included sieve analyses, hydrometer analyses, specific gravities, Atterberg limits, aggregate particle shape/surface texture determinations, standard and modified proctor densities, and vibratory table relative densities.

The granular base material resilient modulus testing program variables included compactive effort, degree of saturation, gradation (open and dense), deviator stress/confining pressure (bulk stress), and geologic source of aggregate (reflecting differences in particle shape/surface texture). Within the confines of the testing program, it was found that the only variables significant to resilient

modulus were bulk stress, degree of saturation, and compactive effort. Results indicated that for granular materials, resilient modulus decreases with decreasing bulk stress, decreasing compactive effort, and increasing degree of saturation. A regression model was developed for the prediction of resilient modulus of unbound granular material which reflected the change in modulus in accordance not only with the above variables, but with the base course position in the pavement structure. Layer coefficients were then determined using the AASHTO Design Guide nomograph method, and the Odemark method. The nomograph equations supplied in the AASHTO Design Guide for determination of layer coefficient a_2 (base course), and a_3 (subbase course) from resilient modulus results are recommended for use. Because modulus is partially a function of the thickness of the base course and its position in the pavement structure, a sliding scale for layer coefficients is necessary, and use of the above-mentioned regression equation is recommended.

Static compressive chord moduli were determined for the two soil sources in the soil-cement portion of the study. The major testing variables were cement content and sand content of the fine-grained soil-sand mixtures. Regression models were developed for the prediction of chord modulus. Layer coefficients were then determined from the cement stabilized base AASHTO Guide nomograph with knowledge of the chord moduli.

A verification analysis was performed. Twelve hypothetical pavements were designed using both the former MHTD method and the AASHTO method. The layer coefficients developed in this study for unbound granular and soil-cement

bases were used. This analysis verifed the use of the AASHTO nomographs for calculation of layer coefficients in most cases.

A sensitivity analysis was also performed. The results indicated that for the granular material, a higher compactive effort could result in a requirement of a substantially thinner base or subbase in certain cases.

TABLE OF CONTENTS

LIST OF FIGURES

LIST OF TABLES

LIST OF TABLES

a_1, a_2, a_3 = layer coefficients for the surface, base, and subbase layers, respectively

m_2, m_3 = drainage coefficients of the base and subbase, respectively

D_1, D_2, D_3 = thickness of surface, base, and subbase layers, respectively.

Drainage coefficients are essentially modifiers of the layer coefficients, and take into account the relative effects of pavement structure internal drainage on performance of the pavement. Determination of the drainage coefficients is addressed under a separate contract in a separate report submitted by UMR to the MHTD concurrent with this study(2).

A preliminary review of the literature indicates that reported values for layer coefficients vary widely (Table 1). The range of layer coefficients determined at the AASHO Road Test are shown in Table 2(3,6).

Table 1. Reported Layer Coefficients.

Layer Coefficient	Material/Layer	Value	Ref.
a_1	asphalt surface	0.30 - 0.57	4-9
a_2	asphalt-treated base	0.10 - 0.62	5-7,9
	cement-treated base	0.12 - 0.50	5-7,9
	lime-treated base	0.12 - 0.26	4,6,7
	unbound granular base	0.03 - 0.23	5,6,8-11
a_3	unbound granular base	0.02 - 0.15	6,10

Table 2. Range of Layer Coefficients at the AASHO Road Test.

Coefficient	Minimum	Maximum	Reported
a_1	0.33[1]	0.78[1]	0.44[1]
a_2	0.12[2]	0.23[2]	0.14[2],0.07[3]
a_3	0.07[4]	0.12[4]	0.11[4]

[1] asphaltic concrete surface layer
[2] unbound crushed stone base
[3] unbound sandy gravel base
[4] unbound sandy gravel subbase

Examination of Eq. 1 indicates that the thickness of any particular layer is, to a significant extent, dependent upon the layer coefficients. Hence, an accurate determination of layer coefficients can have a significant economic impact in regard to the design of the pavement structure.

It has been postulated that the magnitude of any layer coefficient is a function of several factors. For example, the asphalt surface layer coefficient a, is dependent upon mix characteristics, pavement temperature, vehicle speed, layer thickness, traffic level, and compacted mix stiffness. For an unbound granular base, the layer coefficients a_2 and a_3 have been shown to be dependent on the state of stress in the layer, degree of saturation, compactive effort, aggregate properties, base layer thickness, and subgrade stiffness.

As originally used in the AASHO Road Test analysis, layer coefficients were actually regression coefficients which were the result of relating layer thicknesses to road performance under the conditions of the Road Test. The problem is to translate the Road Test findings to other geographic areas where the construction

materials and climate are different. Layer coefficients must be determined in order to use Eq. 1 for design purposes. In a pure sense, layer coefficients are abstract mathematical entities. In a practical sense the layer coefficients must be related to something tangible. Most commonly, layer coefficients are determined on the basis of relative layer material strength or stiffness considerations Over the years since the AASHO Road Test, many methods have been used to determine values for layer coefficients.

OBJECTIVES AND SCOPE

This study is based on methods which optimize the combination of economy, accuracy, and length of study. In brief, the study entails determination of stiffness values for several commonly used MHTD types of pavement materials. The stiffness values were determined by both direct laboratory modulus testing and by approximation techniques. These stiffness values were related to layer coefficients and then verified for reasonableness by comparing several pavement structures designed with the AASHTO method to structures designed with the former MHTD method. The report includes a method suitable for use in routine design which will enable the pavement designer to solve Eq. 1 and hence obtain the desired layer thicknesses

The approach taken for layer coefficient determination was the traditional one (5,12), which is to take some measure of strength, stability, or stiffness of a particular mix or blend and compare it to the same type of measure for the counterpart AASHO Road Test material. The comparisons are usually done by use of one of the AASHTO Design Guide charts or some form of a ratio of the two values. The traditional approach does not specifically address rutting.

In this study, the materials for which layer coefficients were determined were limited to two types of asphalt surface mixes (Types C and IC), one type of bituminous base mix, two types of cement-treated base mixes, and one type of unbound granular base/subbase. The report is separated into two volumes: Volume I(12) covers asphaltic materials; Volume II deals with unbound granular and cement-treated materials.

UNBOUND GRANULAR BASE LAYER

INTRODUCTION

The main thrust of this portion of the study was to determine base and subbase layer coefficients (a_2 and a_3) for Types *1* and 2 unbound aggregates which are used as base material under an asphaltic surface layer or as subbase under asphaltic surface and base layers. Fig. 1 shows the pavement section being modeled. The analysis was based on repeated-load triaxial resilient modulus tests as recommended in the 1986 AASHTO pavement design guide (1). A secondary goal was to develop a regression equation to enable the prediction of resilient modulus without having to actually perform the test.

Pavement engineers are interested in longevity of the pavement. Longevity is a function of pavement durability and response to load. Usually, the pavement is designed structurally to give a favorable response to load. Durability is assured through specification of good materials. The elastic response to load of any material is a function of its stiffness, as defined by some sort of load-deformation modulus.

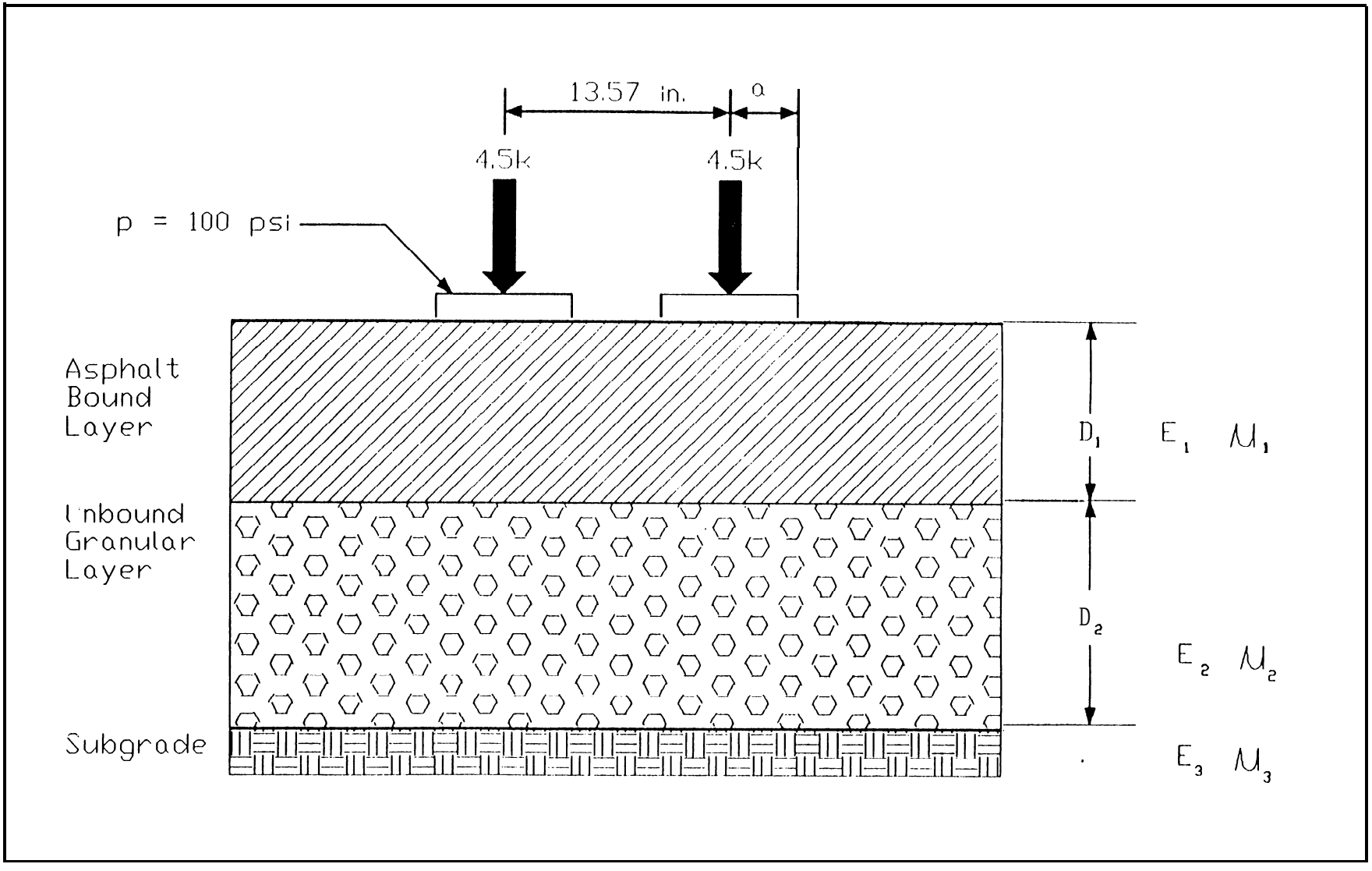

Fig. 1. Pavement Section with Unbound Granular Base,

Thus, direct measurement or estimation of modulus becomes desirable. This has given impetus to the effort by the pavement industry to produce a type of modulus test that is suitable for practical use.

DETERMINATION OF LAYER COEFFICIENTS-METHODOLOGY

Two methods were used to determine the layer coefficients (a_2 or a_3) of Type 1 and Type 2 unbound granular base materials:

1) Direct use of the base and subbase layer nomographs in the 1986 AASHTO guide (1). The necessary input is the resilient modulus of the granular material (E_g). However, resilient modulus of an unbound granular material is dependent on many factors, including stress state. Thus, use of an elastic layered stress analysis was necessary to predict stress states.

2) Use of Odemark's transformation. Stiffness (in the form of resilient modulus) of MHTD aggregate types was related to the modulus of Road Test material at various stress states in a manner similar to that done with the asphalt mixtures (12). Layer coefficients were calculated from Eq. 2, hereafter called the Odemark equation:

$$a_n(MHTD) = a_n(AASHO)\left[\frac{E_g(MHTD)}{E_g(AASHO)}\right]^{1/3} \quad \ldots\ldots\ldots \quad (2)$$

RESILIENT MODULUS

gradation, and particle shape. Of these variables, stress state is the dominant factor in regard to material stiffness. The higher the confining pressure, the higher the modulus. The significance of the other parameters seems less well defined. Higher relative density, or compactive effort, increases modulus, but to varying degrees (10,13-15,22). The significance may be influenced by gradation. A higher degree of saturation has been shown to significantly decrease modulus (10,13-18,21,22). For some aggregates, this effect is of minor significance (10,18). It appears that, as fines content increases, resilient modulus decreases (11,13,14,19). Perhaps with higher fines content, the influence of a high degree of saturation is more pronounced, possibly due to the generation of pore pressures (13). Thus, there may be an interaction between the amount of fines and their moisture content. This may be the reason that several studies have shown that open-graded mixtures have higher modulus values than their dense-graded counterparts. However, several studies have shown the reverse(13,20), or at least that gradation is of negligible significance (17), and others have shown that there is an optimum fines content for maximum modulus(11,22).

In regard to particle shape/texture, a more angular/rough aggregate generally exhibits a higher modulus (14,20), although, in some cases, the reverse seems to be true(20,23). The effect has been shown to be variable in significance(13), of minor significance (14,20) and of major significance(14). Thus the influence and significance of particle shape is not well defined.

Several of the factors that are significant to the magnitude of resilient

modulus were studied in this project. These include: the effect of stress state, compactive effort, degree of saturation and particle shape/texture. The effect of gradation was not in the scope of this study. However, in the companion project (2), a different gradation was used for the same materials which were used in the present study. The results of modulus testing from both projects were examined jointly. Thus a study of the effect of gradation was accomplished and is reported herein.

MATERIAL TYPES AND SOURCES

All unbound aggregates in the study were MHTD-approved materials. The materials were selected and sampled by MHTD personnel. Two Type 1 crushed stone base aggregates were studied. They were selected by MHTD personnel to give a wide range of particle shape and texture. Additionally, in the companion project (2), two Type 2 gravel materials were tested for resilient modulus. Test results for these two gravel materials are also included in this report. The materials, sources, and identification are shown in Table 3.

Table 3. Material Types and Sources.

Nomenclature	Material	Sources	Location
DR-12	Type 1 crushed Burlington limestone	Mertens Quarry	Millersburg
DR-13	Type 1 crushed Jefferson City dolomite	Smith Quarry	Rolla
DR-14	Type 2 Crowley Ridge gravel base	Delta Aggregates	Dexter
DR-15	Type 2 Black River gravel base	Williamsville Stone Co.	Poplar Bluff
Note: All sources are located in Missouri			

LABORATORY INVESTIGATION

General

The principal property determined for unbound granular base materials was the resilient modulus. However, the performance of other tests and procedures was necessary in order to ultimately conduct the resilient modulus testing and analyze the results. These other procedures included sieve analyses, gradation formulation, specific gravity determination, moisture-density relationship testing, particle shape/texture testing, and determination of plasticity of fines. These operations are outlined below.

Gradations

The experimental gradation utilized in this study was characterized as a curve situated midway between the upper and lower limits of the allowable gradation specification band for MHTD Type 1 unbound base material. This gradation was used for both the two crushed stones and the two gravels. At the finer size end, the gradation was extended to include 8% passing the #200 sieve. This value was chosen because 1) it matched one of the gradations used in the drainage study which is the companion project to the present study, and 2) this was approximately the same percentage as both as-delivered gradations of the Type 1 aggregates supplied by MHTD for this project. The gradation plot is termed the "MHTD-Middle" and is shown in Fig. 2.

In the companion study for the determination of drainage coefficients (2), an open gradation (the so-called New Jersey gradation) was also tested for resilient

modulus. The results of that testing is also herein reported. The New Jersey gradation is also shown in Fig. 2.

Gradation Curve Shape/Position

An analysis was performed to determine the effect of gradation upon resilient modulus. The most promising methods were later tried in the development of the E_g predictive equation. To accomplish this, there was a need to characterize the gradations so that a single parameter would represent the shape and position of each gradation curve. Nine different methods to determine the gradation parameter were tried. These are described in detail in Volume I of this report, and are discussed in the "Results" section of this report.

Particle Shape/Texture

Numerous test methods have been devised to quantify particle shape and/or texture. These can be divided into two catagories: 1) direct methods (those that result in measurement of aspects of individual particle shape or texture) and 2) indirect methods (those that measure some sort of bulk aggregate property, such as void content, which is related to particle shape/texture). Recent evaluations of these methods were reported by Kandhal et al. (24) at NCAT (National Center for Asphalt Technology). From the literature, it appears that efforts are being concentrated in the area of fine aggregate evaluation and that there are several methods available which can be used in lieu of the standard test, ASTM D 3398 (25) which is somewhat cumbersome to perform. Kandhal et al. recommended the National Aggregate Association's (NAA) proposed method (A or B) for fine

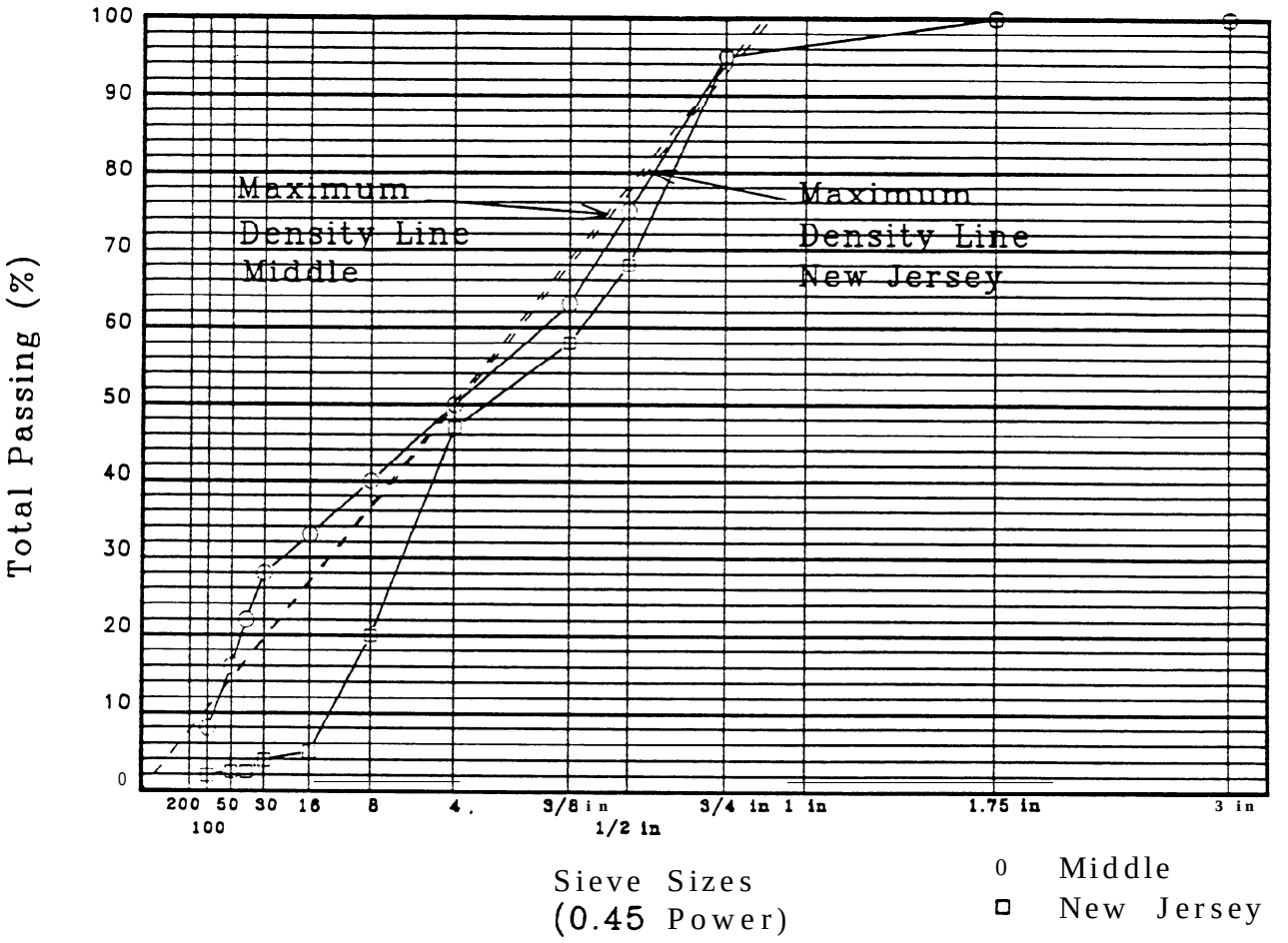

Fig. 2. MHTD – Middle and New Jersey Experimental Gradations.

aggregate (26). Both the standard ASTM method and the proposed NAA method are indirect methods of particle shape determination.

In this study the (-) #8 to (+) #100 sieve size fraction of each aggregate mixture blend was tested using the NAA Method A. The methodology is given in Appendix A of Volume I of this study. For the (+) #4 size, the blends were tested in accordance with ASTM D 3398. This method is recorded in Appendix B of Volume I of this study. The results of both methods were used in developing the resilient modulus regression equations discussed later in the "Results" section of this report. Photographs of the NAA test device and the D 3398 equipment are shown in Figs. 9 and 10 of Volume I of this report (12).

Specific Gravity

Aggregate fractions of each of the two gradations were separated at the #4 and #100 sieve sizes and tested in accordance with AASHTO T85-88 (27) and T84-88 (28) for the (+)#4 material and the (-)#4 to (+)#100 material, respectively. These data were necessary for use in the degree of saturation calculations. Weighted averages of apparent specific gravities were used to calculate the specific gravity for each gradation of each of the four aggregates as follows:

$$G = \frac{100}{\frac{\%\ Passing\ \#4}{ASG} + \frac{\%\ Retained\ \#4}{ASG}} \quad \ldots\ldots\ldots\ldots \quad (3)$$

where:

G = apparent specific gravity weighted average

ASG = apparent specific gravity of each fraction.

Screening

All aggregates were shaken in an air dry state through the appropriate screens in a Gilson shaker. A dust baffle/cover was designed to restrict the movement of particles in order to minimize problems with incorrect sizes of material being retained on any given sieve.

Upon shaking, the split material was stored in 20 gal plastic cans with lids until the aggregate was needed for specimen fabrication.

Moisture - Density Relationship

In order to choose target densities for compaction of resilient modulus specimens, standard and modified proctor tests were performed in accordance with AASHTO T-99 (29) and T-180 (30). Additionally, the maximum density of the open-graded gradation was determined via the vibratory table method (ASTM D4253) (31). For each of the four aggregates, a double amplitude vs dry density curve was obtained in accordance with the dry method to obtain the optimum power setting. This power setting was then used for the determination of density utilizing the wet method. The vibratory table is shown in Fig. 3.

Relative Density

For data analysis purposes, it was necessary to determine the relative density (32) of all E_g test specimens. The equation to calculate relative density is:

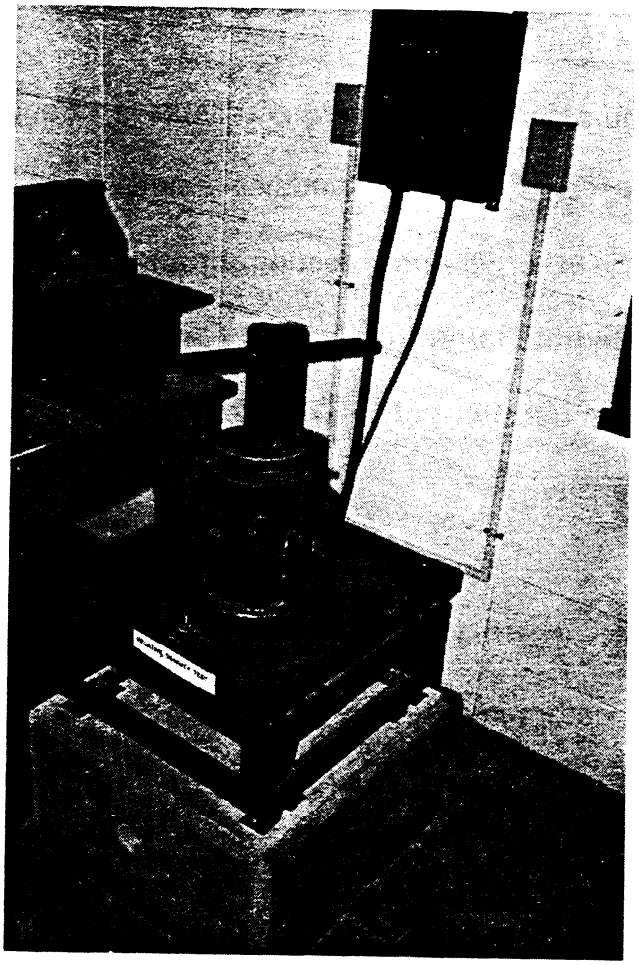

Fig. 3. Vibratory Compaction Table.

$$D_R = \frac{[\gamma_{max}(\gamma - \gamma_{min})]}{[\gamma(\gamma_{max} - \gamma_{min})]} \quad \ldots \quad \ldots\ldots (4)$$

where:

D_R = relative density, pcf

γ_{max} = maximum density for a given gradation and aggregate source - the highest value was used whether it came from a peak target value from T-180 or vibratory testing, or an actual E_g test specimen that exceeded the target, pcf

γ_{min} = minimum density, pcf (ASTM 4253)

γ = test density, pcf.

Plasticity of Fines

To determine whether the plasticity of the fines had an effect on E_g, Atterberg limits were determined for the (-)#40 sieve material of each aggregate source.

Specimen Fabrication

Specimens for unbound granular base were fabricated in accordance with AASHTO T-XXXC91 (33). Each specimen was made by taking the indicated amount of material for each sieve size per the experimental gradation previously discussed. The largest particle size in the gradation was approximately 5/8 in. Thus, the specimen diameter was greater than six times the maximum particle size, in accordance with AASHTO T-XXXC91 . The 4 in diameter 8 in tall specimens were compacted in 1 in lifts with a Dayton air hammer in a split aluminum mold lined with a nitrile rubber membrane. Various membrane materials and thicknesses

were tried, including 0.012 and 0.025 in latex and nitrile rubber. It was found that during compaction the thinner membranes would tear, especially the latex, even if two membranes were used. A 0.06 in thick nitrile rubber membrane was the minimum that was sufficiently rugged. This still met the AASHTO specification which limits membrane thickness to 0.08 in. The specimen was compacted directly on the triaxial cell pedestal. A vacuum of approximately 20 in was applied to the specimen prior to removing the split mold.

Resilient Modulus

General. The relationship between applied stress and the resulting strain of unbound granular base materials is most commonly defined by the resilient modulus test. This test is performed by subjecting a compacted specimen to an all-around confining pressure and then applying a vertical cyclic load. Total applied load (a,), displacement resulting from the load, and confining pressure (σ_3) are monitored. The applied load and confining pressure are varied to achieve a range of stress states which should represent the expected stress states in actual pavement structures. The specimen is encased in a flexible membrane and tested in a triaxial cell. Fifteen combinations of confining (cell) pressure and cyclic applied (deviator) stress were used for each specimen.

The procedure that was followed in this study is essentially in conformance with the 1991 Interim AASHTO method of test (33). The test procedure is also essentially in conformance with SHRP Protocol P46 (34). One notable exception is that the AASHTO stress state sequence (not the SHRP) was followed. And, in

accordance with Claros et al. (35), σ_1/σ_3 ratios were not allowed to exceed three in order to prevent possible excessive specimen straining.

Equipment. The testing equipment setup is shown in Fig. 4. The equipment consisted of an MTS servo-hydraulic load system, a triaxial chamber capable of housing a 4 in diameter specimen while subjected to cyclic loads, and a data acquisition system. Load was measured with an internal 1000 lb capacity load cell and deformation was measured with two LVDT'S mounted externally to the cell. This type of measuring system is allowed in the AASHTO method and is recommended in the SHRP method. Minimum resolution of the vertical LVDT's and the load cell were in accordance with the AASHTO specifications. Actual minimum deformations and loads during the testing were kept at least ten times the minimum resolutions to assure confidence in the test results. Air was used as the confining fluid instead of water in order to protect the internal load cell. Triaxial cell pressure and back pressure were controlled via a Geotest control panel. The Research Engineering triaxial cell that was used has several advantages. First the chamber cylinder wall can be placed after the loading piston is brought into contact with the specimen. Also, end caps can be purged of air very easily by the unique design of the caps.

Test Variables. Four test parameters were controlled as independent variables.

a) Stress State. As previously mentioned, several variables affect the modulus of

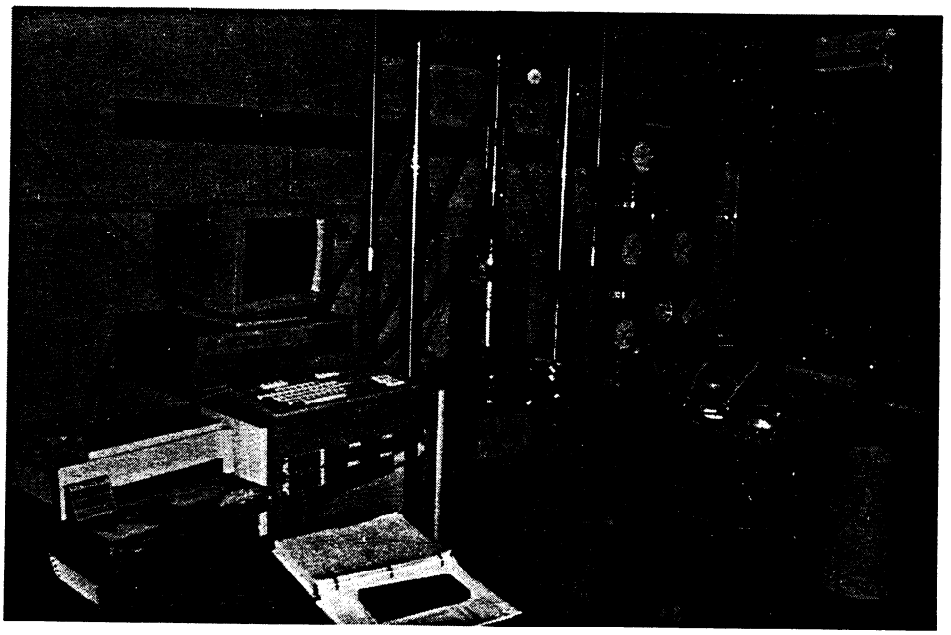

Fig 4. Resilient Modulus Testing Equipment.

granular materials. Stress state is considered to be the most important. As in shear strength, the more confined a granular material is, the higher will be the modulus. In the field, confinement is supplied by: 1) the layer underneath the granular material, 2) the granular material itself in the lateral (tangential and radial) (σ_2 and σ_3) direction, 3) the overburden above the point of interest, and 4) the momentary load from a vehicle. In a triaxial test, the difference between total vertical stress (a,) and the confining pressure (σ_3) is called the deviator stress or stress difference (σ_d). Cell pressure supplies the lateral confinement to the specimen (σ_2 and σ_3). A small static load ($0.1\ \sigma_d$) supplies the "overburden" pressure, and cyclic deviator stress ($0.9\ \sigma_d$) supplies the "vehicle" momentary stress. All of the stresses combined are known as the bulk stress.

$$\Theta = \sigma_1 + \sigma_2 + \sigma_3 \text{ where } \sigma_2 = \sigma_3 \text{ and } \sigma_1 = \sigma_d + \sigma_3$$
$$= (\sigma_d + \sigma_3) + 2\sigma_3$$
$$= \sigma_d + 3\sigma_3$$

E_g is calculated as $0.9\ \sigma_d/\epsilon_{recoverable}$. For each specimen, resilient modulus was determined at 15 stress states where effective confining pressure ranged from 2 to 20 psi and σ_d varied from 2 to 40 psi. This resulted in a range of bulk stress from 8 to 100 psi. This was considered adequate to cover the range of stress states likely to be encountered under field conditions. For instance, as will be shown later, the weighted average Θ in the crushed stone base at the AASHO Road Test was about 14 psi. The testing sequence and stress state schedule is shown in Table 4.

Table 4. Test Sequence for Granular Specimens of Base/Subbase Material.

Phase	Sequence No.	Deviator Stress (σ_d)(psi) *	σ_1	Confining Pressure (psi)	σ_1/σ_3	0	No. of Repetitions **
Specimen Conditioning	1	15	35	20	1.75	75	1000
Testing	2	10	30	20	1.5	70	50
	3	20	40	20	2.0	80	50
	4	30	50	20	2.5	90	50
	5	40	60	20	3.0	100	50
	6	10	25	15	1.67	55	50
	7	20	35	15	2.33	65	50
	8	30	45	15	3.0	75	50
	9	5	15	10	1.5	35	50
	10	10	20	10	2.0	40	50
	11	20	30	10	3.0	50	50
	12	5	10	5	2.0	20	50
	13	10	15	5	3.0	25	50
	14	5	8	3	2.67	14	50
	15	2	4	2	2.0	8	50

Note: 1psi = 6.9kPa

* Cyclic loads = 0.9 σ_d; constant contact loads = 0.1 σ_d

** For all stress states the minimum number of repetitions necessary is 50. The maximum is determined as per the AASHTO method and were redetermined for each confining pressure.

b) Degree of Saturation. In general, an increased water content will cause modulus to decrease. Several degrees of saturation (°S) have been put forth by others as break-points in behavior. Granular base materials are considered to be

relatively "dry" at degrees of saturation 60 percent and less (10,22). AASHO Road Test granular base materials suffered a marked increase in distress above 85 percent saturation. Resilient behavior has been shown to deteriorate above 80 to 90 percent saturation (22). In the present study, each material was tested at two degrees of saturation: approximately 60% and 100%.

c) Degree of Compaction. As previously discussed, modulus generally increases with higher levels of compaction. Two levels of compactive effort were evaluated for each material and gradation. For the dense gradation, specimens were compacted to 100% standard and 100% modified proctor densities. For the New Jersey gradation, one level of compaction corresponded to the maximum index density via vibratory compaction (wet method), while the lower level of density usually corresponded to an impact-type of compaction, such as 100% standard proctor.

d) Particle Shape/Surface Texture. As stated earlier, the effect of particle shape/surface texture is not well-defined. Two crushed stones and two gravels from different geological formations were chosen for delineating the effect of particle shape/surface texture.

Testing Scheme. The testing scheme involved the following variables: two sources of two particle shapes, two compactive efforts, two gradations and two degrees of saturation for a total of 32 "tests". Each test was run with duplicate specimens. The testing scheme is shown in Table 5.

Table 5. Testing Variable Scheme.

		Crushed Stone				Gravel			
		DR-12		DR-13		DR-14		DR-15	
		Mid.	NJ	Mid.	NJ	Mid.	NJ	Mid.	NJ
CE_L	°S = 60	X	X	X	X	X	X	X	X
	°S = 100	x	x	X	X	X	X	X	X
CE_H	°S = 60	X	X	X	X	X	X	X	X
	°S = 100	x	x	X	X	X	X	X	X

Note: Mid. = middle of MHTD Type 1 gradation band
NJ = New Jersey gradation
CE_L = lower compactive effort
CE_H = higher compactive effort
°S = 60 or 100% saturated

Test Procedure. The resilient modulus testing procedure involved the following steps: specimen compaction, assembly of the triaxial cell, consolidation, specimen conditioning at a given stress state, load application through 14 additional stress states at 60% saturation, backpressure saturation to 100% saturation, consolidation, and load application through 14 stress states at 100% saturation. After the load application in the 100% saturation step, the specimen was tested for permeability. The permeability results were used in the drainage project that was concurrent with the layer coefficient project. As a final step, the specimens were allowed to drain overnight in order to calculate their effective porosities.

The specimens were compacted in eight layers of equal thickness with a hand-held air hammer. The material was compacted at about 60% saturation into a split mold. After cell assembly and consolidation, the specimen was conditioned

with 1000 repetitions. Conditioning is used to eliminate the effects of any specimen disturbance due to specimen preparation procedures. It also aids in minimizing the effects of initially imperfect contact between the end platens and the test specimen. The various stress states and loads were then applied in accordance with Table 4. The number of load applications varied from 50 to 200, depending on the number of applications necessary to meet the AASHTO modulus repeatability requirements.

Load and deformation data were taken for every load application over the entire sequence, but only the last five repetitions were used for calculation of resilient modulus.

The load duration for each repetition was 0.1 sec followed by 0.9 sec rest. The stress pulse shape was haversine in nature. Repeated load equipment deflection was determined through the use of an aluminum dummy specimen and was subtracted from total deflections for each stress state. Initially, calibration of the load cell and LVDT's was performed before each test, but the interval was increased upon determining that the drift in calibration was insignificant. The change in specimen height was constantly monitored. None of the specimens approached the maximum allowable permanent strain of 5%.

In an effort to determine the effect of drainability on pavement bases, the tests at 60% saturation were performed in a drained condition while the 100% saturation tests were run in an undrained state.

RESULTS OF THE LABORATORY INVESTIGATION

As-Received Gradations

The as-received gradations of the four granular materials are shown in Table 6. The two experimental gradatons are shown in Table 7.

Table 6. As-Received Gradations.

Sieve Size	Percent Passing			
	DR-12	DR-13	DR-14	DR-15
1 in	100	100	100	100
1/2 in	96	83	72	83
#4	68	50	46	50
16	--	26	37	26
40	24	18	17	12
100	12	13	2	5
200	8	7	1	4

Table 7. Experimental Gradations.

Sieve Size	% Passing	
	Middle	NJ
3 in.	100	100
1 1/2	100	100
3/4	(95)	(95)
1/2	75	68
3/8	(63)	(58)
#4	50	47
8	(40)	(20)
16	33	5
30	(28)	(4)
40	25	3
50	(22)	(2.5)
100	(16)	(2.5)
200	8	2
( ) = estimated from plot		

Gradation Curve Shape/Position

In an attempt to determine the effect of gradation on resilient modulus, a parameter that described gradation curve shape/position was required. Nine different methods were explored. Sieve size data from both experimental gradation curve types (Middle and NJ) were used for calculation of various parameters. The parameters were then used in the development of the multiple regression model of resilient modulus to see which method increased the accuracy of the model the most. This was judged from the adjusted - R^2 statistic of the equation. The nine

methods or parameters were as follows: fineness modulus (FM), coefficient of uniformity (C_u), coefficient of skew (C_z), surface fineness (SF), specific surface factor (SSF), a combination of SF and SFF (SF/SSF), Hudson's $\bar{A}$, slopes-of-gradation-curve, and the percent passing or retained on individual sieves. Values for these parameters are shown in Tables 8 and 9. The parameters are discussed in Volume I of this report. The slopes-of-gradation-curve (M) method was altered from that which was in Volume I to better match the natural break points of the granular base experimental gradation curves. The slopes of each curve were determined between the *1* in and #4 sieve, the #4 and #16 sieves, and the #16 and #200 sieves.

Table 8. Gradation Shape Results.

	Mid.	NJ
FM	4.53	5.66
C_u	82.6	5.29
C_z	1.19	0.21
SF	1588	1938
SSF	294.4	65.8
SF/SSF	5.40	29.4
$\bar{A}$	4.55	3.36
M_{n-n}	e-o--	-----
3/4, #4, 16, 200	-----	-----

The results of the regression model analysis indicated that it made very little

difference as to which gradation parameter was used (except $\bar{A}$ was somewhat less effective, and no more than one "M" could be used at a time due to collinearity problems).

Table 9. Experimental Gradation Slopes.

Gradation	M_{1-4}	M_{4-16}	M_{16-200}
Middle	94.3	78.0	138.9
NJ	100.0	192.7	16.7

Moisture-Density Relationships and Specific Gravities

Moisture-density relationship and apparent specific gravity information was determined in regard to the two test gradations for each of the four granular materials. The data are shown in Table 10.

Table 10. Specific Gravity and Moisture Density Data.

Material	Gradation	Apparent Sp. Gravity	Density, minimum (pcf)	T-99		T-I 80		D4253	
				MDD (pcf)	OMC (%)	MDD (pcf)	OMC (%)	MDD (pcf)	OMC (%)
DR-12	MHTD Mid	2.69	113.2	136.5	7.0	137.6	7.4	--	--
	NJ	2.69	101.7	--	--	131.2	9.0	121.1	12.2
DR-13	MHTD Mid	2.78	114.3	138.3	7.7	141.0	5.9	--	--
	NJ	2.78	100.8	--	--	135.2	8.3	124.1	13.0
DR-14	MHTD Mid	2.65	109.9	132.5	7.8	134.5	6.7	--	--
	NJ	2.65	99.9	119.0	8.0	--	--	122.8	12.0
DR-15	MHTD Mid	2.65	110.2	134.4	7.6	136.9	6.1	--	--
	NJ	2.65	96.2	109.5**	8.9	--	--	114.3	14.0

Note: T-99 = Standard proctor
T-180 = Modified proctor
D4253 = Vibratory table
**. T-99, T-180, and D4253 densities were very close. To get a wider difference in values, a surcharge weight was used which was different than that which was used to obtain the other D4253 data

Some difficulty was experienced with performing the impact-type of moisture-density tests for certain materials when graded according to the New Jersey gradation, therefore, the vibratory table density (wet) method was also performed. It is believed that this compaction method gives a density value more comparable to that which will be achieved in the field. The tests were performed in a dry state at different power settings to determine the optimum setting which would result in the highest density. The test was then run with the material in a moisture state which was more in line with field compaction conditions. A typical vibratory table test result is shown in Fig. 5. In Fig. 6 are shown the moisture-density relationships for each of the four granular materials.

Relative Density

Minimum density test results are also listed in Table 10. The minimum and maximum density values were used in Eq. 4 to calculate the relative density of each E_g specimen, as listed later in Table 13. Relative density values give a wider spread of values than "percent of T-180 values", and therefore are more useful in analysis of behavior.

Particle Shape and Surface Texture

Particle shape/texture characteristics were quantified by use of ASTM D 3398 for the (+) #4 sieve material and by NAA Method A for the (-) #8 through (+) #100 material for each aggregate source. Both are measures of void content of bulk aggregate. Void content has been shown to be related to particle shape/texture. D3398 results in a "Particle index" (IP) while the NAA Method A

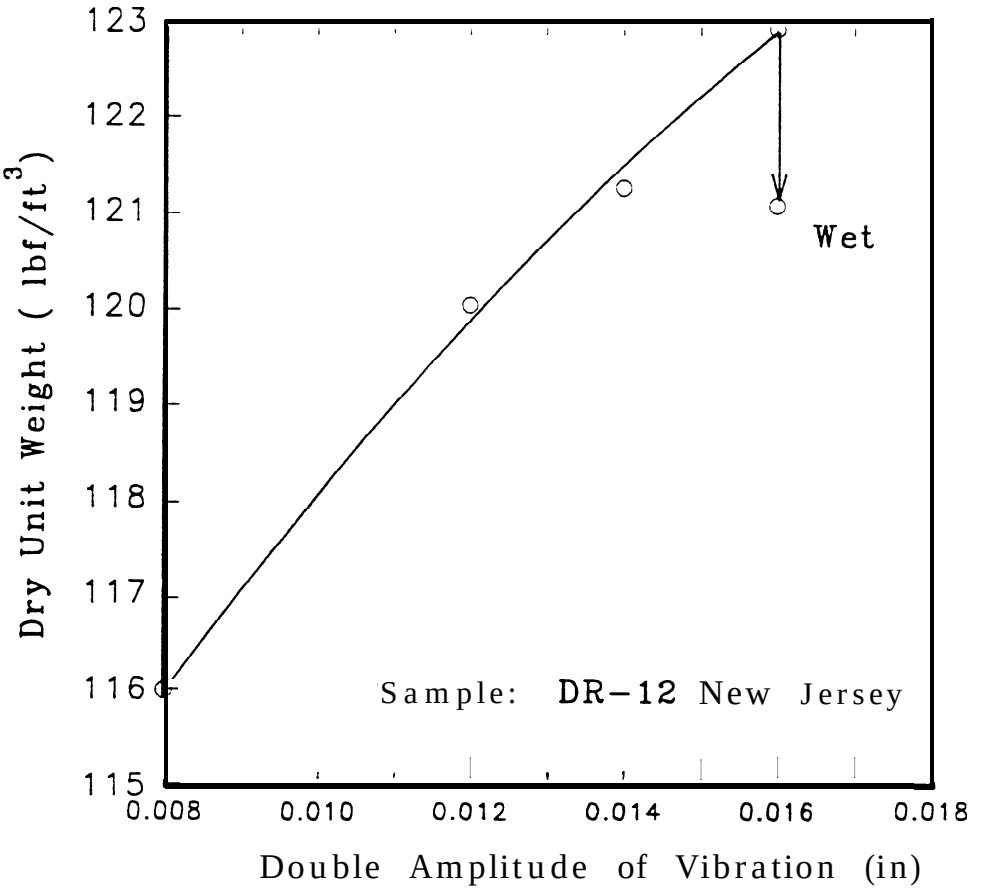

Fig. 5. Typical Vibratory Table Test Result.

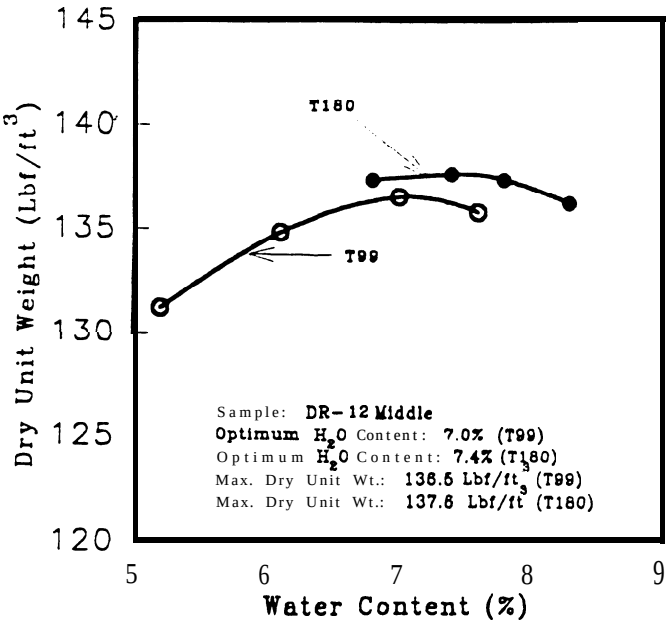

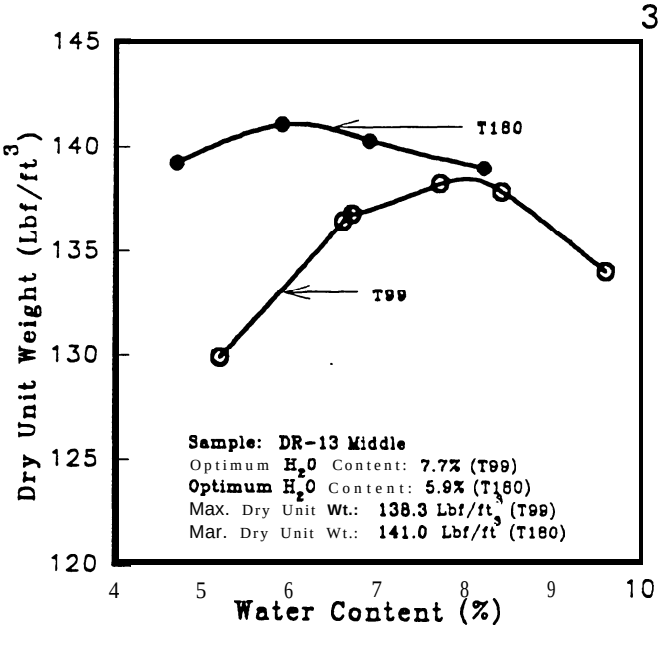

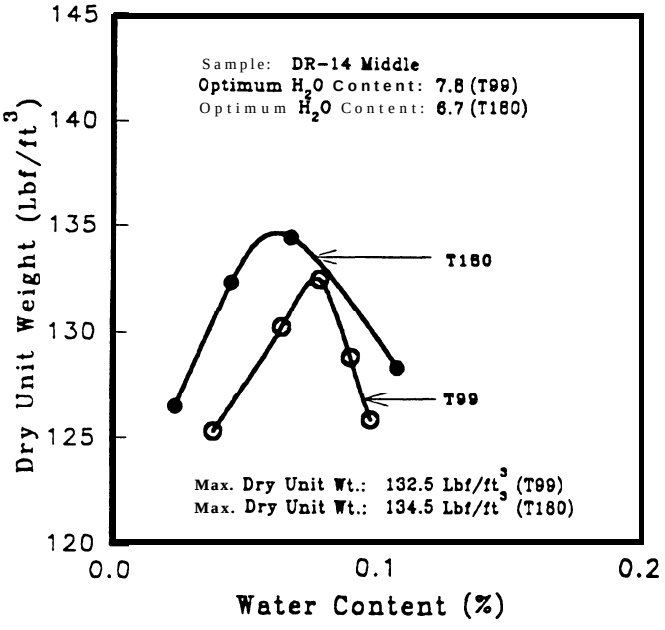

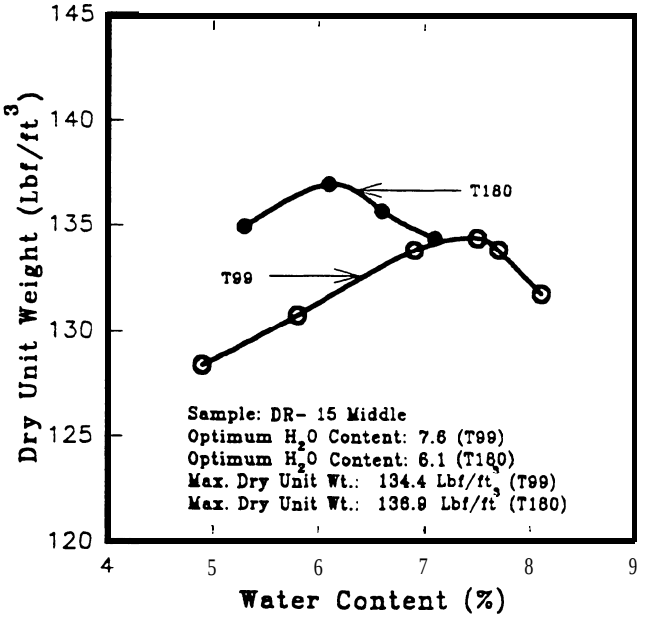

Fig. 6. Moisture – Density Relationships for MHTD Middle Unbound Granular Materials.

gives an "Uncompacted Voids Percent" (U). The results are shown in Table 11.

Table 11. Particle Shape/Texture Results.

Aggregate	Particle Index (IP)	Uncompacted Voids (U) %
DR-12	12.5	43.6
DR-13	11.9	45.3
DR-14	10.0	41.2
DR-15	10.4	40.6

Round, smooth particles give IP's of 6 or 7, while angular, rough particles result in values of more than 15. The range of IP's of the aggregates in this study was 10.0 to 12.5. The Particle Index was determined for the coarse aggregate fraction of each gradation and the Uncompacted Voids content was determined for the fine aggregate fraction.

Looking at Particle index and especially the Uncompacted Voids values, the crushed aggregates were somewhat more angular than the gravels, as expected, but the ranges were limited.

Plasticity of Fines

The results of the Atterberg Limits testing are shown in Table 12. All four aggregates were essentially non-plastic in nature.

gives an "Uncompacted Voids Percent" (U). The results are shown in Table 11.

Table 11. Particle Shape/Texture Results.

Aggregate	Particle Index (IP)	Uncompacted Voids (U) %
DR-12	12.5	43.6
DR-13	11.9	45.3
DR-14	10.0	41.2
DR-15	10.4	40.6

Round, smooth particles give IP's of 6 or 7, while angular, rough particles result in values of more than 15. The range of IP's of the aggregates in this study was 10.0 to 12.5. The Particle Index was determined for the coarse aggregate fraction of each gradation and the Uncompacted Voids content was determined for the fine aggregate fraction.

Looking at Particle Index and especially the Uncompacted Voids values, the crushed aggregates were somewhat more angular than the gravels, as expected, but the ranges were limited.

Plasticity of Fines

The results of the Atterberg Limits testing are shown in Table 12. All four aggregates were essentially non-plastic in nature.

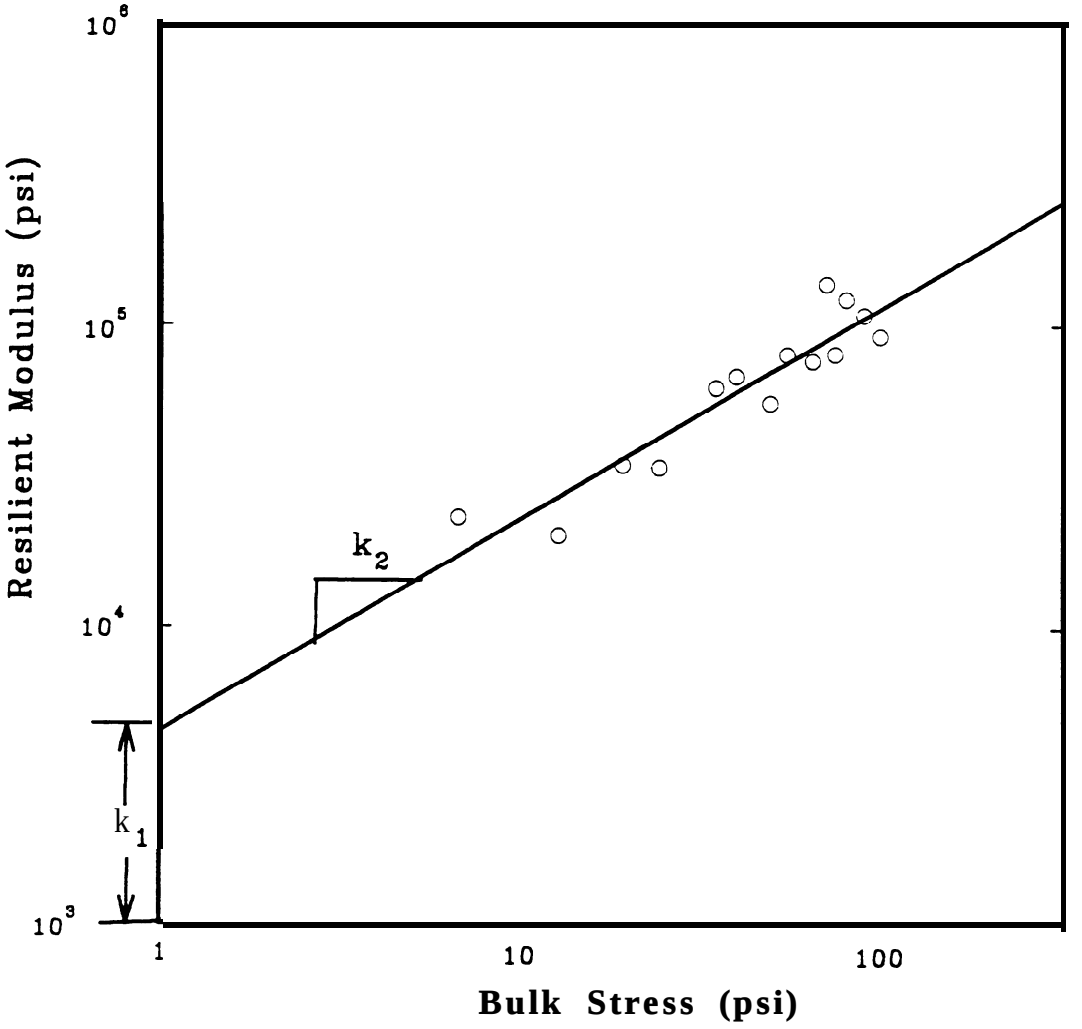

Fig. 7. Typical Resilient Modulus Test Results.

$$E_g = k_1 \Theta^{k_2} \quad \ldots\ldots\ldots\ldots\ldots\ldots\ldots\ldots (6)$$

where:

k_1 = intercept of E_g at Θ = 1 psi, log-log plot

k_2 = slope of line, log-log plot.

The results of all resilient modulus testing are tabulated in Table 13.

Fig. 8 shows the relationship of coefficients k_1 and k_2 as reported by Rada and Witczak (22), with the results of the present study also plotted. As can be seen, the present study data falls in the range of data that has been reported elsewhere.

Fig. 9 shows the effect of aggregate source on E_g. It appears that in the range of stresses encountered in highway pavements, there is no clear trend in the effect of aggregate source on E_g. This may be a result of the limited range of particle shapes/textures of the materials used in this study.

The effect of increased degree of saturation is shown in Fig. 10. The general trend is a loss of E_g as the degree of saturation increases from a moist state to a saturated state. This is similar to the trend reported by Rada and Witczak and others.

The interaction between gradation, compactive effort, and degree of saturation is shown in Fig. 11. It appears that open-graded material suffers somewhat more of a loss in E_g than dense-graded material as indicated by steeper curve slopes. The percent loss for the dense graded materials with low and high compactive efforts was 9.8 and 11.0, while the loss for the open graded materials

Table 13. Resilient Modulus Test Data.

Material	Gradation/CE	Dry Density (pcf)		MADD		D_R	°Sat. (%)	k_1 (psi)	k_2	E_q (psi)*
		Target	As-tested	(pcf)	(%)					$\theta = 10$
DR-12	Mid (low)	136.5	136.4	138.9	98.2	92.1	61.4	3040	0.85	21,522
DR-12	Mid (low)	136.5	136.4	138.9	98.2	92.1	100	2958	0.86	21,428
DR-12	Mid (high)	137.6	138.4	138.9	99.6	98.4	62.5	3828	0.82	25,295
DR-12	Mid (high)	137.6	138.4	138.9	99.6	98.4	100	3758	0.80	23,437
DR-12	NJ (low)	121.1	120.5	131.2	91.8	69.3	59.6	4307	0.72	22,865
DR-12	NJ (low)	121.1	120.5	131.2	91.8	69.3	100	1940	0.90	15,584
DR-12	NJ (high)	131.2	127.7	131.2	97.3	90.5	53.1	5134	0.74	27,890
DR-12	NJ (high)	131.2	127.7	131.2	97.3	90.5	100	2706	0.92	22,508
DR-13	Mid (low)	138.3	138.2	141.0	98.0	91.3	63.8	4212	0.76	24,238
DR-13	Mid (low)	138.3	138.2	141.0	98.0	91.3	100	3606	0.80	22,752
DR-13	Mid (high)	141.0	139.5	141.0	98.9	95.2	59.8	8312	0.58	31,967
DR-13	Mid (high)	141.0	139.5	141.0	98.9	95.2	100	5918	0.62	24,390
DR-13	NJ (low)	124.1	125.9	135.2	93.1	78.3	63.8	3470	0.81	22,407
DR-13	NJ (low)	124.1	125.9	135.2	93.1	78.3	100	2824	0.82	18,658
DR-13	NJ (high)	135.2	134.1	135.2	99.2	97.5	58.8	3164	0.90	25,428
DR-13	NJ (high)	135.2	134.1	135.2	99.2	97.5	100	2997	0.86	21,963
DR-14	Mid (low)	132.5	131.1	135.4	96.8	85.9	58.6	4443	0.60	17,688
DR-14	Mid (low)	132.5	131.1	135.4	96.8	85.9	100	3401	0.68	16,278
DR-14	Mid (high)	134.5	134.4	135.4	99.3	96.8	67.2	5468	0.64	23,869
DR-14	Mid (high)	134.5	134.4	135.4	99.3	96.8	100	5793	0.67	27,096
DR-14	NJ (low)	122.8	121.1	125.8	96.2	84.7	58.2	6618	0.56	24,309
DR-14	NJ (low)	122.8	121.1	125.8	96.2	84.7	100	4504	0.72	23,369
DR-14	NJ (high)	125.8	124.1	125.8	98.6	94.7	55.1	7639	0.53	25,884
DR-14	NJ (high)	125.8	125.0	125.8	99.3	97.4	100	3569	0.74	19,840

DR-15	Mid (low)	134.4	131.5	136.9	96.0	83.1	51.4	5058	0.55	17,946
DR-15	Mid (low)	134.4	131.5	136.9	96.0	83.1	100	2645	0.69	12,955
DR-15	Mid (high)	136.9	135.4	136.9	98.9	95.2	59.7	4498	0.65	20,090
DR-15	Mid (high)	136.9	135.4	136.9	98.7	94.5	100	2702	0.75	15,194
DR-15	NJ (low)	109.5	110.4	115.8	95.3	76.1	58.9	4554	0.57	16,920
DR-15	NJ (low)	109.5	110.4	115.8	95.3	76.1	100	2358	0.76	13,569
DR-15	NJ (high)	114.3	115.8	115.8	100	100	63.6	3012	0.72	15,807
DR-15	NJ (high)	114.3	115.8	115.8	100	100	100	1338	0.96	12,203

CE = Cornpactive effort
MADD = Maximum Attainable Dry Density
D_R = Relative Density
$^*E_g = k_1 \theta^{k2}$

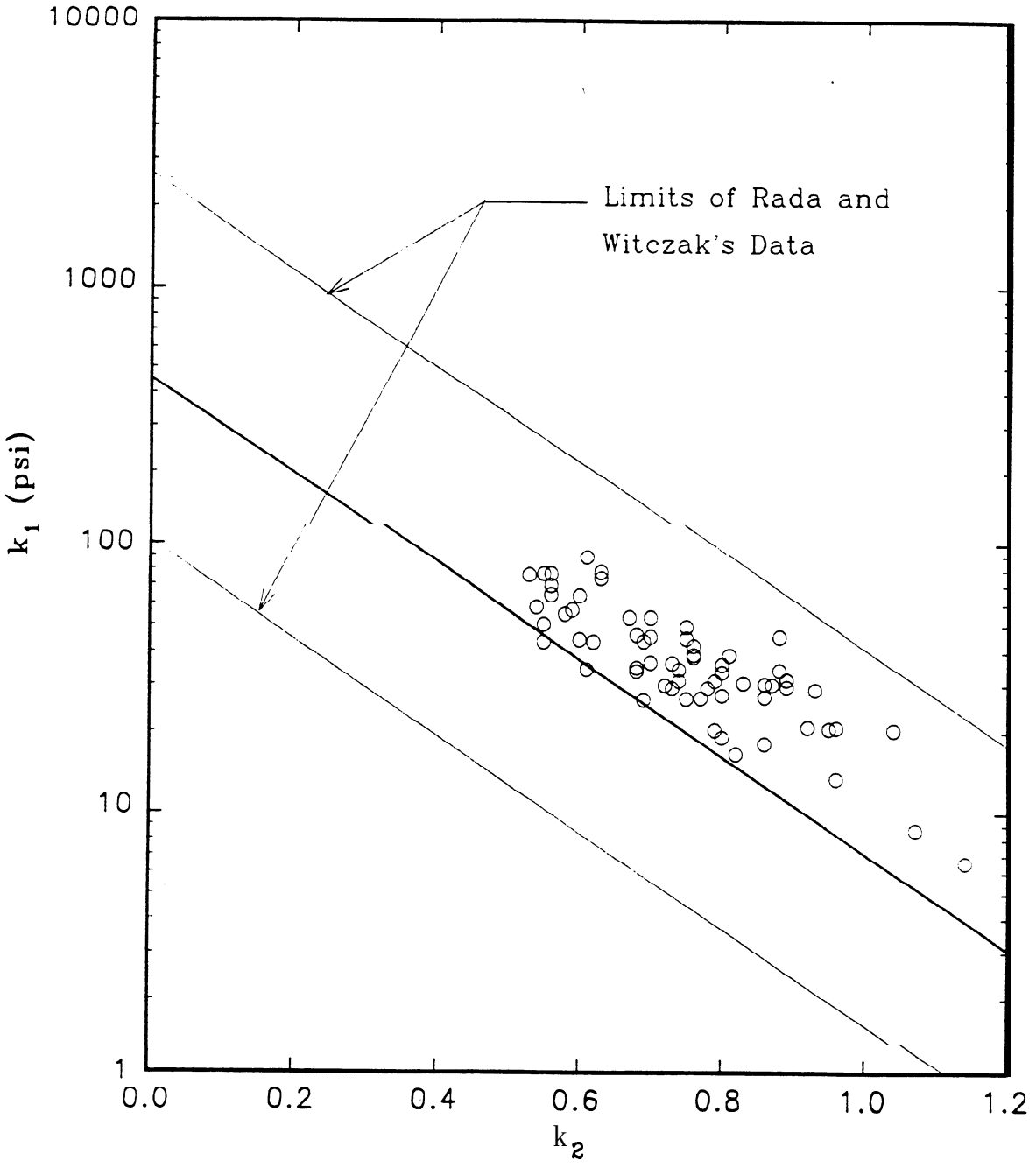

Fig. 8: Relationship Between Experimentally Derived Factors (k_1 and k_2) for the Theta Model.

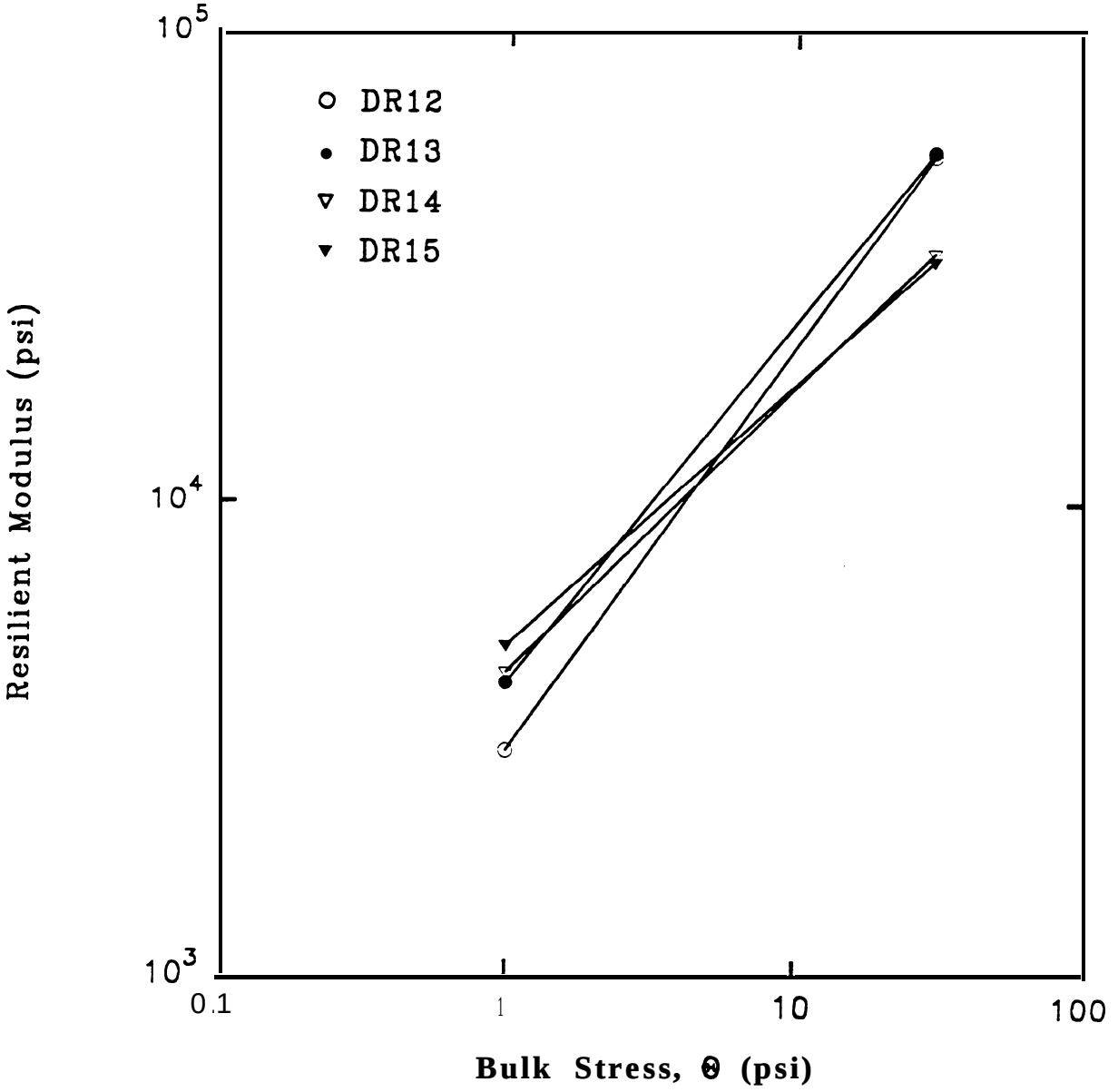

Fig. 9. Effect of Agregate Source on Resilient Modulus.

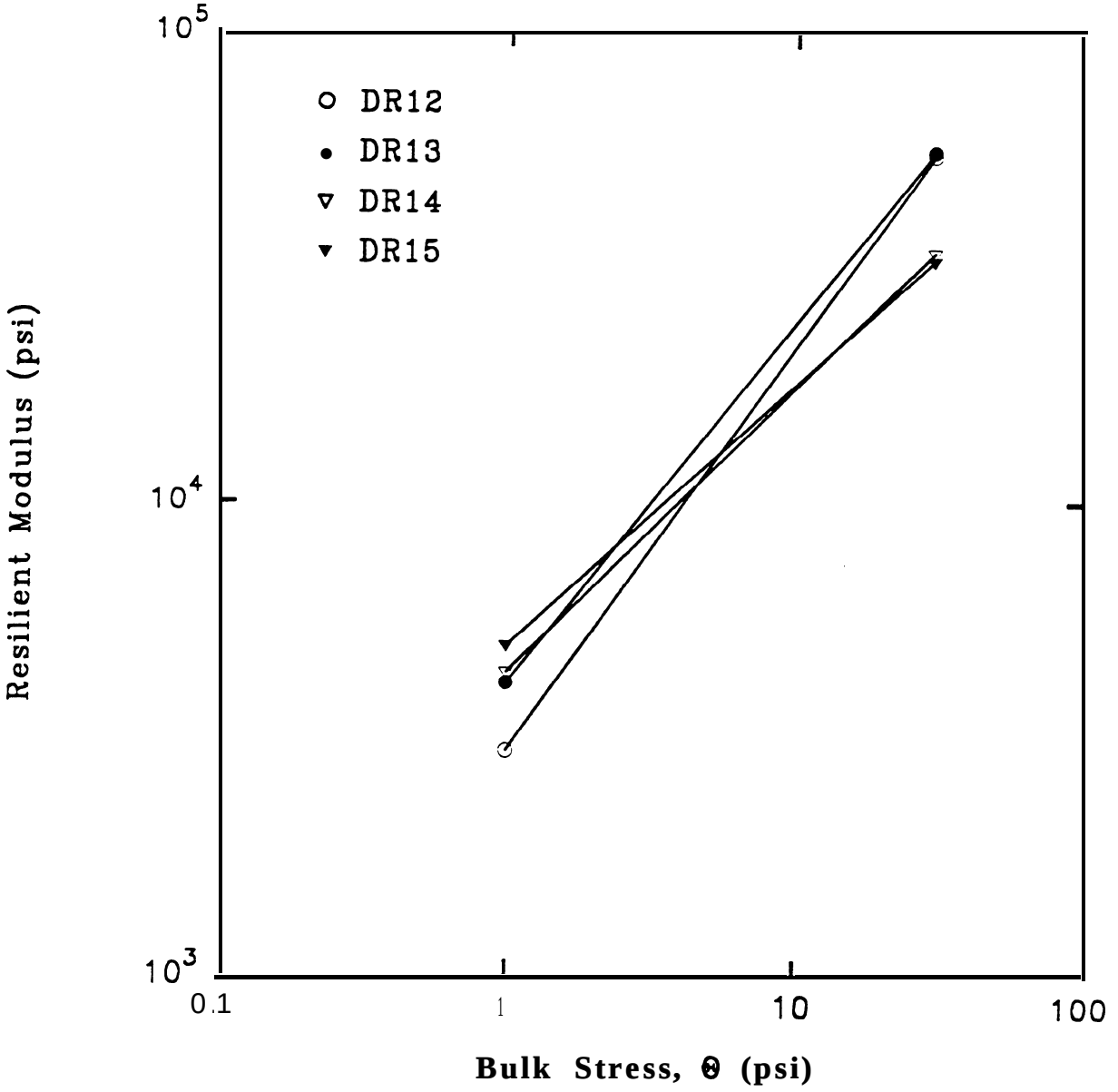

Fig. 9. Effect of Agregate Source on Resilient Modulus.

was 17.7 and 19.5, respectively. However, the effect on E_g of providing a drained base can also be seen from Fig. 11 by looking at the dashed lines. For both the low and high compactive effort cases, there is a benefit from changing from a dense graded material which will remain saturated for extended periods of time to an open graded material which will remain in a drained state most of the time.

Additionally, the effect of compactive effort is apparent. For both the dense and open graded materials, an increase in compactive effort from close to 100% T-99 density to 100% T-180 density leads to an increase in E_g.

Statistical Analysis

A statistical analysis was conducted to determine the effect of the four independent variables on E_g. Paired-t tests were performed to see if there was a significant difference between the means of all E_g data of 1) a low degree vs a high degree of saturation, 2) a low compactive effort vs a high one, and 3) a dense gradation vs an open gradation. Additionally, a Tukey HSD analysis was performed to determine if aggregate source made a significant difference in E_g results and, if so, which source(s) were significantly different. The results are shown in Table 14. As can be seen, degree of saturation, compactive effort, and aggregate source were significant to differences in E_g at the 0.05 level, and the interaction of gradation and saturation was significant at the 0.088 level. Gradation by itself was not statistically significant. Reduction in E_g came from increasing the saturation from 60 to 100%, reducing the level of compaction from about 100% T-180 to 100% T-99 density, and having a saturated, dense graded

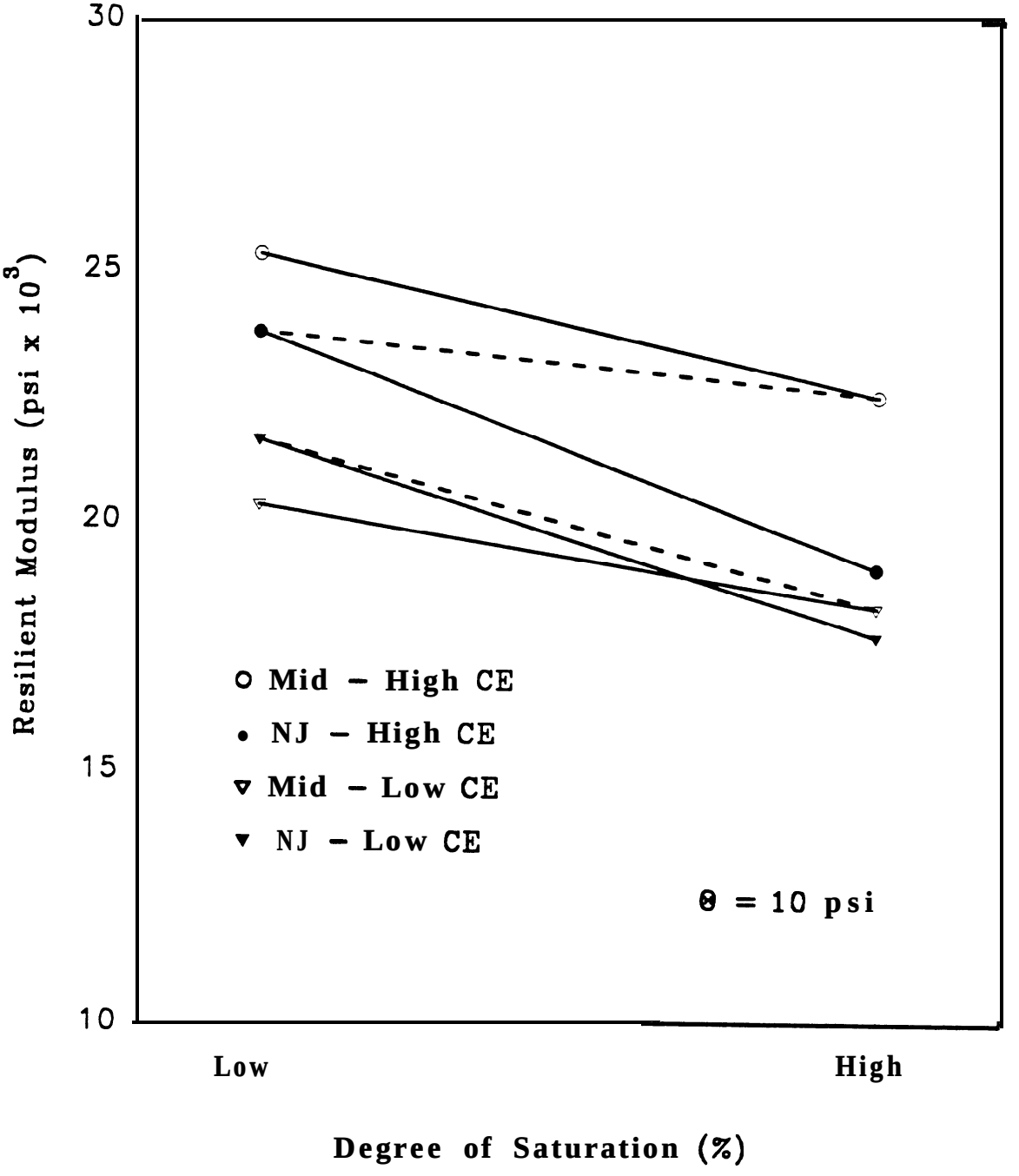

Fig. 11. Effect of Gradation, Degree of Saturation, and Compactive Effort on Resilient Modulus.

Table 14. Significance of Variables to Resilient Modulus.

E_g at θ = 10 psi (psi)				
Condition	Maximum	Minimum	Difference	Significance at 0.05 level
All Mixtures:				
°Saturation, low vs high	22,706	19,452	3254	yes
Gradation, dense vs open	21,634	20,562	1072	no
Comp. effort, high vs low	22,679	19,518	3161	yes
Agg. Source,				
*DR 12 vs DR 15	22,541	15,585	6956	yes
DR 13 vs DR 15	23,975	15,585	8390	yes
DR 14 vs DR 15	22,330	15,585	6745	yes
Gradation and saturation: open graded drained vs dense graded undrained	22,704	20,442	2262	yes at 0.088 level
*All other combinations: not significantly different				

material as opposed to a drained, open-graded material. In regard to aggregate source, the DR-15 had a significantly lower modulus than the other three sources (which were all about the same). However, this does not appear to be a function of particle shape or plasticity of fines, because the U and IP values of the DR15 were close to those of the DR14, and the plasticity Index all four sources was about the same. A possible explanation is that the as-tested density of the DR-15 specimens was somewhat low compared to the target density.

ESTIMATION OF RESILIENT MODULUS

Introduction

The layer coefficients a_2 or a_3 for an unbound granular base or subbase material are found from a relationship with resilient modulus, E_g. The resilient modulus for a given material can be found by test using the "theta model", or by use of an estimation regression equation. The development of the regression equation is outlined below.

It has been shown that the resilient modulus of a granular material is a function of stress state:

$$E_g = k_1 \theta^{k_2}$$

where:

θ = bulk stress = $\sigma_1 + \sigma_2 + \sigma_3$

σ_1 = major principal stress

= $\sigma_d + \sigma_c$ in triaxial cell test

(σ_d = deviator stress; σ_c = confining pressure)

σ_1 = $\sigma_z + \gamma_1 z_1 + \gamma_2 z_2$ in pavement, under centerline of load

(σ_z is vertical stress induced from a single wheel load as computed by elastic layer analysis; γ_1 and γ_2 are unit weights of each overlying material; z's are thicknesses of each layer overlying the point of stress computation)

σ_2 = intermediate principal stress

σ_3 = minor principal stress

$\sigma_2 = \sigma_x + k_o (\gamma_1 z_1 + \gamma_2 z_2)$

$\sigma_3 = \sigma_y + k_o (\gamma_1 z_1 + \gamma_2 z_2)$

σ_x = horizontal stress in x-direction induced by wheel load, psi

σ_y = horizontal stress in y-direction induced by wheel load, psi

k_o = coefficient of earth pressure at rest

= 1 - sin ϕ for granular materials (ϕ = angle of internal friction)

k_1, k_2 = regression coefficients as determined from laboratory cyclic triaxial testing.

Thus, in a pavement structure:

$$\theta = [\sigma_z + (\gamma_1 z_1 + \gamma_2 z_2)] + [\sigma_x + k_o(\gamma_1 z_1 + \gamma_2 z_2)] + [\sigma_y + k_o(\gamma_1 z_1 + \gamma_2 z_2)]$$
$$= \sigma_z + \sigma_x + \sigma_y + (\gamma_1 z_1 + \gamma_2 z_2)(1 + 2 k_o) \quad . \quad (7)$$

In order for E_g to be calculated by use of Eq. 6 $\left(E_g = k_1 \theta^{k_2}\right)$, values for k_1, k_2, and θ are necessary. The following discussion shows the methods by which these three parameters were determined.

$\underline{k_1 \text{ and } k_2}$

The parameter k_1 represents the granular material condition and characteristics: gradation, particle shape and texture, degree of saturation, and relative density. A larger k_1 indicates a superior material/condition.

The constants k_1 and k_2 can be determined for a given material by cyclic triaxial testing (CTX) as shown in Fig. 7. Alternately, in order to be able to estimate k_1 (and hence E_g) without performing a CTX test, regression equations were developed by use of the statistical software package SYSTAT (36) from the

test data produced in the present study. Numerous linear multiple regression models were developed and analyzed to estimate k_1 from certain test data. Many combinations of variables were analyzed. Data to develop the equations came from Tables 7, 9, and 10. The equation of best fit had a low degree of accuracy and is not shown here, but it was helpful in indicating trends and for estimation of k_1 values to set up boundary conditions for other models in the study. A second method of k_1 estimation will be presented later in this report.

k_2 has been shown (22) to correlate with k_1 as follows:

$$k_2 = \frac{4.657 - \log k_1}{1.807} \quad \ldots\ldots\ldots\ldots\ldots\ldots \quad (8)$$

Thus, k_1 can be estimated from physical properties of the aggregate (as shown later), and k_2 can be estimated from a relationship with k_1.

Bulk Stress (θ)

Bulk stress in an unbound granular base layer is a function of applied load (P) and contact pressure (p), stiffness (E_1) and thickness (D_1) of the overlying asphalt-bound layer, stiffness (E_{sg}) of the subgrade underlying the base layer, stiffness (E_g) and thickness (D_2) of the base layer, and unit weight of the overlying layers. Because E_g is a function of θ, and θ is a function of E_g, an iterative procedure was necessary in order to reconcile the E_g and θ. The method of successive approximations is shown below..

A load of 9000 lbs (one half of an 18k axle load) and a contact pressure of 100 psi (average U.S. truck tire pressure) was used.

1. An initial E_g was assumed.
2. An elastic layer analysis was performed with KENLAYER (37) a commercially available analysis program. Output included σ_z, σ_x, σ_y and geostatic stresses resulting from the static overburden of the pavement layers.
3. Bulk stress was calculated from $\theta = \sigma_z + \sigma_x + \sigma_y$ + geostatic stresses.
4. E_g was calculated via Eq. 6.
5. If E_g (calculated) was not close to E_g (initial), a new E_g was computed.

The process was automatically repeated until satisfactory convergence was achieved. KENLAYER was used with the elastic non-linear option. Reconciling E_g with θ was not a separate process; rather, it was integral to determining the E_g algorithm as explained below in the section "Resilient Modulus Algorithm".

Corrected Bulk Stress

Granular materials normally cannot sustain tension, discounting any cementing action or residual compressive stress from compaction. So, in KENLAYER, if the computed θ became negative, an arbitrary minimum modulus was assigned.

Resilient Modulus Regression Equation

To circumvent the necessity of the above iterative procedure, Witczak and Smith (38) developed a predictive equation:

$$E_g = (10.447)(D_1)^{-0.471}(D_2)^{-0.041}(E_1)^{-0.139}(E_{sg})^{0.287}(k_1)^{0.868} \quad . \quad . \quad . \quad (9)$$

A predictive equation of resilient modulus could be constructed from E_g test data which reflected the effect of saturation, density, and bulk stress, θ. Unfortunately, θ is not normally known. Results of numerous runs of KENLAYER indicated that θ could typically vary from 3 to 33 psi. This is too wide a variance to merely assume a value for θ. Bulk stress could be calculated for a variety of cross-sections, but the θ values would be dependent on the particular value of k_1 that had been assumed. Additionally, it was anticipated that the typical design situation would involve a trial-and-error solution for D_1 and D_2, with θ therefore varying. Thus, an assumption (or determination by test) of a k_1 value seems to be unavoidable.

In the formulation of Eq. 9, Witczak and Smith assumed a constant value for k_2. However, it has been shown in the present study and others (22) that k_2 varies significantly with k_1, and k_1 is a function of several material characteristics, including degree of saturation. When saturation increases above 90%, there is a substantial drop in k_1 and an increase in k_2 (22). This was verified in the present study. To reflect the effect of the change in k_2, a different regression equation was developed in the present study:

$$\log E_g = 2.708 - 0.458\log D_1 + 0.426\log k_1 - 0.107\log E_1 + 0.207\log E_{sg} + 0.067\log D_2 \quad . \quad . \quad . \quad (10)$$

$$\text{or} \quad E_g = (510.505)(D_1)^{-0.458}(k_1)^{0.426}(E_1)^{-0.107}(E_{sg})^{0.207}(D_2)^{0.067}$$

where k_1 can be obtained by test. If it is necessary to estimate k_1, values may be

approximated as shown in Table 15, which is based on the results of the present study and a previous study (22). It must be emphasized that k_1 values vary considerably within an aggregate source class, and it is quite possible for a given gravel to have a k_1 value greater than a given crushed stone.

Table 15. Estimated Values of k_1.

Material	k_1	
	SCE (100%)	MCE (100%)
Gravel	4300	5000
Crushed stone	4800	6100

Note:
at $\leq$ 60% saturation; minus #200 $\leq$ 10%
SCE = standard compactive effort
MCE = modified compactive effort

The modulus calculated by use of Eq. 10 will approximate the modulus from Eq. 6 that has been reconciled with θ. The other terms in Eq. 10 are necessary to compute bulk stress conditions. As E_1 and D_1 increase, less stress is transmitted to the base layer, hence E_g decreases. As E_{sg} decreases, the base layer is less confined under loading, hence E_g decreases. Note that Eq. 10 can only be used for a single granular layer sandwiched between an asphalt layer and the subgrade. For more complicated sections, use of programs such as KENLAYER are recommended to calculate E_g (base) and E_g (subbase).

Eq. 10 was developed by calculation of granular E_g by use of Eq. 6

$(E_g = k_1\theta^{k_2})$. In the regression equation development, resilient modulus was varied by use of 237 combinations of k_1, k_2, and θ in the program KENLAYER. These combinations represented three levels of the following variables: layer thicknesses (D_1 and D_2), subgrade modulus (E_{sg}), asphalt layer modulus (E_1), and granular material constants k_1 and k_2:

Stress state: D_1 = 2,8,15 in

D_2 = 4,12,18 in

E_1 = 130,000; 500,000; 2,100,000 psi

E_{sg} = very soft, medium, stiff

k_1 = 1800; 3000; 11,000 psi

k_2 = 0.776, 0.653, 0.341

The following paragraphs show how the above values were determined.

Granular Material k_1 and k_2. k_1 = 1800; 3000; 11,000 psi, which represented three levels:

1) 60% saturation; 95% SCE; dense gradation with 35% minus #16 sieve material; gravel representing U = 5; contaminated with plastic fines
2) 60% saturation; 100% SCE; dense gradation with 35% minus #16 sieve material; crushed stone representing U = 13; non-contaminated
3) 10% saturation; 100% MCE; open gradation with 5% minus #16 sieve material; crushed stone representing U = 15; non-contaminated

k_2 = 0.776, 0.653, 0.341 from Eq. 8.

For each of the 237 combinations, KENLAYER calculated the bulk stress θ in

the granular base and the deviator stress σ_d in the subgrade soil from an applied load, The different cross-sections represented by the model are shown in Fig. 12.

Asphalt Modulus (E_1). The asphalt layer was characterized as linearly elastic, while the granular base and subgrade materials were characterized as non-linearly elastic. For the asphalt layer, three conditions of stiffness were characterized using the relationship of temperature and resilient modulus for MHTD 1990 mix designs as developed in Volume I of this report. The highest modulus was determined by choosing the stiffest 1990 mix at the coldest individual Missouri weather station's reported average monthly temperature (pavement temperature T_p = 33.4°F). The smallest asphalt modulus utilized the least stiff 1990 mix at the warmest individual weather station's average monthly temperature (T_p = 92.3°F). A middle value for modulus was found by using a 1990 mix of average stiffness with the overall average monthly pavement temperature for all Missouri weather reporting stations (T_p = 64.2°F). This resulted in asphalt mixture moduli of 2,100,000; 500,000, and 130,000 psi. Pavement temperatures were calculated from air temperatures by use of Witczak's equation as discussed in Volume I.

Subgrade Modulus (E_{sg}). The resilient modulus of fine-grained soils can be computed by use of the program KENLAYER. The modulus is a function of soil type, degree of saturation, compacted density, and state of stress within the pavement structure. In KENLAYER, the soil modulus was characterized as being very soft, medium, or stiff. The soils were described as shown in Fig. 13. As can be seen, the curves of each of these three soils has the same general shape and

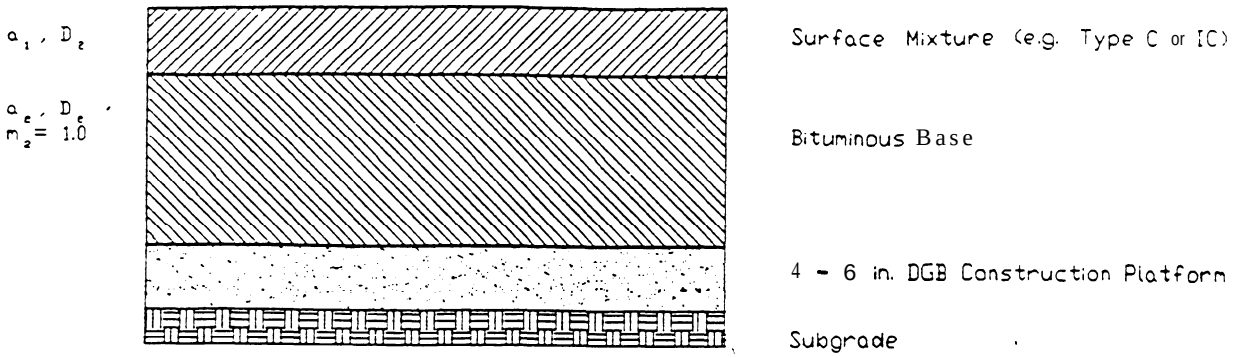

a. Two Layer Full Depth Asphalt Section.

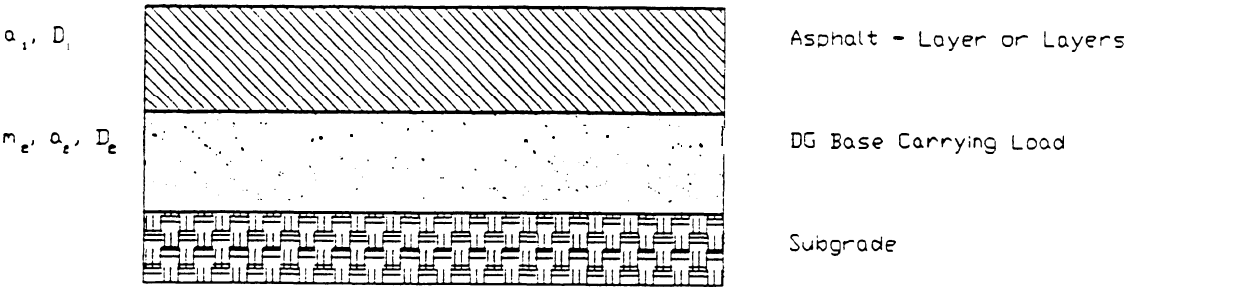

b. Two Layer Flexible Pavement With Dense Graded Unbound Base Carrying Part of Load.

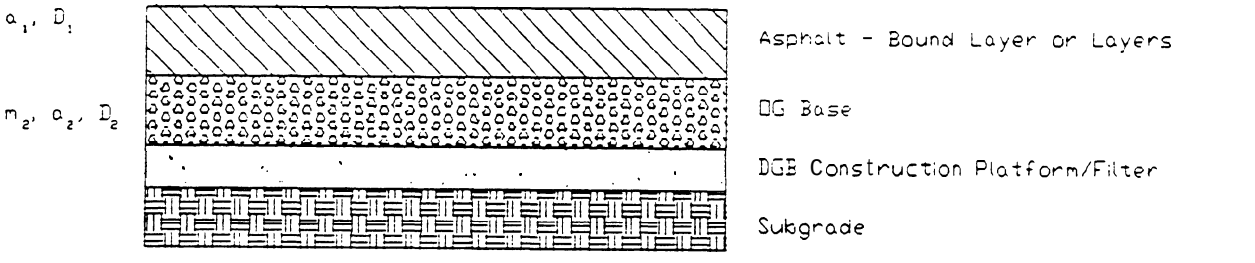

c. Two Layer Flexible Pavement With Open Graded Unbound Base Carrying Part of Load

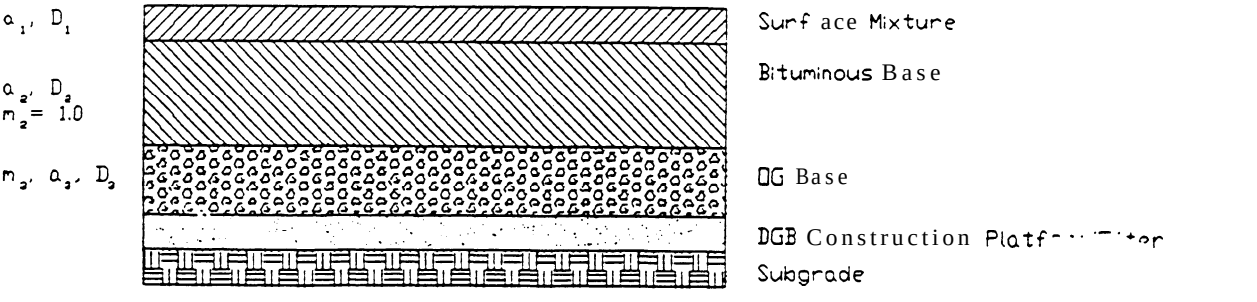

d. Three Layer Flexible Pavement.

Fig. 12. Definitions of Layer Variables.

equal line slopes (K_3 and K_4). The parameters that distinguish one soil's consistency from another are the maximum and minimum moduli (boundary conditions on a possible spectrum of stiffness) and K_1, except for the very soft material which has a K_4 of zero.

input values to describe the three soils are shown in Table 16.

Table 16. Typical input Soil Constants for KENLAYER Analysis.

Soil Consistency	K_1 (psi)	K_2 (psi)	K_3	K_4	E_{sg} (max) (psi)	E_{sg} (min) (psi)
very soft	1000	6.2	1110	0	5662	1000
medium	7680	6.2	1110	178	12,342	4716
stiff	12,340	6.2	1110	178	17,002	7605

From Fig. 13 it is seen that E_{sg} is also a function of stress state. Thus, there is an interaction between the stress transmitted to the base and to the subgrade, with the modulus of both materials fluctuating with stress state. KENLAYER performs numerous iterations to reconcile the base, subase, and subgrade moduli and stress states.

Table 16 is based on work by Thompson and Robnett (39). Note that with the exception of very soft soils, the slopes of the lines in Fig. 13 are all the same. The most significant variable is K_1. K_1 is the input in KENLAYER which sets the curve position. KENLAYER computes deviator stress, σ_d, and E_{sg} is thus determined by moving along the curve in accordance with the point where σ_d intersects. K_1 can be determined by test (resilient modulus testing of subgrade

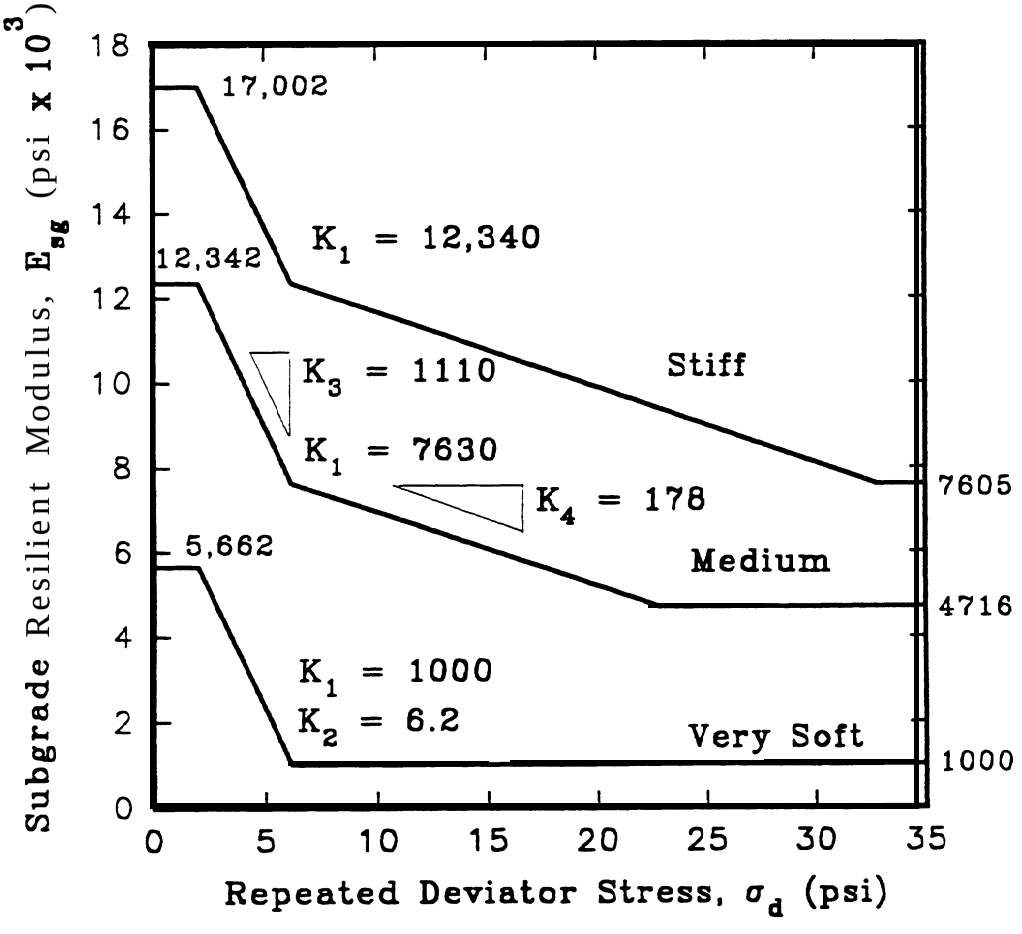

Fig. 13. Relationship of Subgrade Resilient Modulus and Deviator Stress for Three Types of Subgrade.

soil) or by approximation from the following equation (39):

$$K_1 = 3.63 + 0.1239(P_{CLAY}) + 0.4792(PI) + 0.0031(P_{SILT}) - 0.3361(GI) \quad . \quad . \quad . \quad (11)$$

where:

K_1 = resilient modulus of soil at $\sigma_d = 6.2$ psi, ksi

P_{CLAY} = material finer than 0.002 mm, %

PI = plasticity index

P_{SILT} = material between 0.05 and 0.002 mm, %

GI = group index, "new" method (infinite scale)

= $(P_{200}-35)(0.2 + 0.005(LL-40)) + 0.001(P_{200}-15)(PI-10)$ in accordance with AASHTO M145

P_{200} = material finer than #200 sieve, %

LL = liquid limit.

Thus, by performing Atterberg limits, sieve analyses, and hydrometer analyses, K_1 can be estimated. Again, K_2, K_3, and K_4 are as shown in Table 15 for any fine-grained soil.

The K_1 equation is based on a dry density equal to 95% standard proctor (T-99) maximum and at optimum moisture content (OMC). For an increase in density to 100%, an increase of about 1.4 ksi is suggested (39). For densities between 95 and 100%, Eq. 12 can be used:

P_{COMP} = in-service compaction, %.

K_1 is corrected by adding to it "Denscor". This is only done for increasing density from 95% to 100% T-99 maximum density on the dry side of OMC. If the in-service moisture content will be greater than OMC, the use of the Denscor should be omitted.

More significantly, the in-service moisture content must be estimated. An increase above OMC will reduce K_1 as follows:

$$Satcorr = 0.334\ (Sat_{OMC} - Sat_{SVC}) \quad \ldots\ldots\ldots\ldots \quad (13)$$

where:

Satcorr = correction to K_1 for increase in moisture content above OMC, ksi

Sat_{SVC} = in-service degree of saturation, at the in-service dry density, %

$$Sat_{SK} = \frac{MC_{IS}}{\frac{62.4}{(P_{comp}/100)(MDD)} - \frac{1}{sp.grav.}} \quad \ldots\ldots\ldots\ldots \quad (14)$$

Sat_{OMC} = degree of saturation at T-99 OMC, at 95% maximum standard proctor dry density, %

$$Sat_{SVC} = \frac{OMC}{\frac{62.4}{(0.95)(MDD)} - \frac{1}{sp.grav.}} \quad \ldots\ldots\ldots\ldots \quad (15)$$

MDD = maximum dry density, pcf

where moisture is in "%". Note the "dry density" may be different in Sat_{SVC}

P_{COMP} = in-service compaction, %.

K_1 is corrected by adding to it "Denscor". This is only done for increasing density from 95% to 100% T-99 maximum density on the dry side of OMC. If the in-service moisture content will be greater than OMC, the use of the Denscor should be omitted.

More significantly, the in-service moisture content must be estimated. An increase above OMC will reduce K_1 as follows:

$$Satcorr = 0.334\ (Sat_{OMC} - Sat_{SVC}) \quad \ldots\ldots\ldots\ldots \quad (13)$$

where:

Satcorr = correction to K_1 for increase in moisture content above OMC, ksi

Sat_{SVC} = in-service degree of saturation, at the in-service dry density, %

$$Sat_{SK} = \frac{MC_{IS}}{\frac{62.4}{(P_{comp}/100)(MDD)} - \frac{1}{sp.grav.}} \quad \ldots\ldots\ldots\ldots \quad (14)$$

Sat_{OMC} = degree of saturation at T-99 OMC, at 95% maximum standard proctor dry density, %

$$Sat_{SVC} = \frac{OMC}{\frac{62.4}{(0.95)(MDD)} - \frac{1}{sp.grav.}} \quad \ldots\ldots\ldots\ldots \quad (15)$$

MDD = maximum dry density, pcf

where moisture is in "%". Note the “dry density” may be different in Sat_{SVC}

subgrade.

At some point during routine design, the E_{sg} must be determined, but the use of KENLAYER may not be possible or appropriate. In this case E_{sg} can be estimated by calculating K_1 (corrected) as shown above, followed by estimation of σ_d. several options for estimation of σ_d are open. In the performance of the 237 runs of KENLAYER which represented pavement cross-sections of a range from 2 in asphalt over a 4 in base to 15 in asphalt over an 18 in base, the following σ_d values were noted: 2.1 psi minimum, 12.2 psi maximum, and 5.1 psi average. The 5.1 psi average σ_d is less than 6.2 (the "knee" in Fig. 13), thus the E_{sg} is situated on the steep-sloped portion of the curve (Fig. 13) and E_{sg} would be greater than K_1. On the other hand, by use of $\sigma_{d\ max}$ (12.2 psi), E_{sg} would be less than K_1.

When determining resilient modulus on a given curve, the following equations are useful:

$$E_{sg} = K_1(corr) + K_3(K_2-\sigma_d) \quad when\ \sigma_d < K_2 \quad (17)$$

$$E_{sg} = K_1(corr) - K_4(\sigma_d-K_2) \quad when\ \sigma_d > K_2 \quad (18)$$

where:

$K_2 = \sigma_d$ at the knee of the curve; 6.2 psi is used in KENLAYER

K_3 = upper slope of curves, 1 .110 is used in KENLAYER

K_4 = lower slope of curve, 0.178 is used in KENLAYER.

Note that E_{sg} (minimum) = K_1 when K_1 = 1000 psi or less.

The selection of 5.1 psi is the least conservative option, and Elliot (42) suggests that it is not even appropriate. Conversely, use of $\sigma_{d\ max} = 12.2$ psi may be unduly conservative. Thus, it is suggested here that a value of 6.2 psi be used and thus E_{sg} should be set at the K_1 (corrected) value. This would be considered the "normal" condition. The 1986 AASHTO Guide recommends that a further correction should be used to account for seasonal moisture changes, freezing, and length of season. This final weighted average E_{sg} ("effective resilient modulus") should be the value used in Eq. 10 for estimation of the E_g of unbound granular base material.

E_g was reconciled with θ by the method of successive approximations, as explained earlier. The entire set of results is shown in Appendix A.

Model Statistics. Once the 237 different values of E_g were calculated, a regression model was developed by use of SYSTAT. The criteria for model acceptance were as follows:

1. The highest adjusted squared multiple correlation (adj-R^2) for the models that met all the below listed criteria. This statistic reflects the overall goodness of fit of the equation. It describes how well an equation will predict a population of data, not the sample data. Thus it is usually a little lower than the R^2 value,, which is for the sample data. The adjusted R^2 for the model chosen was 0.909
2. The standard error of estimate was low compared to the mean resilient modulus ($\bar{Y}$): The SEE was 0.070 and the mean log E_g was

3.591.

3. The analysis of variance F-statistic indicated that the relationship was significant at the 0.01 level.
4. Residuals were normally distributed.
5. Residuals had constant variance.
6. All members of the population were described in the same model.
7. No serious problems of variable collinearity existed.
8. No single observation influenced the regression coefficients excessively.
9. Each independent variable contributed significantly to the model.

The relationship of observed E_g (calculated from KENLAYER) and E_g estimated from Eq. 10 is shown in Fig. 14.

Usage. Eq. 10 can be used by the designer to approximate E_g of granular material which is functioning either as a base under an asphalt layer or as a subbase under an asphalt surface layer and a bituminous base layer. If the latter is the case, E_1 should represent a combination of the two asphalt bound layers (E_{eq}) as follows:

$$E_{eq} = \left[\frac{D_{1a}(E_{1a})^{0.333} + D_{1b}(E_{1b})^{0.333}}{D_{1a} + D_{1b}}\right]^3 \quad \text{(19)}$$

where:

E_{eq} = combined modulus of both asphalt bound layers

E_{1a} = modulus of the asphalt surface layer, psi

D_{1a} = thickness of the asphalt surface layer, in

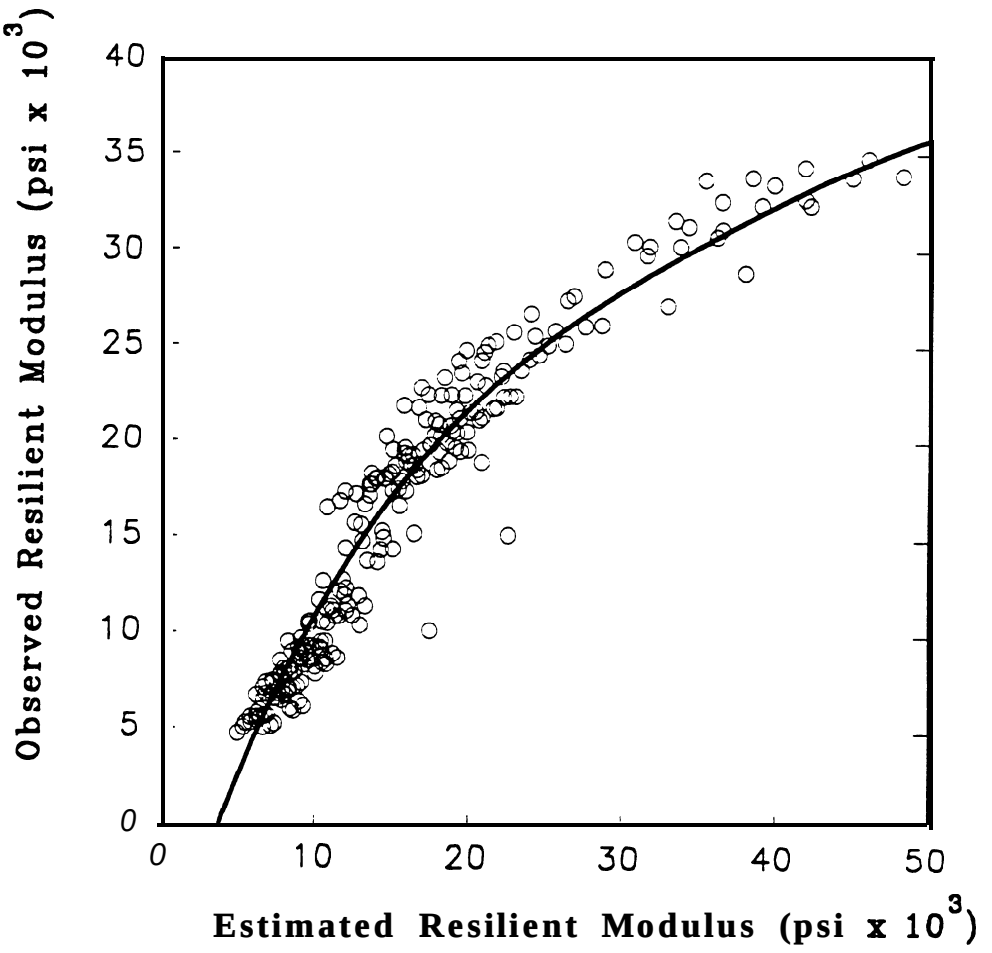

Fig. 14. Observed vs. Estimated Resilient Modulus of Unbound Granular Material.

E_{1b} = modulus of the asphalt base layer, psi

D_{1b} = thickness of the asphalt base layer, in.

So, to use Eq. 10, the designer should:

1. Assume a D_1 and D_2 for a particular trial.
2. Determine E_1 by either test or by the approximation technique detailed in Volume I knowing mixture design characteristics and approximate pavement temperature.
3. Calculate E_{sg} from the procedure given above.
4. Determine k_1 of the granular material by test or by assumption (see Table 15).

Other trials of cross-section would only entail further assumptions of D_1 and D_2.

Once E_g is determined, it can be converted to a layer coefficient a_2 or a_3 as shown in the next section.

Effects of Pavement Cross-section and Material Variables

As can be seen from Fig. 15, E_g increases with a decrease in asphalt layer thickness or stiffness. This is because higher stress is transferred to the base layer which increases E_g. Fig. 16 shows that as E_{sg} increases, bulk stress in the base increases which increases E_g. As compactive effort increases, k_1 increases, and thus E_g increases. And in Fig. 17 it is seen that an increase in base thickness has only a small effect on base E_g (taken as a whole).

Summary

To obtain layer coefficients, the E_g of the granular material must be

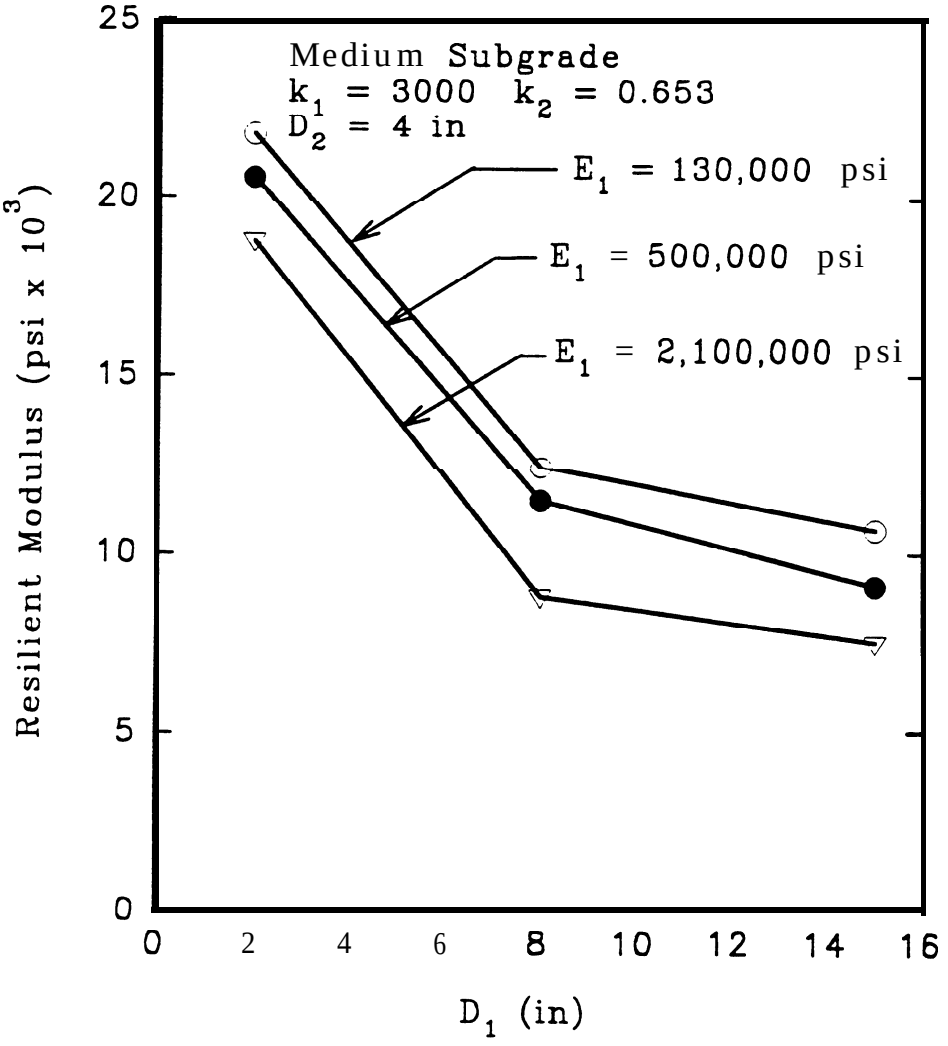

Fig. 15. Effect of Asphalt Layer Thickness and Stiffness on Base Resilient Modulus.

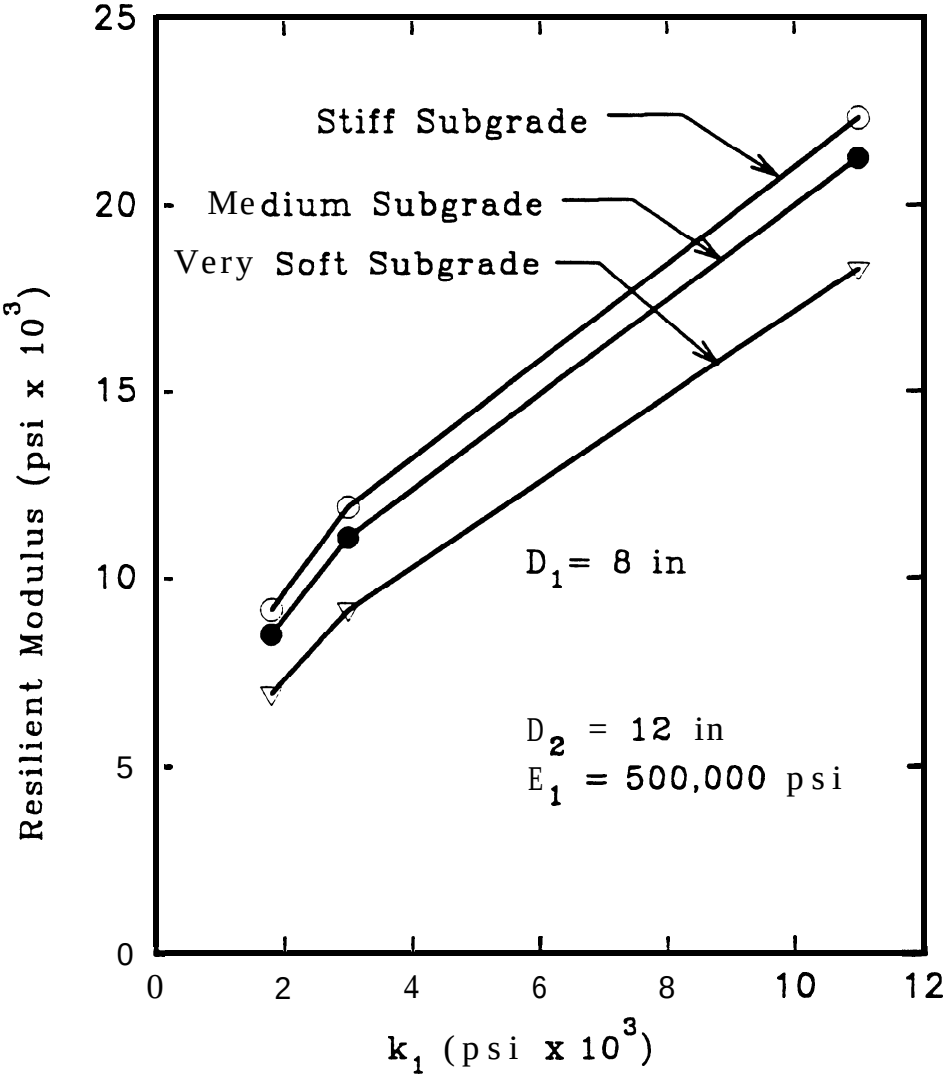

Fig. 16. Effect of Granular k_1 and Subgrade Stiffness on Base Resilient Modulus.

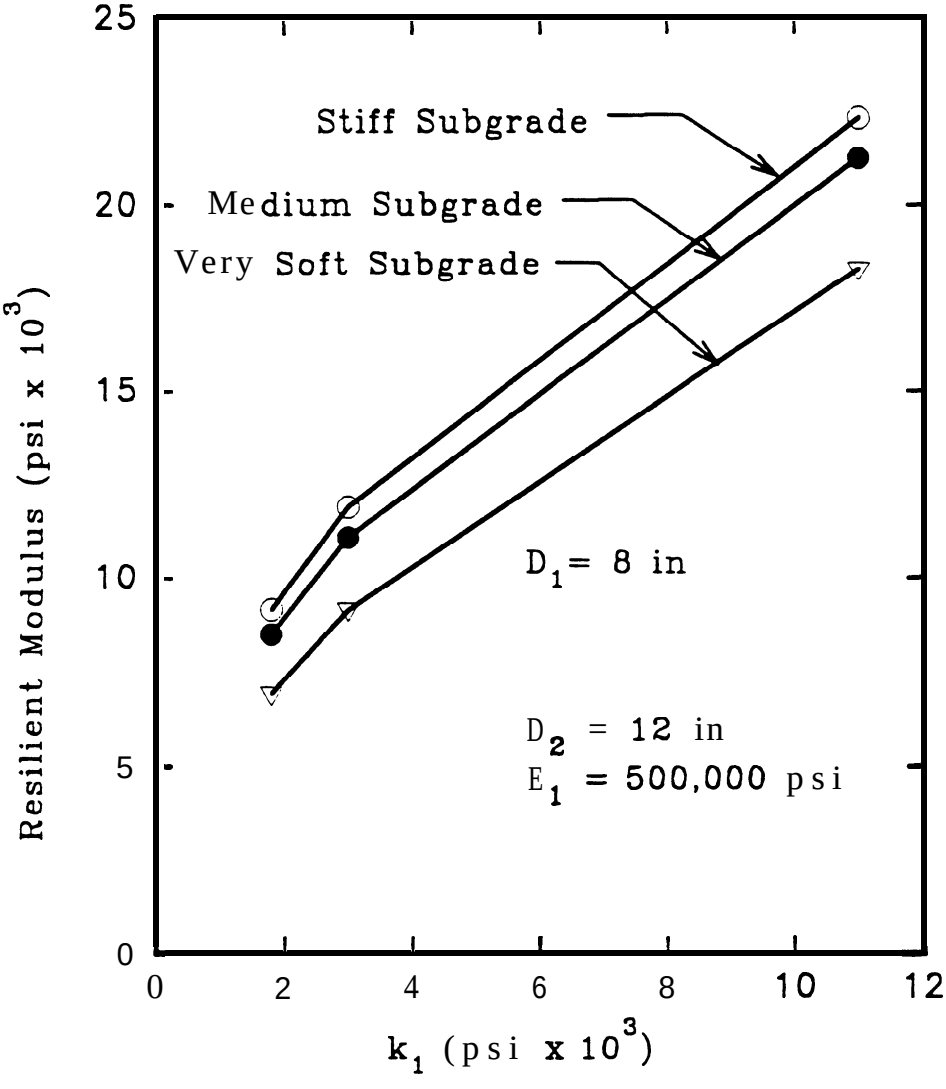

Fig. 16. Effect of Granular k_1 and Subgrade Stiffness on Base Resilient Modulus.

determined. This can be done in two ways. The most accurate way is to run, say, 14 E_g tests at different θ values and define the E_g-θ relationship (Fig. 7). Then, θ must be determined from a program such as KENLAYER, knowing D_1, E_1, D_2, and E_{sg} (E_{sg} can be determined by test or by estimation). Finally, knowing θ, E_g is determined from the E_g-θ relationship. The second method is to estimate E_g from Eq. 10 by knowing, as above, D_1, E_1, D_2, and E_{sg}. Additionally, k_1 must be estimated -- hence the lesser accuracy of this second method.

DETERMINATION OF LAYER COEFFICIENTS

Matching Layer Coefficient with Layer Position

When designing a pavement, values of a,, a_2, a_3, D_1, D_2 and D_3 must be assigned. In this study, the development of layer coefficients was done with the assignment of the definitions of layer variables, as shown in Fig. 12. Note that for asphalt bound layers, a, and a_2 are determined from the procedures given in Volume I of this study (12). The drainage coefficients m_2 and m_3 are determined from the procedures given in the companion study to this report (2). The layer coefficients a_2 and a_3 for unbound materials are determined in accordance with the procedures developed below,

AASHTO Nomographs

The nomographs available in the 1986 Guide (1) as shown in Fig. 18 and 19 relate layer coefficients a_2 and a_3 to base or subbase resilient modulus (E_{gb} or E_{gsb}) as per the following (10):

$$a_2 = 0.249 \log E_{gb} - 0.977 \quad \text{. . . . . (20)}$$

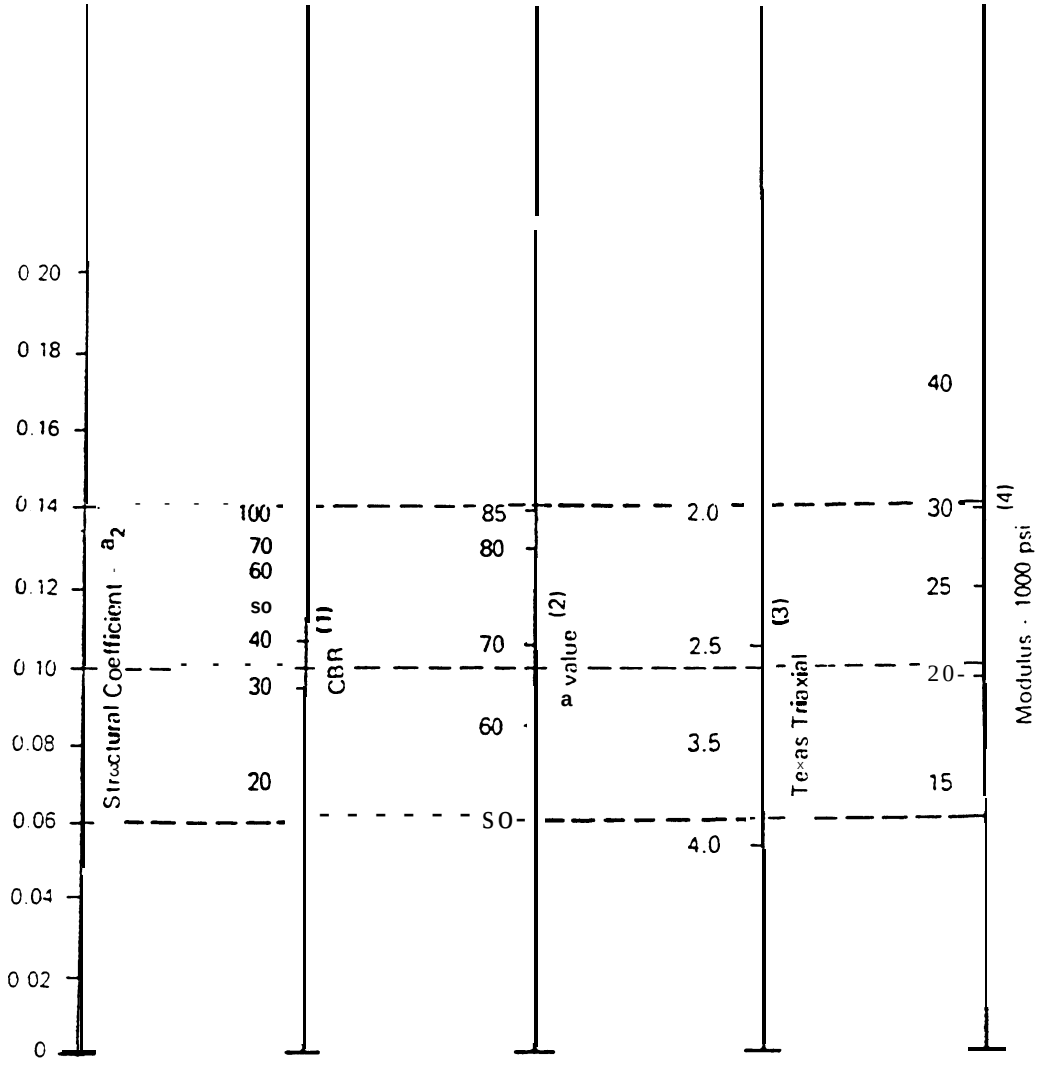

(1) **Scale derived by averaging correlations obtained from Illinois.**
(2) Scale **derived by averaging correlations obtained from** California, **New** Mexico and **Wyoming.**
(3) **Scale derived by** averaging **correlations** obtained **from** Texas
(4) **Scale derived on** NCHRP **project** *(3).*

Fig. 18. **AASHTO** Unbound Granular Base Layer Coefficient (a,> **Nomagraph.**

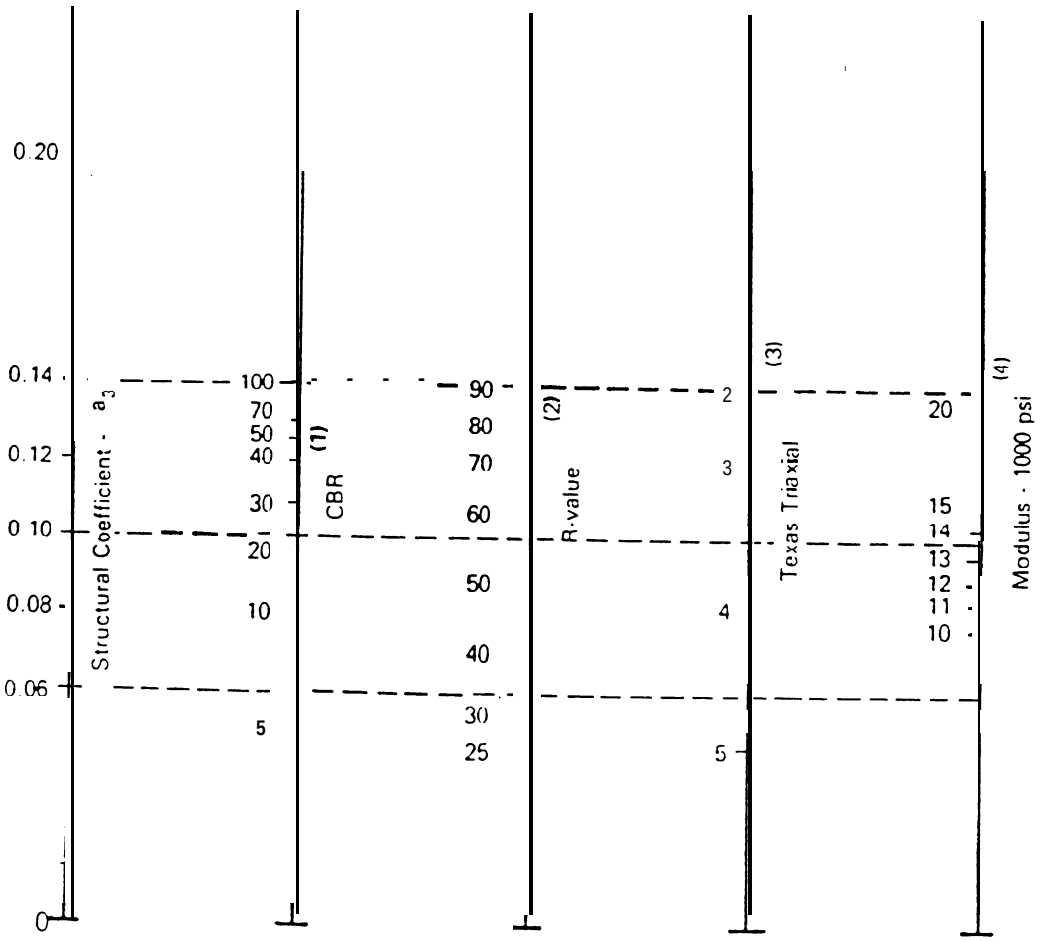

(1) Scale derived from **correlations from** Illinois.

(2) Scale derived from **correlations obtained from** The **Asphalt** Institute, California, New Mexico **and Wyoming.**

(3) **Scale** derived **from correlations** obtained **from Texas.**

(4) **Scale** derived on NCHRP project *(3).*

Fig. 19. AASHTO Unbound Granular Subbase Layer Coefficient **(a_3) Nomagraph.**

$$a_3 = 0.227 \log E_{gsb} - 0.839 \quad \ldots\ldots\ldots\ldots\ldots \quad (21)$$

Once the E_g value for a given situation is known, either by test or by use of Eq. 10, a_2 or a_3 can be easily calculated from Eqs. 20 or 21, or the AASHTO nomographs.

Eq. 10 was developed with degrees of saturation of $\leq 60\%$. The effects of a variation in degree of saturation are addressed through the use of drainage (m) coefficients. The determination of m-coefficients is the subject of the companion project to the present study (2).

Equivalent Stiffness

Introduction. A second method of calculating layer coefficients was by use of Odemark's transformation. As was done in Volume I of the study with the asphalt mixtures (12), stiffnesses (in the form of resilient modulus) of MHTD aggregate types were related to the modulus of the Road Test base material at various stress states. Layer coefficients were calculated from Eq. 2:

$$a_n(MHTD) = a_n(AASHO) \left[\frac{E_g(MHTD)}{E_g(AASHO)} \right]^{1/3} \quad \ldots\ldots\ldots \quad (2)$$

Three variables are required to solve Eq. 2: a_2 or a_3 (AASHO), E_g (MHTD), and E_g (AASHO). These were determined as follows: 1) The layer coefficient a_2 for unbound crushed stone base at the Road Test is reported in the literature as 0.14. 2) The value for E_g (MHTD) will vary with several factors. E_g can be determined by *test* or from Eq. 10. Knowledge of the stress state (or pavement

geometry/load condition) is necessary to determine E_g. For the present analysis, the stress state for the average Road Test section was determined and used in Eq. 2 for both MHTD and AASHO E_g values. 3) The E_g (AASHO) was determined as follows.

Road Test Modulus. In the AASHTO Guide (1), Fig. 2.6 gives a relationship between a_2 and resilient modulus. It states that the basis of the nomograph is a_2 = 0.14 at E_g = 30,000 psi. The question is, where did the 30,000 psi value come from? First, a search of the literature was made. In the Guide, an equation was given to be used in lieu of the nomograph which has been presented earlier in this study. The reference given is Rada and Witczak (10). However, Rada and Witczak state that the equation was based on the nomograph. Thus, it seems that Rada and Witczak either found the source of the nomograph (but did not elaborate on it) or they just calculated the equation from the nomograph. Apparently they did not originate the nomograph. In the Guide (1), Appendix GG is referenced as a source for an explanation of the origin of the layer coefficients. A reading of Appendix GG reveals no such explanation. However, it is stated that Road Test moduli varied from 15,000 to 30,000 psi. It does not state the origin of these data. The nomograph is shown with E_g = 30,000 psi corresponding to a_2 = 0.14. The reference is given as NCHRP 128 (6). NCHRP 128 states that elastic values for all the Road Test materials were assigned on the basis of four references: Seed et al. (43), Shook and Fang (44), Coffman et al. (45), and Skok and Finn (46). State DOT studies of layer coefficient derivation are described in

Appendix C of NCHRP 128. Very few are actually referenced, indicating that they were unpublished internal reports. Apparently none involved resilient modulus testing. Of the four references mentioned above, Seed et al. dealt with soil, Shook and Fang reported index tests and so forth, but no resilient modulus testing, and Coffman et al. tested static triaxial properties of Road Test granular materials and estimations of dynamic properties. No estimations of dynamic modulus exceeded 20,000 psi, and for Road Test vehicle speeds, from the authors' calculations it appears that the base and subbase E_g would have been considerably lower than 20,000 psi. Skok and Finn summarized other studies. In their paper, it appears that a value of 15,000 psi was assigned to the Road Test base based on plate load tests. Skok and Finn emphasized that this was very approximate. So, references tied to NCHRP 128 do not shed light on the matter. The question remained - where did the 30,000 psi value come from? Several sources or methods of calculation were explored as follows.

NCHRP 291. Pursuing the question of the base modulus further, several references were found to aid in calculation of Road Test E_g. In the AASHTO Guide, the value for the gravel subbase was given as 15,000 psi. It was stated that E_g values came from NCHRP 291(21). NCHRP 291 stated that the Road Test base and subbase were tested by the Asphalt Institute, but no reference is given. Apparently, this is another internal report. The testing was done under conditions of low moisture, medium moisture, and high moisture. Although test data were not given, Table 17 is a summary of the seasonal moduli equations that were

presented. For some unstated reason, September was omitted. Neither seasonal moduli nor an overall single modulus were given. Thus, to compute the Road Test moduli, in the present study elastic layer analysis was used to calculate the seasonal moduli from the given equations. By use of the program ELSYM 5 (47), numerous iterations were run for each season to reconcile the stress state (Θ) and modulus values. ELSYM 5 allowed the use of the subgrade modulus model shown in Table 17. To perform the analysis, an average pavement cross-section and a representative load application were used. This is shown in Fig. 20.

Table 17. Elastic Moduli/Equations for AASHO Road Test Materials.

Material	Seasonal Moduli/Equations (psi)			
	Dec-Feb	Mar-Apr	May-Aug	Sept-Nov
Asphalt Concrete, E_1	1.7×10^6	0.71×10^6	0.23×10^6	0.45×10^6
Base, E_{gb}	50,000	$3200\ \Theta^{0.6}$	$3600\ \Theta^{0.6}$	$4000\ \Theta^{0.6}$
Subbase, E_{gsb}	50,000	$4600\ \Theta^{0.6}$	$5000\ \Theta^{0.6}$	$5400\ \Theta^{0.6}$
Subgrade, E_{sg}	50,000	$8000\ \sigma_d^{-1.06}$	$18{,}000\ \sigma_d^{-1.06}$	$27{,}000\ \sigma_d^{-1.06}$
Note: σ_d = deviator stress, psi				

From the Road Test reports (3), the average thickness for asphalt surface plus binder, crushed stone base, and gravel subbase were calculated from the main factorial study loop sections. The load application details (18 k SAL, 2 tires, tire spacing, tire pressure) were taken from NCHRP 128 and Witczak (48). Poisson's

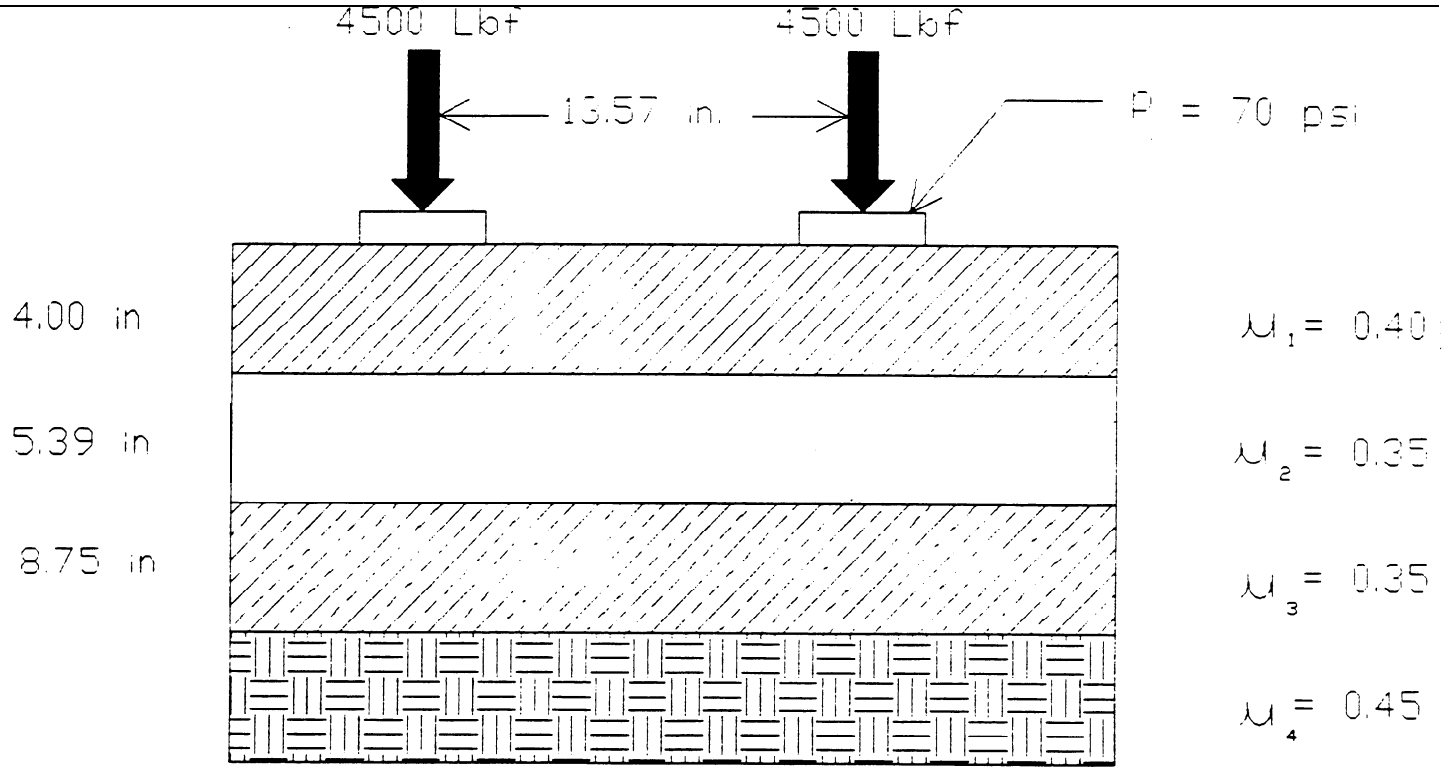

Fig. 20. Average AASHO Road Test Cross Section.

ratios for each material were taken from Appendix DD of the AASHTO Guide. From all this, the seasonal moduli and bulk stress values were calculated, and are shown in Table 18. Winter moduli were assumed to be 50,000 psi for the base, subbase, and subgrade in NCHRP 291 . Assuming September should be included with October and November, the average moduli for each material (weighted for the number of months per season) were calculated and are shown in Table 18. As can be seen, even with the inclusion of September into the highest modulus season and assuming a frozen base in winter, the base modulus is still only 25 to 26,000 psi, not 30,000. In this analysis, the subbase seems high at 24,000, and the subgrade seems very high at 17,000. Most references place the AASHO Road Test soil at 3000 to 5000 psi. Use of KENLAYER puts it at 5543 psi. So, inclusion of frozen conditions seems questionable. Thus, the average moduli (and stress states) were recalculated, omitting the frozen months. These somewhat lower values are shown in the right-hand column in Table 18. The subgrade (5800 psi) seems much more reasonable. The subbase (15,000 psi) now lines up with that which was stated in the AASTHO Guide. However, the base is 18,000 psi, only 60% of the reported 30,000.

Table 18. Seasonal Moduli/Bulk Stress of AASHO Road Test Materials.

Material	Seasonal Moduli/Bulk Stress (psi)					
	Dec-Feb	Mar-Apr	May-Aug	Sept-Nov	Weighted Average	Weighted Average *
Asphalt Concrete	1,700,000	710,000	230,000	450,000	732,000	732,000
Base	50,000	12,000	19,000	20,000	26,000	18,000
Subbase	50,000	11,000	16,000	17,000	24,000	15,000
Subgrade	50,000	3200	5500	8000	17,000	5800
Base Θ	--	9.2	16.3	14.2	--	14.0
Subbase Θ	--	4.3	6.8	6.6	--	6.2
σ_d	--	2.37	3.06	3.15	--	2.94

* Excluding winter values.

The results of Road Test trench studies (50) indicated that the average moisture content of the crushed stone base was 4.3% (0.1% above T-99 optimum). NCHRP 291 considered optimum moisture content as “moist” (as opposed to “dry” or “wet”) and from Table 17, “moist” test results indicate k_1 = 3600 psi. At Θ = 14 psi (see Table 17), this corresponds to an E_g = 18,000 psi. The average moisture content of the gravel subbase was 5.65%, which was considerably higher (for a granular material) than the optimum of 3.8%. Thus this could be considered either “moist” or “wet” with corresponding k_1 values of 4600 or 5000 psi. The corresponding E_g values at Θ = 6.2 are 14,000 and 15,000 psi, respectively.

Traylor. Traylor (49) tested the Road Test base material and reports moduli relationships as shown in Table 19. Traylor measured the base and subbase moisture contents as 4.3 and 5.7%, respectively, which compares favorably with Road Test trench studies. Thus, at these average conditions, from Table 19 it appears that the average base modulus would be about 27,000 psi and the subbase would be about 11,000 psi. Traylor also tested the subgrade for moisture and E_{sg}. The average moisture content was 15.8% and the average E_{sg} was 3472 psi. The AASHO Road Test subgrade T-99 optimum moisture content was 13.3%. Road Test trench studies showed the average subgrade moisture in the top 4 in to be 16.6%.

Table 19. AASHO Road Test Moduli from Traylor.

	Moisture contents, %			
	4.0	5.5	7.0	Road Test
Base				
Equation	$10{,}360\ \Theta^{0.35}$	$11{,}795\ \Theta^{0.34}$	$2850\ \Theta^{0.62}$	$*10{,}647\ \Theta^{0.35}$
E_{gb}, psi				26,815
Subbase				
Equation	$6840\ \Theta^{0.32}$	$6270\ \Theta^{0.30}$	$4075\ \Theta^{0.40}$	$**6270\ \Theta^{0.32}$
E_{gsb}, psi				10,839

* interpolated k_1 and k_2 at moisture = 4.3%; Θ = 14.0 psi

** at moisture = 5.5%; Θ = 6.2 psi

NCHRP 128. Fig. 18 of NCHRP 128 indicates that, from an elastic layer analysis for E_1 = 450,000 (the given value) psi and D_1 = 4 in., E_{gb} equals 30,000 psi.

The analysis is based on equivalent sections which render equal vertical subgrade compressive strain.

KENLAYER. In the present study, KENLAYER was used to calculate E_{gb} and E_{gsb}. Input included E_1 = 656,800 psi (best estimation of Road Test average asphalt layer, in accordance with Vol. I of this report), k_1 = 10,647 psi and k_2 = 0.35 for the base (as per Traylor), k_1 = 6270 psi and k_2 = 0.32 for the subbase, and K_1 of the subgrade = 5619 psi. K_1(corr) was calculated from Eqs. 16 with the following input from Road Test data:

Table 20. Road Test Data Input to KENLAYER.

Parameter	Value
minus #200, %	81
Liquid limit	29
PI	13
GI (new)	8.6
amount clay, %	15.3
amount silt, %	27
average compaction, %	97.7
avg. max. dry density, pcf	116.4
97.7% max. dry density, pcf	113.7
95% max dry density, pcf	110.6
optimum moisture content, %	15.1
Specific gravity	2.71
average in-service moisture, %	16
calculated K_1, psi	8759
K_1 (corrected), psi	5619

The analysis is based on equivalent sections which render equal vertical subgrade compressive strain.

KENLAYER. In the present study, KENLAYER was used to calculate E_{gb} and E_{gsb}. Input included E_1 = 656,800 psi (best estimation of Road Test average asphalt layer, in accordance with Vol. I of this report), k_1 = 10,647 psi and k_2 = 0.35 for the base (as per Traylor), k_1 = 6270 psi and k_2 = 0.32 for the subbase, and K_1 of the subgrade = 5619 psi. K_1(corr) was calculated from Eqs. 16 with the following input from Road Test data:

Table 20. Road Test Data Input to **KENLAYER.**

Parameter	Value
minus #200, %	81
Liquid limit	29
PI	13
GI (new)	8.6
amount clay, %	15.3
amount silt, %	27
average compaction, %	97.7
avg. max. dry density, pcf	116.4
97.7% max. dry density, pcf	113.7
95% max dry density, pcf	110.6
optimum moisture content, %	15.1
Specific gravity	2.71
average in-service moisture, %	16
calculated K_1, psi	8759
K_1 (corrected), psi	5619

Table 21. Subgrade Rutting Prediction.

E_{gb} (psi	D_2			
	5.39 in		14.14 in	
	ϵ_v	N_{fr}	ϵ_v	N_{fr}
5,000	0.001162	18,802	0.0009997	36,884
10,000	0.001127	21,561	0.0007064	174,555
30,000	0.0009577	44,686	0.0003814	2,756,077
Note: $D_1 = 4$ in, $E_1 = 450{,}000$ psi				

To examine the effect on pavement life from a decrease in base layer coefficient in accordance with the AASHTO structural number equation, the following analysis was performed.

The basic design equation in the 1986 AASHTO Guide was used to back-calculate SN values:

$$\log w_{18} = Z_R S_0 + 9.36 \log (SN+1) - 0.20 + \frac{\log\left[\frac{\Delta PSI}{42.-2.5}\right]}{0.40 + \frac{1094}{(SN+1)^{5.19}}} + 2.32 \log E_{sg} - 8.07 \quad (23)$$

where:

W_{18} = number of 18k ESAL (500,000; 50,000; 5000)

S_0 = overall standard deviation (0.45)

Z_R = statistic related to reliability (0.000 was used which represents 50% reliability)

SN = structural number

Δ PSI = loss of Present Serviceability Index (4.2 to 2.5 was used)

E_g = roadbed resilient modulus (3000 psi).

Then, knowing Road Test average layer thicknesses, the following was used to back calculate a_2 values:

$$a_2 = \frac{SN - a_1 D_1}{D_2} \quad \ldots\ldots\ldots\ldots\ldots\ldots \quad (24)$$

where:

a_1 = 0.44 (Road Test asphalt layer coefficient)

D_1 = 4 in (average Road Test asphalt layer thickness)

D_2 = 14.14 in (average Road Test total granular material thickness).

From the AASHTO a_2 nomograph knowing a_2 values, E_{gb} values were obtained. The results of this analysis is shown in Table 22.

Table 22. Backcalculation of a_2 Values.

N_{18} (18k SAL)	SN	a_2*	E_{gb}** (psi)
500,000	3.6	0.140	30,000
50,000	2.5	0.052	13,568
5,000	1.7	-0.004	8065

* Backcalculated from Eq. 24
** Backed out of nomagraph

As can be seen, when modulus is reduced nearly an order of magnitude, the allowable traffic diminishes by about two orders of magnitude. Table 21 tends to

SN = structural number

Δ PSI = loss of Present Serviceability Index (4.2 to 2.5 was used)

E_g = roadbed resilient modulus (3000 psi).

Then, knowing Road Test average layer thicknesses, the following was used to back calculate a_2 values:

$$a_2 = \frac{SN - a_1 D_1}{D_2} \quad \ldots\ldots\ldots\ldots\ldots\ldots \quad (24)$$

where:

a_1 = 0.44 (Road Test asphalt layer coefficient)

D_1 = 4 in (average Road Test asphalt layer thickness)

D_2 = 14.14 in (average Road Test total granular material thickness).

From the AASHTO a_2 nomograph knowing a_2 values, E_{gb} values were obtained. The results of this analysis is shown in Table 22.

Table 22. Backcalculation of a_2 Values.

N_{18} (18k SAL)	SN	a_2*	E_{gb}** (psi)
500,000	3.6	0.140	30,000
50,000	2.5	0.052	13,568
5,000	1.7	-0.004	8065

* Backcalculated from Eq. 24
** Backed out of nomagraph

As can be seen, when modulus is reduced nearly an order of magnitude, the allowable traffic diminishes by about two orders of magnitude. Table 21 tends to

Conclusions

It is recommended that layer coefficients a_2 and a_3 can be obtained by 1) solution for E_g via Eq. 10 or by use of KENLAYER and then 2) solution for a_2 and a_3 by AASHTO nomographs or Eqs. 20 or 21.

CEMENT-TREATED BASE

INTRODUCTION

The third part of this study was to determine layer coefficients for cement-treated soil base. The analysis is based upon the static compressive chord modulus test as recommended by the 1986 AASHTO Guide (1). A secondary goal was to develop a regression equation to assist in the estimation of static modulus for the soils analyzed in this report. Once the modulus is determined, the layer coefficient (a_2) can be obtained directly from the base layer nomograph contained in the 1986 AASHTO Guide.

As with portland cement concrete, the magnitude of compressive chord modulus of soil-cement materials is related to unconfined compressive strength. Thus, factors that affect compressive strength will likely affect compressive chord modulus. These factors include gradation (material retained on #4 sieve, material finer than the #270 sieve, and material retained between #270 sieve and 0.005 mm), dry density, plasticity index, and cement content.

MATERIAL TYPES AND SOURCES

Two soils were chosen by MHTD personnel to be stabilized with portland

cement. The Lintonia (DR-16) is a fine sand, whereas the Knox (DR-17) is a clayey silt. It was intended that the Knox was to be mixed with Missouri River sand (DR-17s). All materials were sampled and delivered to the UMR laboratory by MHTD personnel.

The materials, sources, and identification codes are shown in Table 24.

Table 24. Material Types and Sources.

Nomenclature	Material	Sources	Location
DR-16	Lintonia Soil	--	Malden
DR-17	Knox soil	--	Callaway Co.
DR-17s	Missouri River Sand	Capitol City Sand	Jefferson City
DR-18	Portland cement, Type I	Monarch Cement	--
Note: All sources are located in Missouri			

LABORATORY INVESTIGATION

Soil Classification

The three materials were classified by utilizing results of washed sieve analyses and index testing. The results are shown in Table 25.

Experimental Material Proportions and Moisture Density Relationships

To reflect the significance of compressive strength on static modulus, each soil-cement mixture was tested at three cement contents. Additionally, the DR-17 soil was mixed with the DR-17s sand. Records supplied by the MHTD indicated that a reasonable spread of soil-sand proportions would include 23, 30, and 37% soil content. Because essentially all the DR-17 soil passed the #200 sieve and

Table 25. Soil Classification.

Sieve Size	DR-16 % passing	DR-17 (soil) % passing	DR-17s (sand) % passing
3/8 in.	100.0	100.0	100.0
#4	100.0	100.0	98.5
10	100.0	100.0	79.9
40	97.1	99.9	16.0
60	43.6	99.8	5.1
200	3.6	99.2	0.3
270	3.4	98.2	0.2
0.005 mm	--	34.0	--
0.002 mm	0.3	30.0	0
ASG	2.652	2.74	2.547
LL	--	42	--
PI	NP	18	NP
Classification	A-3	A-6	A-3

virtually all of the DR-17 sand was retained on the #200 sieve, this meant that the percent passing the #200 sieve for the three mixtures would be 23, 30 and 37%. The gradations, Atterberg limits, and AASHTO soil classifications are shown in Table 26. Also shown are the results of gradation curve characterization via Hudson's $\bar{A}$ and the slopes-of-gradation curve calculations. These were used later in the regression analysis portion of the study. Calculation of Hudson's $\bar{A}$ and the slopes was discussed earlier in the unbound aggregate section. However, different sieve sizes were used for the soil/sand mixtures to better reflect their gradation

Table 26. **Soil/Sand** Mixture Characteristics.

Sieve Size	23/77	30/70	37/63	DR 16
1½ in	100	100	100	100
3/4	100	100	100	100
3/8	100	100	100	100
#4	99	99	99	100
8	88	89	so	100
16	69	71	73	99
30	46	50	54	98
50	30	36	42	70
100	26	31	38	21
200	23	30	37	4
$\bar{A}$	6.81	7.06	7.33	7.92
M_{4-10}	0	167.1	153.1	136.7
M_{10-40}	33.9	574.8	510.6	469.7
M_{40-200}	1092.4	143.7	130.9	123.8
LL	34	35	35	--
PI	17	17	18	--
GI	1	1	2	0
Soil Classification	A-2-6	A-2-6	A-6	A-3

curve shapes.

The **PCA** Soil-Cement design manual **(51)** (tempered with **MHTD** experience) indicated that for preliminary purposes, the amount of cement for the **DR-1 6** and **DR-1** 7 combination materials should be 9 and **8%,** by dry weight of soil or soil-sand, respectively. Consequently, **T-99 moisture-density relationships were**

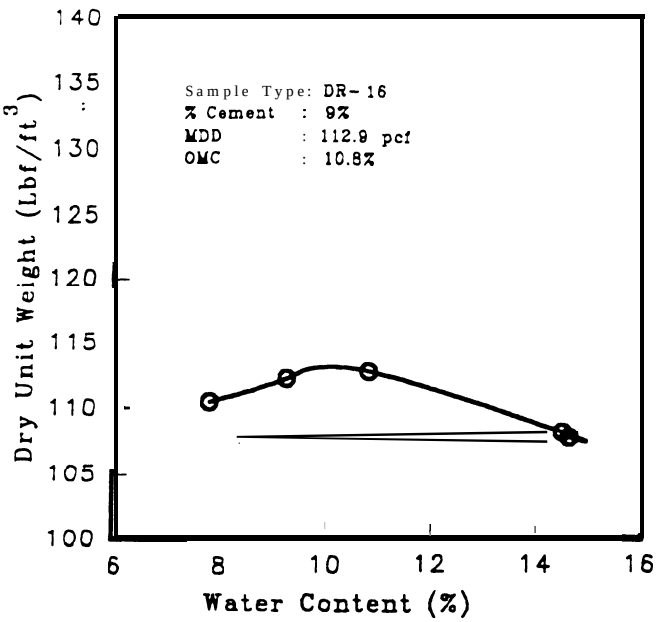

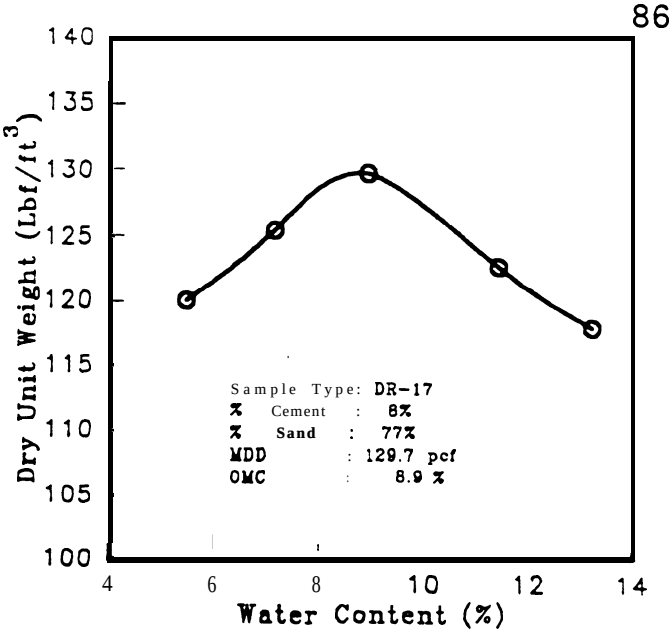

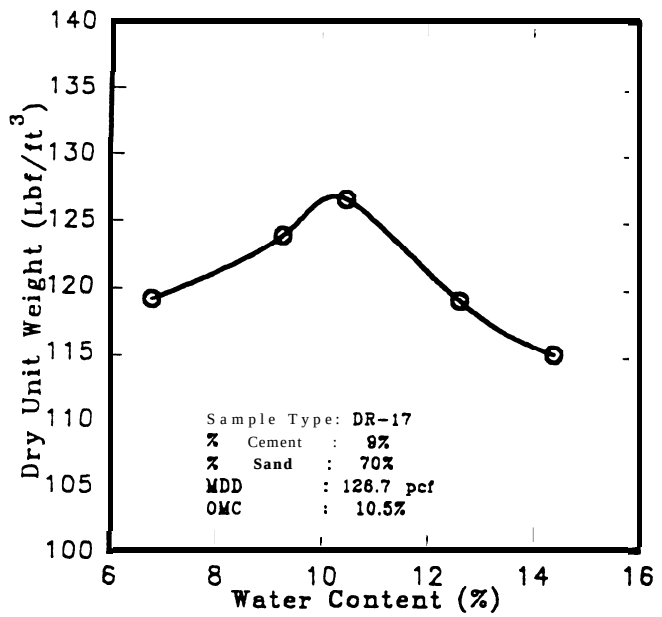

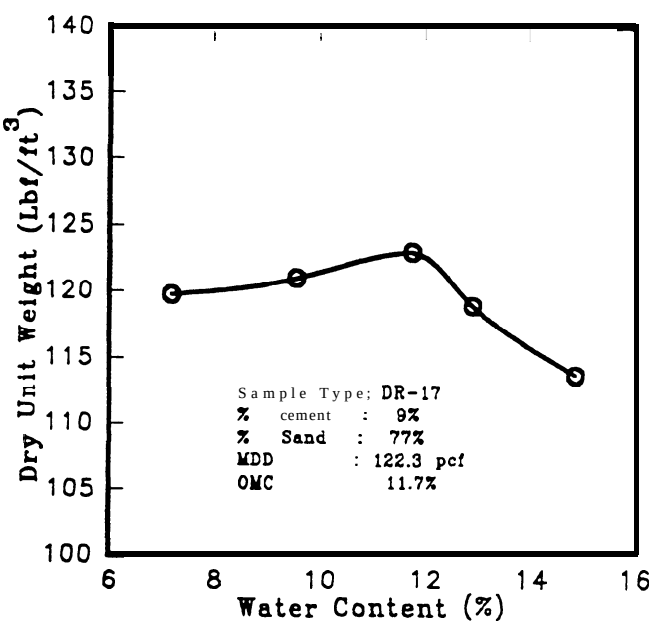

Fig. 21. Soil Cement Material Moisture-Density Relationships

determined for the DR-16, DR-17 (23/77), DR-17 (30/70), and DR-17 (37/63) materials. The results are shown in Fig. 21. As expected, for soil/sand mixtures (DR17), the more granular the material, the higher the dry density and the lower the optimum moisture content.

In the final cement content determination, Table 2 of the PCA manual indicates that the DR-16 soil should contain 9% cement. However, in the PCA manual, Fig. 36 indicates 10%. MHTD records indicated that 6.9% has been specified. Consequently, to cover this range, three sets of specimens were made with cement contents of 6, 8, and 10%. For the DR-17 (23/77), DR-17 (30/70), and DR-17 (37/63) mixtures, the PCA Table 2 indicates cement requirements of 5, 5, and 6% respectively. PCA Fig. 36 indicates 6, 6, and 7%, while MHTD records show 4 to 10% recommended or specified, with 7.4% as the most recent and most similar in density to materials used in this study. Thus, mixtures were prepared with 5, 7, and 9% cement. in Table 27 is shown the mixture proportion schedule.

Table 27. Soil-Cement Mixtures.

% Cement	DR-16	DR-17		
		(23/77)	(30/70)	(37/63)
5		X	X	X
6	X			
7		X	X	X
8	X			
9		X	X	X
10	X			

Specimen Fabrication

For the DR-17 (23/77) and DR-17 (30/70) materials, the material for four replicate specimens was prepared by adding the amount of water necessary to bring the cement, soil (and sand) mixture to its optimum moisture content (as determined by the T-99 analysis), and mixing in a Lancaster counterflow 3.0 cu ft mixer. Subsequently, for the rest of the specimens, the material was dry mixed in the mixer for better mixture control. Then for each lift, the amount of water necessary to bring the mixture to its optimum content was added. A representative sample was taken for moisture determination.

Specimen size and method of compaction were two factors that had to be considered. Several mold diameters and height-to-diameter ratios are presented in the literature (51-52). When measuring modulus, height-to-diameter ratios of 2.0 are usually used; this was the case in this study. Specimens were 6 in in diameter. The most common method of compaction is an impact type similar to the T-99 standard effort. This method was used in the present study, with additional effort via vibration by air hammer and plate to bring each lift to its required density. The specimens were compacted into steel split molds with a 5.5 lb hammer and a 12 in drop. Each layer received a varying number of blows which resulted in a compaction effort similar to the T-99 effort. Specimens were compacted at optimum moisture content to 100% maximum dry density as determined by the T-99 analysis. After compaction, the specimens were placed in a moist room at 73°F, then demolded. The DR-17 specimens were demolded after

two days, while the DR-1 6 specimens were demolded after three days because of their more fragile nature. After a total of seven days moist curing, the specimens were removed from the moist room and capped with a proprietary sulfur compound. Two replicate specimens were made for modulus testing and one for compression testing, then one or both of the modulus specimens were also tested in compression.

Unconfined Compressive Strength

Each strength specimen was tested for ultimate compressive strength in a 200,000 lb Tinius-Olsen compression machine in accordance with AASHTO T 22-90 (53). The results of the replicate specimens were used for determination of the modulus test load for each soil-cement mixture. Also, the results were used in the modulus regression equation which was developed from the data.

Modulus of Elasticity

The chord modulus of elasticity was determined as per ASTM C469-87a (54). In brief, each specimen was capped with a proprietary sulfur compound. A compressometer yoke was mounted on the specimen which held an LVDT (linear variable differential transducer) for measurement of vertical deformation. The gage length of the specimen was 8 in. A pressure transducer measured pressure which was then converted to load and displayed on a digital display. The load and deformation conditioned signals were transmitted to an IBM XT via a 12 bit analog/digital board and stored in an ASCII file. The data file was then loaded into QUATTROPRO (55) where the load and deformation data was parsed and

converted to stress and strain. The stress and strain data were then loaded into the data-fitting program TABLECURVE (56). A best-fit line was fit through the data. The chord modulus was calculated by determining the x-y coordinates of two points on the curve: 1) the load at 0.000050 strain, and 2) the load and strain at 40% ultimate compressive strength. Two load runs were made and thus the modulus was determined twice for each specimen ; then the results were averaged. The modulus was calculated as follows:

$$E_c = \frac{\sigma_1 - \sigma_2}{\epsilon_1 - \epsilon_2} \quad \ldots\ldots\ldots\ldots\ldots\ldots \quad (25)$$

where:

E_C = chord modulus, psi

σ_1 = 40% of ultimate strength, psi

σ_2 = stress at 0.000050 in/in strain

ϵ_1 = strain at σ_1, in/in

ϵ_2 = 0.000050 in/in.

The equipment is shown in Fig. 22.

RESULTS OF LABORATORY INVESTIGATION

Results of the compressive strength and modulus testing are shown in Table 28. As can be seen, both strength and modulus increased with increasing cement content. Also, as sand content of the DR-17 specimens increased, strength and modulus increased. This is shown in Figs. 23 through 25. The relationship between strength and modulus is shown in Figs. 26 and 27. The best-fit equation

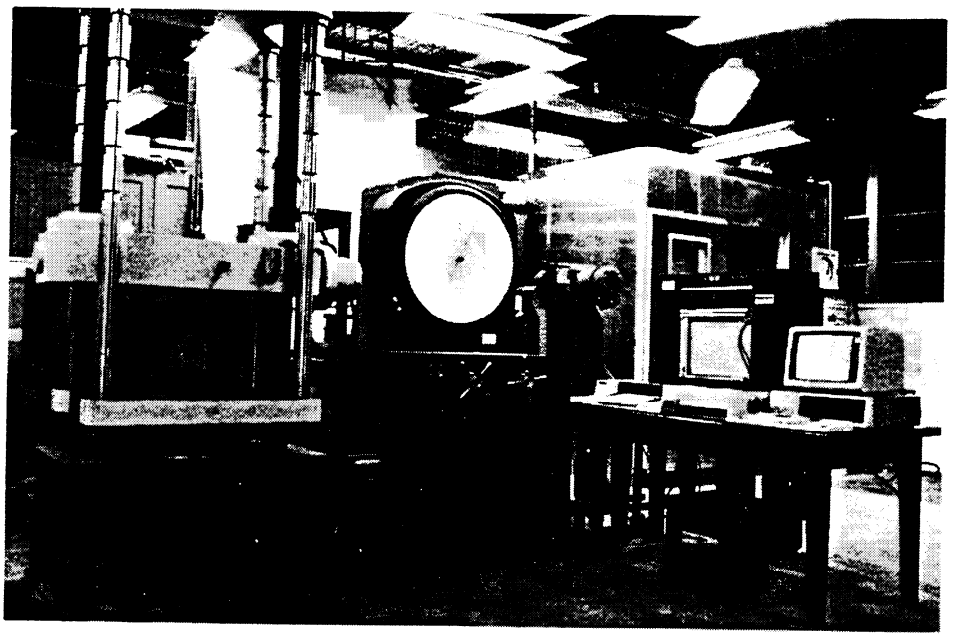

Fig. 22. Static Chord Modulus Equipment.

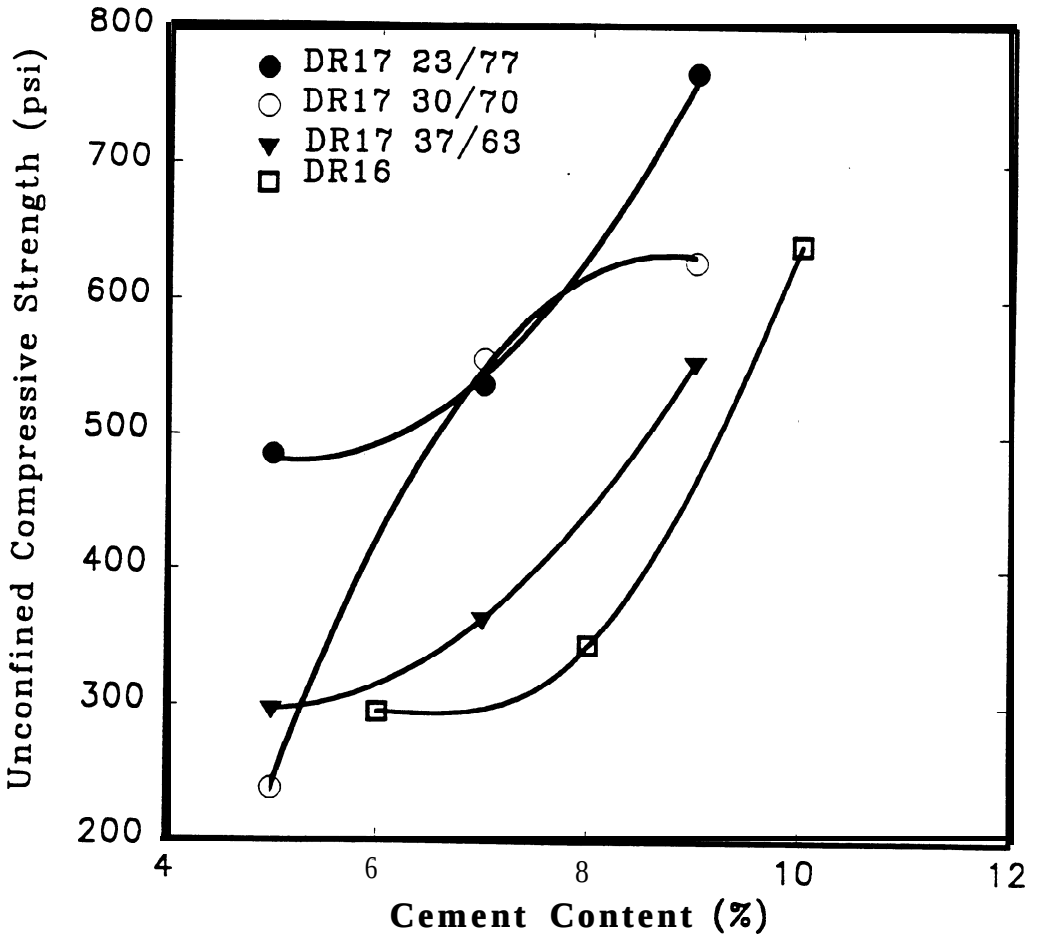

Fig. 23. Effect of Cement Content on Unconfined Compressive Strength.

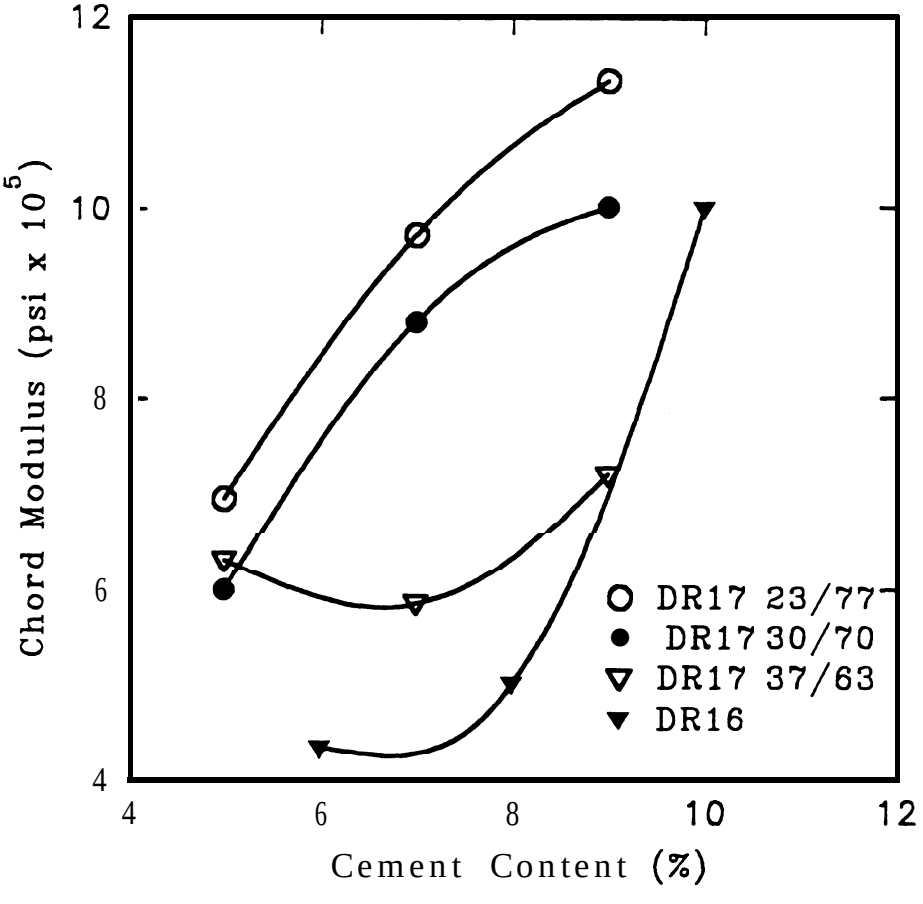

Fig 24. Effect of Cement Content on Chord Modulus.

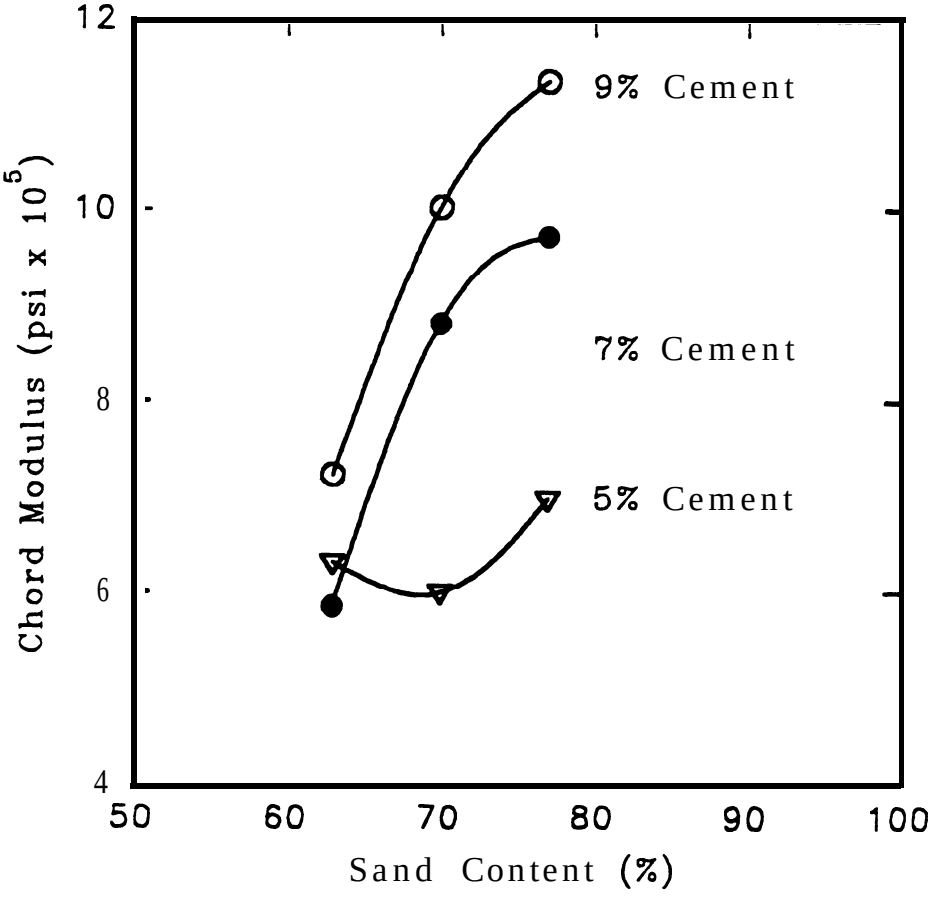

Fig. 25. Effect of Sand Content on Chord Modulus.

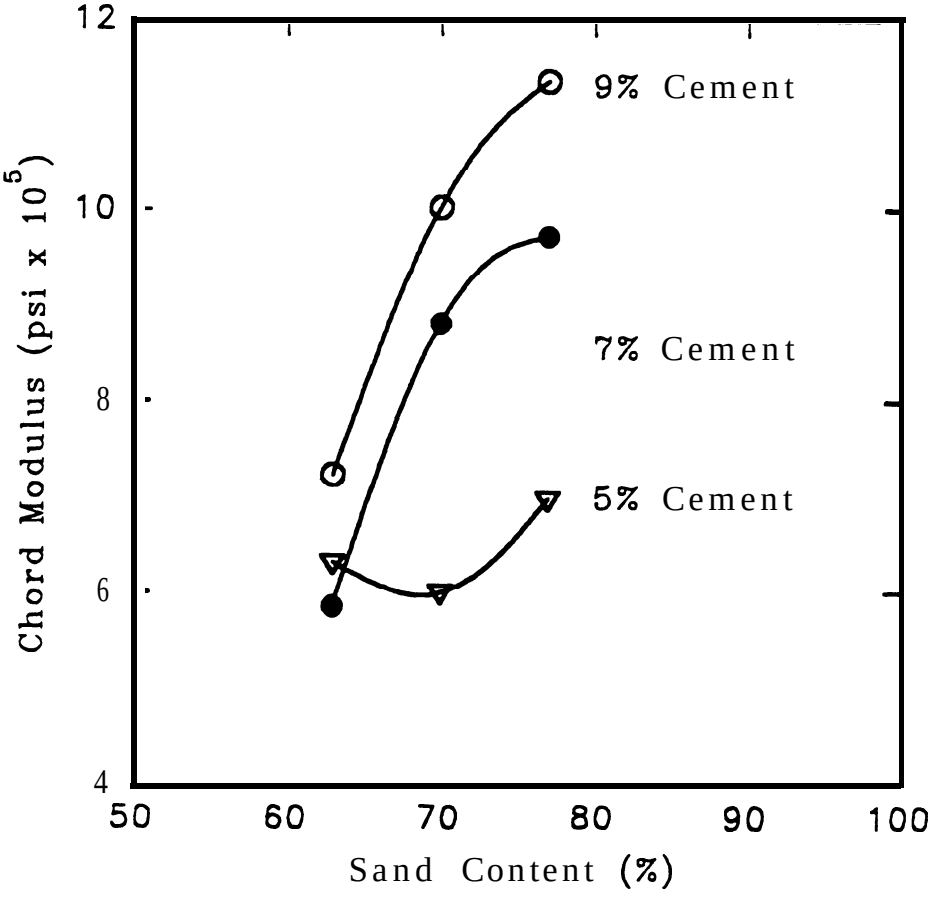

Fig. 25. Effect of Sand Content on Chord Modulus.

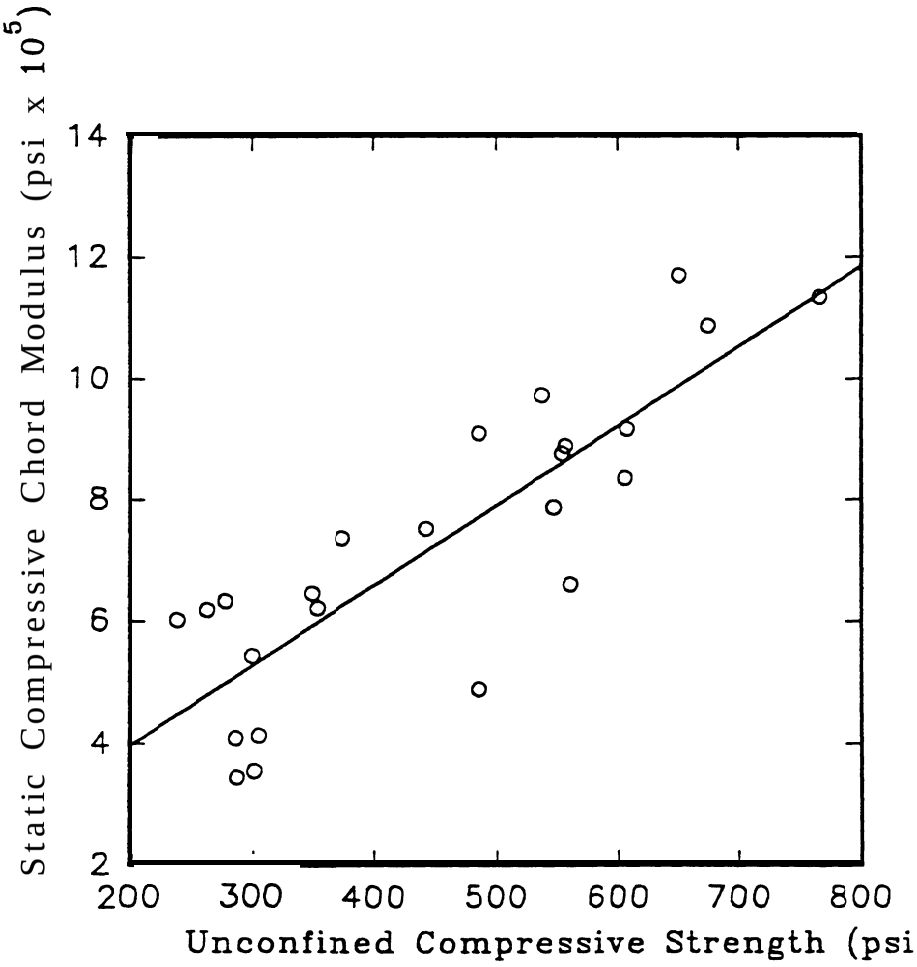

Fig. 27: Overall Relationship of Unconfined Compressive Strength and Static Compressive Chord Modulus for Soil – Cement Mixtures.

Table 28. Compressive Strength and Chord Modulus Results.

Mix	Soil/Sand Proportions (%)	Cement Content (%)	Dry Density (pcf)	Comp. strength (psi)	Chord Modulus (psi)
DR-16	--	6	112.3	300	435,700
		8	112.4	345	503,000
		10	112.4	640	1,001,600
DR-17	23/77	5	--	485	698,400
		7	126.9	538	972,700
		9	130.0	766	1,134,000
	30/70	5	126.4	239	601,300
		7	127.0	554	882,100
		9	127.0	628	1,003,100
	37/63	5	122.2	297	632,400
		7	123.0	364	679,000
		9	122.6	554	724,000

(adjusted $R^2 = 0.704$) of the line is:

$$E_C = 132{,}772 + 1314.9\ q_u \quad \text{(26)}$$

This is similar to that which is reported by Felt and Abrams (52). For sand and soil/sand mixtures similar to the present study, they noted increasing modulus and increasing compressive strength as cement content increased, and usually as sand content increased. Their sandy soil's seven day compressive strength at 6%

seven day compressive strengths at 6 and 10% cement were 400 and 600 psi, respectively. The compressive moduli for the 10% (-) #200 material mixtures at 3, 6, and 10% cement contents were 0.3, 1.0, and 1.5 x 10^6 psi, respectively.

ESTIMATION OF STATIC CHORD MODULUS

A multiple regression model was fit to the data. The criteria for model acceptance was the same as presented earlier for E_g in Eq. 10. The R^2 statistic = 0.601, the adjusted R^2 = 0.562, and the SEE = 158,433. The best fit model is as follows:

$$E_c = -2{,}575{,}557 + 84{,}084(C) + 22{,}349(\gamma_d) \quad \ldots\ldots\ldots \quad (27)$$

where:

E_C = chord modulus, psi

C = cement content, %

γ_d = dry density, pcf.

Various parameters were tried in the model, including PI, activity of fines, percent passing #200 sieve and #270 sieve, A, slopes-of-curve, percent retained on #4 sieve, amount 0.005 mm material, and percent finer than 0.002 mm. None of them improved the model nor were any statistically significant to the model. A plot of the relationship of the estimated and observed soil cement chord moduli is shown in Fig. 28. In comparing this relationship to the one delineated by Eq. 26, it is seen that modulus can be more accurately estimated by use of unconfined compressive strength.

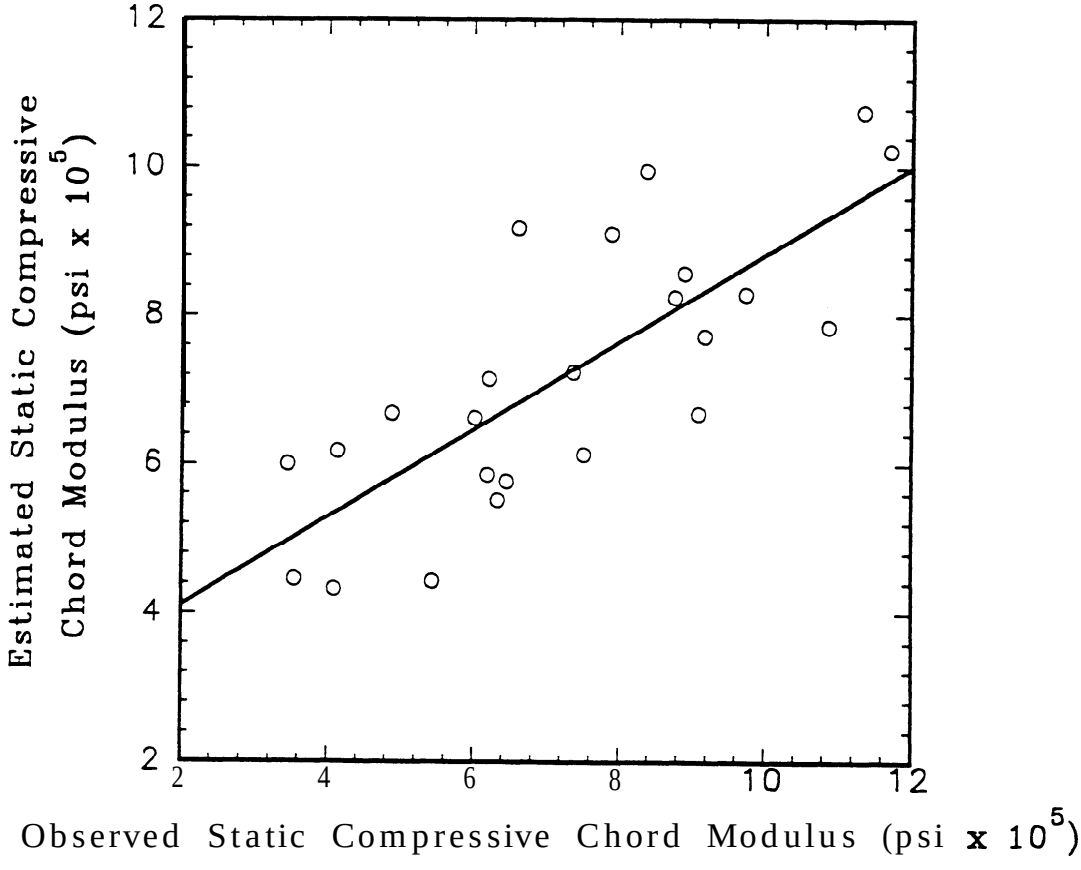

Fig. 28: Relationship of Estimated and Observed Chord Modulus of Soil – Cement Mixtures.

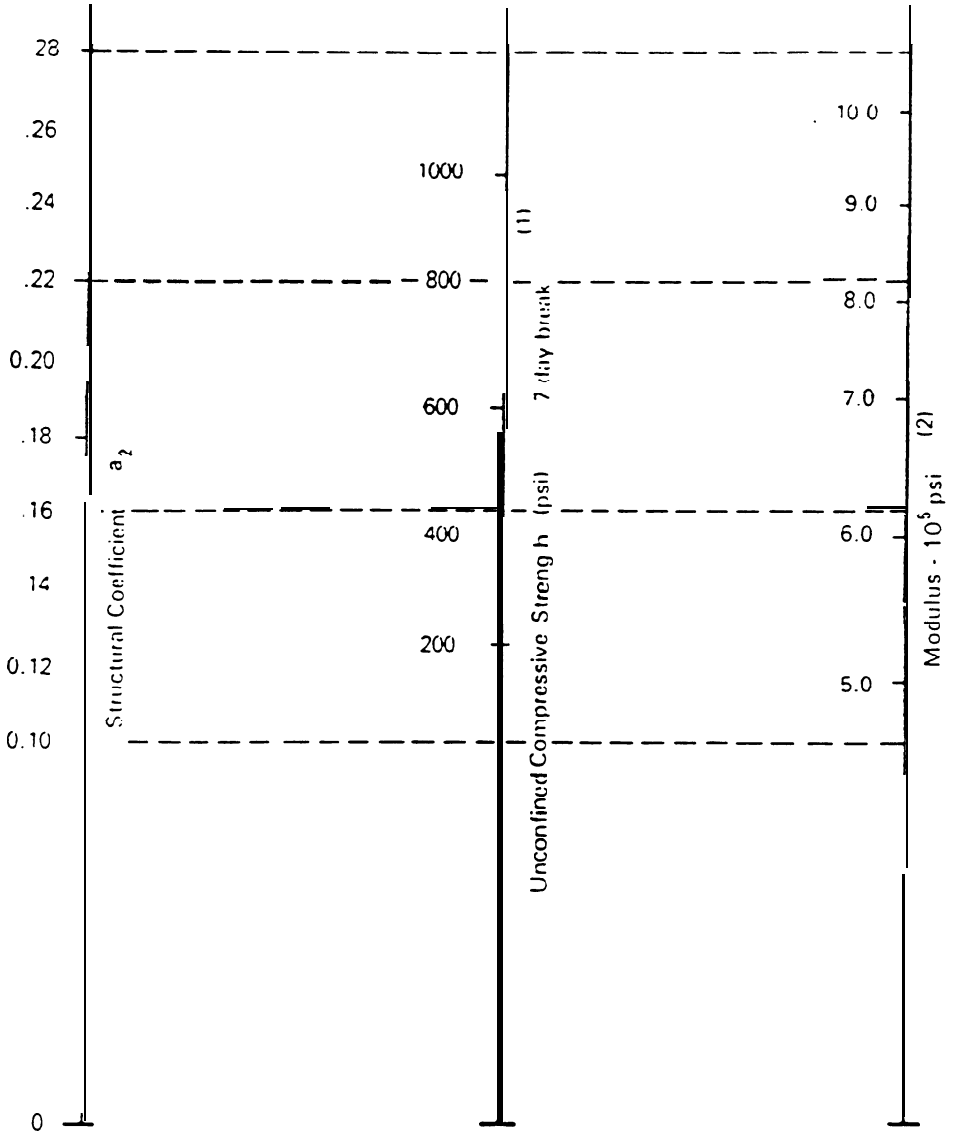

(1) Scale derived by averaging **correlations** from Illinois. Louisiana and Texas.
(2) Scale derived on NCHRP project (3).

Fig. 29. **AASHTO Nomagraph** for Determination of a_2 for Cement Treated Base.

DETERMINATION OF LAYER COEFFICIENTS

Layer coefficients were determined by use of the AASHTO nomograph, which is shown in Fig. 29. The equation for the relationship of a_2 and modulus was derived from the nomograph and is:

$$a_2 = -2.7170 + 0.49711 \log E_c$$ (illegible)

where:

E = chord modulus, psi.

Substitution of elastic moduli into Eq. 28 resulted in the layer coefficients that are shown in Table 28.

VERIFICATION

COMPARISON TO PUBLISHED DATA

In Table 1 are listed unbound aggregate base and cement-treated base layer coefficients as reported by others. The layer coefficients shown in Table 29 seem to be reasonable in comparison to those in Table 1.

DESIGN VERIFICATION

In order to further check the reasonableness of the layer coefficients, 18 design situations were examined to compare standard MHTD designs vs. AASHTO designs using the layer coefficients developed in this study. Subgrade soil and traffic conditions were varied to give a wide range of pavement thickness. The MHTD Flexible Pavement Thickness Design Chart was used to determine total pavement thicknesses and recommended asphaltic layer thicknesses. Additionally, the unbound crushed stone base thicknesses were converted to the required

Table 29. Soil-Cement Layer Coefficients,

Mix	Soil/sand Proportions (%)	Cement Content (%)	a_2
DR-16	--	6	0.09
		8	0.12
		10	0.27
DR-17	23/77	5	0.19
		7	0.26
		9	0.29
	30/70	5	0.16
		7	0.24
		9	0.27
	37/63	5	0.17
		7	0.18
		9	0.20

thicknesses of soil-cement base by use of a 1.5:1 equivalency ratio as recommended in the MHTD method. Traffic levels were chosen so that each of four design curves (2 through 5) in the MHTD chart could be used.

To obtain equivalent AASHTO designs, the use of a traffic correlation provided by Murray (57) was used to convert the MHTD 2 axle equivalents to 1 8^kESAL as used in the AASHTO method. Also, the subgrade was characterized to have a Group Index (old) of 6, 9, and 17. Eqs. 17 and 18 were used to calculate E_{sg} values. These values represent the soils predominant in Missouri. Data from the MHTD Geology and Soils Manual (58) were analyzed and it was determined that the average GI (old) of the soils reported was 10 and the standard

deviation was 4, which indicates that about two thirds of the soil types have a GI between 6 and 14. The asphaltic layer thickness was held constant for both design methods. In the AASHTO method, initial Present Serviceability Index (PSI) was assumed to be 4.2 and terminal PSI was chosen as 2.5 for a $\Delta PSI = 1.7$. Reliability was taken as 50%, and standard deviation as 0.45. From the 1986 AASHTO Guide design equation (Eq. 23) the resulting required structural numbers were calculated. To solve for D_2 in an asphalt-over-unbound base section:

$$D_2 = \frac{SN - a_1 D_1}{a_2}$$

To solve for D_3 in an asphalt-over-bituminous base-over-unbound subbase section:

$$D_3 = \frac{SN - (a_1 D_1 + a_2 D_2)}{a_3}$$

The layer coefficient (a,) for the asphaltic layers was taken as 0.42 and a_2 = 0.34 (as per Volume I of this report), and the layer coefficients a_2 and a_3 for the unbound base and subbase at various thicknesses were obtained from Eqs. 20 and 21. E_b values for the granular base and subbase were calculated using Eq. 10. Input included D_1, D_2, and E_{sg} values as shown in Tables 30 and 31 . An E_1 of 457,351 psi was used, which represents the average resilient modulus of 1990 MHTD mix designs (see Volume I). Values of k_1 for the base and subbase were taken from Table 15: 6100 psi for the base and 4300 psi for the subbase. The soil-cement layer coefficient was determined from Table 29 assuming a DR-1 7 37/63 blend with 7% cement (a_2 = 0.18). The results of the analysis are shown

in Tables 30 and 31:

Granular a_2

In studying Table 30, the design base (D_2) thickness for the granular material based on the AASHTO nomograph is similar to MHTD designs for the 6 and 17 GI soils for most traffic levels. For GI = 9, the nomograph a_2 - derived designs are conservative. The Odemark a_2-derived designs are conservative for GI = 9, but are thinner than MHTD designs for GI's of 6 and 17.

Granular a_3

Table 31 indicates that the nomograph-based designs are close to MHTD designs for soils of GI = 6, are conservative for GI = 9, and are thinner for GI = 17. The Odemark-based designs are conservative for GI = 9 and thinner than MHTD designs for GI = 6 and 17. However, underdesign at GI = 17 may not be of practical significance if a subgrade cap is used, as mentioned in the MHTD design method for soils with a GI greater than 16.

Thus, two options are presented for possible use by MHTD. If an evaluation by MHTD of its granular base design thicknesses reveals them to be either on-target or inadequate, then the AASHTO nomograph-based layer coefficients are recommended. If an evaluation indicates that MHTD base designs are excessive, then the Odemark-based method of layer coefficient calculation is recommended.

Soil Cement a_2

Table 30 indicates that for a_2 = 0.18, AASHTO-derived cement stabilized base thicknesses are comparable for GI = 9, would be the same for GI = 6 (if

in Tables 30 and 31:

Granular a_2

In studying Table 30, the design base (D_2) thickness for the granular material based on the AASHTO nomograph is similar to MHTD designs for the 6 and 17 GI soils for most traffic levels. For GI = 9, the nomograph a_2 - derived designs are conservative. The Odemark a_2-derived designs are conservative for GI = 9, but are thinner than MHTD designs for GI's of 6 and 17.

Granular a_3

Table 31 indicates that the nomograph-based designs are close to MHTD designs for soils of GI = 6, are conservative for GI = 9, and are thinner for GI = 17. The Odemark-based designs are conservative for GI = 9 and thinner than MHTD designs for GI = 6 and 17. However, underdesign at GI = 17 may not be of practical significance if a subgrade cap is used, as mentioned in the MHTD design method for soils with a GI greater than 16.

Thus, two options are presented for possible use by MHTD. If an evaluation by MHTD of its granular base design thicknesses reveals them to be either on-target or inadequate, then the AASHTO nomograph-based layer coefficients are recommended. If an evaluation indicates that MHTD base designs are excessive, then the Odemark-based method of layer coefficient calculation is recommended.

Soil Cement a_2

Table 30 indicates that for a_2 = 0.18, AASHTO-derived cement stabilized base thicknesses are comparable for GI = 9, would be the same for GI = 6 (if

Table 31. Comparison of AASHTO Designs to MHTD Designs for a_3.

Subgrade		Traffic		SN	D_1 and D_2 (asphalt-bound)				a_3		
GI		2AE	18^{k}SAL (thous.) (thous.)		MHTD		AASHTO		Nom.	Ode.	M
Old	New				D_1 (in)	D_2 (in)	D_1 (in)	D_2 (in)			
6	5	500	450	2.3	1.25	3.75	1.25	3.75	0.11	0.15	
6	5	1000	875	2.6	1.25	3.75	1.25	3.75	0.12	0.15	
9	9	500	450	2.8	1.25	3.75	1.25	3.75	0.11	0.14	
9	9	1000	875	3.1	1.25	3.75	1.25	3.75	0.11	0.14	
17	30	500	450	3.0	1.25	5.75	1.25	5.75	0.09	0.11	
17	30	1000	875	3.3	1.25	5.75	1.25	5.75	0.09	0.12	

minimum thickness of 6 in is used as per MHTD practice), and are somewhat thinner for two traffic levels on GI = 17 soil. On balance, the layer coefficients seem reasonable. However, the wide range in coefficients reported in Table 29 emphasize the importance of testing the actual materials and assigning the proper coefficient, as opposed to assigning a single coefficient for all materials.

SENSITIVITY ANALYSIS

A sensitivity analysis was performed by looking at the effect of mixture variables on required pavement thickness.

UNBOUND GRANULAR MATERIAL

As discussed previously, only compactive effort and degree of saturation were significant in their effect on E_g. An analysis was performed to ascertain the effect on base and subbase layer thickness by varying compactive effort. The effect of saturation is examined in the companion study (2). For the a_2 coefficient analysis, thickness of the surface (asphalt) layer was held constant at 4 in. Thickness of the base layer was varied at 6 in and 12 in. Three levels of compactive effort (CE) were looked at: most significant change in the UMR data set, least significant change in the UMR data set, and average change for all blends. For instance, looking at Table 13, the largest change in E_g as a result of a change of CE occurred with the DR-14 Mid high CE material as CE went from high (E_g = 27,096) to low (E_g = 16,278 psi). The least change occurred where the DR-14 NJ high CE material went from high (E_g = 25,884) to low CE (E_g = 24,309). The "average" condition was simply a comparison of the average of the

E_g's for the four aggregate sources lowest CE to the average of the E_g's for the four aggregate sources highest CE. In each case, CE was changed from high to low with a resulting change in E_g. Then the resulting change in layer coefficient (a_2) was calculated from the AASHTO nomograph. Finally, the required change in thickness was computed as needed to maintain the initial structural number rendered by the initial assumption of layer thicknesses. The results are shown in Table 32. For example, what is the average change in required base layer thickness for an initial thickness of 6 in when compactive effort is changed from high to low? Looking at row 1 in Table 32, the E_g for the high CE (of the pair which resulted in the most loss of modulus) is 27,096 psi. Moving to the low CE results in a reduction to 16,278 psi. Using the AASHTO nomograph, the corresponding loss in a_2 is 0.055. The structural number (SN) provided by the high CE is $SN = a_1D_1 + a_2D_2$ or $SN = (0.42)(4) + (0.127)(6) = 2.44$. When the layer coefficient is reduced from 0.127 to 0.072, the new required thickness $D_2 = (SN - a_1 D_1)/a_2 = \frac{2.44-(4*0.42)}{0.072} = 10.6$ in or, an additional requirement of 4.6 in. This is quite significant in a practical sense. A similar analysis was undertaken for the subbase layer coefficient a_3. D_1, a_1, D_2, and a_2 were held constant. D_{32} was calculated as $D_3 = (SN-a_1 D_1 - a_2 D_2)/a_{31}$. The results are shown in Table 33.

From Tables 32 and 33, it appears that, on the average, changes in unbound base layer compactive effort are significant for both 6 in and 12 in layers. The thicker the granular base or subbase layer, the more pronounced is the effect.

E_g's for the four aggregate sources lowest CE to the average of the E_g's for the four aggregate sources highest CE. In each case, CE was changed from high to low with a resulting change in E_g. Then the resulting change in layer coefficient (a_2) was calculated from the AASHTO nomograph. Finally, the required change in thickness was computed as needed to maintain the initial structural number rendered by the initial assumption of layer thicknesses. The results are shown in Table 32. For example, what is the average change in required base layer thickness for an initial thickness of 6 in when compactive effort is changed from high to low? Looking at row 1 in Table 32, the E_g for the high CE (of the pair which resulted in the most loss of modulus) is 27,096 psi. Moving to the low CE results in a reduction to 16,278 psi. Using the AASHTO nomograph, the corresponding loss in a_2 is 0.055. The structural number (SN) provided by the high CE is $SN = a_1D_1 + a_2D_2$ or $SN = (0.42)(4) + (0.127)(6) = 2.44$. When the layer coefficient is reduced from 0.127 to 0.072, the new required thickness $D_2 = (SN - a_1 D_1)/a_2 = \frac{2.44-(4*0.42)}{0.072} = 10.6$ in or, an additional requirement of 4.6 in. This is quite significant in a practical sense. A similar analysis was undertaken for the subbase layer coefficient a_3. D_1, a_1, D_2, and a_2 were held constant. D_{32} was calculated as $D_3 = (SN-a_1 D_1 - a_2 D_2)/a_{31}$. The results are shown in Table 33.

From Tables 32 and 33, it appears that, on the average, changes in unbound base layer compactive effort are significant for both 6 in and 12 in layers. The thicker the granular base or subbase layer, the more pronounced is the effect.

Table 33. Subbase Thickness Sensitivity to Changes in Compactive Effort.

CHANGE IN DRY DENSITY *										
D_{31} (in)	CASE	M_{R1} (psi)	M_{R2} (psi)	E_g diff (psi)	a_{31}	a_{32}	a_3 diff	SN	D_{32} (in)	D_3 diff (in)
6	Worst	17,030	10,160	6870	0.121	0.071	0.050	3.55	10.3	4.3
12		17,030	10,160	6870	0.121	0.071	0.050	4.28	20.6	8.6
6	Avg	14,455	12,090	2365	0.105	0.088	0.017	3.45	7.2	1.2
12		14,455	12,090	2365	0.105	0.088	0.017	4.08	14.4	2.4
6	Least	17,926	16,299	1627	0.126	0.117	0.009	3.58	6.5	0.5
12		17,926	16,299	1627	0.126	0.117	0.009	4.34	13.0	1.0

Note: a_3 from AASHTO nomograph
D_1 = 1.25 in, a_1 = 0.42; D_2 = 6.75 in, a_2 = 0.34
E_g at θ = 5 psi
* = Data includes both gradations, both degrees of saturation, all aggregate sources

constant at 4 in. Thickness of the base layer was varied at 6 in and 12 in. Three levels of cement content or sand content were studied: most significant change in the UMR data set, least significant change in the UMR data set, and average change for all mixes. For instance, looking at Table 28, the largest change in E_c as a result of a change of cement content occurred with the DR-16 soil as cement content went from 6% (E_c = 435,700) to 10% (E_c = 1,001,600 psi). The least change occurred where the 37/63 DR-17 blend went from 5% (E_c = 632,000) to 9% (E_c = 724,000) cement content. The "average" condition was simply a comparison of the average of the E_c's for the four soil blends' lowest cement contents to the average of the E_c's for the four soil blends' highest cement contents. Cement or sand content was changed from high to low with a resulting

change in E_c. Then the resulting change in layer coefficient (a_2) was calculated from the AASHTO nomograph. Finally, the required change in thickness was computed as needed to maintain the initial structural number rendered by the initial assumption of layer thicknesses. The results are shown in Table 34. For example, what is the average change in required base layer thickness for an initial thickness of 6 in when cement content is changed from high to low? Looking at row 1 in Table 34, the E_c for the high cement content (of the pair which resulted in the most loss of modulus) is 1,001,000 psi. Moving to the low cement content results in a reduction to 435,700 psi. Using the AASHTO nomograph, the corresponding loss in a_2 is 0.18. The structural number (SN) provided by the fine side mix is $SN = a_1D_1 + a_2D_2$ or $SN = (0.42)(4) + (0.27)(6) = 3.30$. When the layer coefficient is reduced from 0.27 to 0.09, the new required thickness $D_2 = (SN - a_1D_1)/a_2 = \frac{3.30-1.68}{0.09} = 18$ in, or, an additional requirement of 12 in. This is quite significant in a practical sense.

From Table 34, it appears that all changes in cement content and sand content are significant for both 6 in and 12 in layers. For thicker layers, the effect becomes more important. Thus, it appears that optimizing sand and cement contents is important to the resulting layer coefficient.

SUMMARY AND CONCLUSIONS

The purpose of this report was to determine layer coefficients for Type 1 dense-graded unbound granular base, open-graded unbound granular base, and soil-cement base. The methodology included the determination of the moduli of the various materials and then conversion to layer coefficients. The study included

Table 34. Thickness Sensitivity to Changes in Cement Content and Sand Content.

D_{21} (in)	CASE	E_{21} (psi)	E_{22} (psi)	E diff (psi)	a_{21}	a_{22}	a_2 diff	SN	D_{22} (in)	D_2 diff (in)
CEMENT CONTENT CHANGE										
6	Worst	1,001,600	435,700	595,900	0.27	0.09	0.18	3.30	18	12
12		1,001,600	435,700	595,900	0.27	0.09	0.18	4.92	36	24
6	Avg	965,675	591,950	373,725	0.26	0.15	0.11	3.24	10.4	4.4
12		965,675	591,950	373,725	0.26	0.15	0.11	4.80	20.8	8.8
6	Least	724,000	632,400	91,600	0.20	0.17	0.03	2.88	7.1	1.1
12		724,000	632,400	91,600	0.20	0.17	0.03	4.08	14.1	2.1
SAND CONTENT CHANGE										
6	Worst	1,134,000	724,000	410,000	0.29	0.20	0.09	3.42	8.7	2.7
12		1,134,000	724,000	410,000	0.29	0.20	0.09	5.16	17.4	5.4
6	Avg	935,033	678,467	256,566	0.25	0.18	0.07	3.18	8.33	2.33
12		935,033	678,467	256,566	0.25	0.18	0.07	4.68	16.67	4.67
6	Least	698,400	601,300	97,100	0.19	0.16	0.03	2.82	7.1	1.1
12		698,400	601,300	97,100	0.19	0.16	0.03	3.96	14.25	2.25

Note: For all sections, D_1 = 4 in and a_1 = 0.42.

the following testing and analysis.

1. The materials under study included two sources of crushed stone, two gravels, and two soils (to be mixed with cement). Additionally, a concrete sand was supplied for combining with one of the soils. One soil was a fine sand, while the other was a silty clay. All materials were selected, sampled, and delivered to UMR by MHTD personnel.

2. For the granular base study, two gradations of granular material were chosen: one followed the midpoint of the MHTD Type 1 gradation acceptance band, and the other was the so-called New Jersey open-graded gradation.

Table 34. Thickness Sensitivity to Changes in Cement Content and Sand Content.

D_{21} (in)	CASE	E_{21} (psi)	E_{22} (psi)	E diff (psi)	a_{21}	a_{22}	a_2 diff	SN	D_{22} (in)	D_2 diff (in)
CEMENT CONTENT CHANGE										
6	Worst	1,001,600	435,700	595,900	0.27	0.09	0.18	3.30	18	12
12		1,001,600	435,700	595,900	0.27	0.09	0.18	4.92	36	24
6	Avg	965,675	591,950	373,725	0.26	0.15	0.11	3.24	10.4	4.4
12		965,675	591,950	373,725	0.26	0.15	0.11	4.80	20.8	8.8
6	Least	724,000	632,400	91,600	0.20	0.17	0.03	2.88	7.1	1.1
12		724,000	632,400	91,600	0.20	0.17	0.03	4.08	14.1	2.1
SAND CONTENT CHANGE										
6	Worst	1,134,000	724,000	410,000	0.29	0.20	0.09	3.42	8.7	2.7
12		1,134,000	724,000	410,000	0.29	0.20	0.09	5.16	17.4	5.4
6	Avg	935,033	678,467	256,566	0.25	0.18	0.07	3.18	8.33	2.33
12		935,033	678,467	256,566	0.25	0.18	0.07	4.68	16.67	4.67
6	Least	698,400	601,300	97,100	0.19	0.16	0.03	2.82	7.1	1.1
12		698,400	601,300	97,100	0.19	0.16	0.03	3.96	14.25	2.25

Note: For all sections, D_1 = 4 in and a_1 = 0.42.

the following testing and analysis.

1. The materials under study included two sources of crushed stone, two gravels, and two soils (to be mixed with cement). Additionally, a concrete sand was supplied for combining with one of the soils. One soil was a fine sand, while the other was a silty clay. All materials were selected, sampled, and delivered to UMR by MHTD personnel.

2. For the granular base study, two gradations of granular material were chosen: one followed the midpoint of the MHTD Type 1 gradation acceptance band, and the other was the so-called New Jersey open-graded gradation.

ranged from 2 to 20 psi and cyclic deviator stress ranged from 2 to 40 psi. Thirty-two specimens were fabricated. The total number of tests run was 896.

The results of the testing indicated that E_g increases with increasing bulk stress, increasing compactive effort, and lower degree of saturation. For the materials tested, the effects of particle angularity and gradation were not significant.

7. A statistical analysis was performed to determine the significance of the variables. Paired-t tests indicated that change in density or degree of saturation gave significantly different results at the 0.05 level, but gradation did not. Tukey HSD analysis indicated that one of the two gravels gave significantly different results than the other gravel and the two crushed stones. The particle shape analysis indicated that the shapes of the two gravels were about the same, but they were both different from the two crushed stones. All of this taken together indicated that particle shape was not significant. Finally, in comparing saturated dense-graded material with drained open-graded material, there was a significant (0.088 level) increase in E_g with superior drainage.

8. A multiple regression model was developed for the parameter k_1 but the relationship was relatively weak.

9. To assist the pavement designer who may not be able to obtain actual E_g data, a regression model was developed for E_g by analyzing 237 pavement

sections which varied in asphaltic layer thickness (D_1 = 2,8,15 in), asphaltic layer modulus (E_1 = 130,000, 500,000, and 2,100,000 psi), unbound base thickness (D_2 = 4,12,18 in), subgrade modulus (E_{sg} = 1000 to 17,000), granular material constant k_1 (1800, 3000, 11,000 psi), and granular material constant k_2 (0.341, 0.653, 0.776). The most accurate model was:

$$E_g = 510.505\ (D_1)^{-0.458}\ (k_1)^{0.426}\ (E_1)^{-0.107}\ (E_{sg})^{0.207}\ (D_2)^{0.067}$$

This model had an adjusted $R^2 = 0.909$.

The model indicates that E_g increases with increasing k_1 of the granular base, increasing K_1 and E_{sg} of the subgrade soil, increasing D_2, decreasing D_1, and decreasing E_1.

10. For comparison purposes, layer coefficients were computed in two different manners. First, E_g values were substituted into the AASHTO nomographs for unbound granular base and subbase to obtain a_2 and a_3 directly. Second, Odemark's equivalent stiffness was used for comparing MHTD aggregates to Road Test materials (and stress states). An analysis indicated that it is preferable to use the AASHTO nomographs.

11. Because layer coefficients are directly affected by resilient modulus, the practical impact of the trends is that higher layer coefficients can be obtained by greater compactive effort and lower degree of saturation (better drainage).

12. The Knox soil (A-6) was mixed with concrete sand in three proportions of soil to sand: 23/77, 30/70 and 37/63. Specimens were made with 5, 7,

and 9% cement contents by weight. The Lintonia (A-3) soil was mixed with 6, 8, and 10% cement contents. Specimens were tested for compressive strength and static chord modulus. In general, strength and modulus increased with increasing cement contents and increasing dry densities.

13. Two regression equations were developed for estimation of static chord modulus:

$E_c = 2{,}575{,}557 + 84{,}084\ (C) + 22{,}349\ (\gamma_d)$ adj $R^2 = 0.562$

$E_c = 132{,}772 + 1314.9\ q_u$ adj $R^2 = 0.704$

where C is cement content, γ_d is dry unit weight and q_u is compressive strength.

14. Layer coefficients were obtained for the soil-cement mixtures by use of the AASHTO nomograph. Values ranged from 0.09 to 0.27. Most of these fit into the range of values reported elsewhere.

15. A verification analysis was performed. Twelve hypothetical pavements were designed by use of both the former MHTD method and the AASHTO method using the layer coefficients developed in this study for unbound base and soil-cement. This analysis tended to verify the choice of using the AASHTO nomographs for calculation of layer coefficients, although use of the Odemark method may be preferrable under certain conditions.

16. A sensitivity analysis was performed. The results indicated that a higher compactive effort could result in a reduction of up to 2 in in base thickness for a 12 in thick base.

An increase in degree of saturation acts to lower k_1 and raise k_2 of the granular material, and to lower subgrade support, all of which act to lower the E_g of the granular material. This phenomenom is addressed by use of drainage coefficients, as developed in the companion study of this report (2). Thus, the layer coefficients developed in this report are representative of average degrees of saturation of about 60%. For significantly greater or smaller magnitudes of saturation, m-coefficients should be used in the equation:

$$SN = a_1 D_1 + m_2 a_2 D_2 + m_3 a_3 D_3$$

RECOMMENDATIONS

1. Layer coefficients for unbound granular base or subbase materials should be determined in the following manner:

   a. Determine a_2 or a_3 from the 1986 AASHTO Guide nomographs, or more accurately:

   $$a_2 = 0.249 \log E_g - 0.977$$

   $$a_3 = 0.227 \log E_g - 0.839.$$

   b. E_g (resilient modulus of granular material) for a pavement section with a single granular layer can be determined by use of an elastic layer analysis program such as KENLAYER or by the following equation:

   $$E_g = 510.505(D_1)^{-0.458}(k_1)^{0.426}(E_1)^{-0.107}(E_{sg})^{0.207}(D_2)^{0.067}$$

   For multiple granular layers, use of a program such as KENLAYER is recommended.

   c. D_1 and D_2 (D_1 = asphalt bound layer, D_2 = granular base or subbase

layer thickness) are assumed for a particular design trial. (Note: D_1 is the combined thickness of all asphalt-bound layers.)

d. E_1 (asphalt material resilient modulus), is determined at a given design temperature as developed in Volume I of this report knowing either resilient modulus or mix design characteristics. If more than one asphalt layer is involved, the weighted average can be obtained by Eq. 19:

$$E_{eq} = \left[\frac{D_{1a}(E_{1a})^{0.333} + D_{1b}(E_{1b})^{0.333}}{D_{1a} + D_{2a}}\right]^3$$

e. E_{sg} (subgrade soil modulus) can be calculated in accordance with the section "Resilient Modulus Regression Equation Subgrade Modulus".

f. k_1 can be determined by resilient modulus testing of the granular material, or by estimation. See Table 15 for guidance.

2. Layer coefficients for cement treated soil base can be determined in the following manner:

a. Determine a_2 from the 1986 AASHTO Guide nomograph, or more accurately

$$a_2 = -2.717 + 0.49711 \log E_c$$

b. E_c can be determined by static compressive modulus testing or by

$$E_C = 132,772 + 1314.9\ q_u$$

or less accurately

$$E_C = -2,575,557 + 84,084\ C + 22,349\ (\gamma_d)$$

where:

E_c = static compressive chord modulus, psi

q_u = unconfined compressive strength, psi

C = cement content, %

γ_d = dry density, pcf.

FUTURE RESEARCH NEEDS

1 A wider range of granular material sources needs to be tested to determine the effects of particle shape and gradation on E_g. This would include several other gradations to better define the effect of fines content.

2 A regression equation for prediction of k_1 of granular materials needs to be developed to facilitate the prediction of E_g.

3 Because the E_g of granular materials is dependent on the resilient modulus of the subgrade, the prediction of E_{sg} needs to be better defined.

4 The effects of permanent deformation of granular material needs to be tied into the layer coefficient concept.

5 More sources of soil for cement treatment need to be included in the E_c regression equation.

ACKNOWLEDGEMENT

The authors wish to thank the MHTD for its sponsorship and support of this research project. They also thank the UMR Department of Civil Engineering for its support. Special thanks go to Mr. Kevin Hubbard for his assistance in the figure preparation portion of the study, and to Aswath V. Rao for assistance in the laboratory work.

REFERENCES

REFERENCES

1 AASHTO 1986 Guide for Design of Pavement Structures, AASHTO, Washington, DC., 1986.

2. Richardson, D.N., W.J. Morrison, and P.A. Kremer, "Determination of AASHTO Drainage Coefficients," MCHRP Final Rpt. Study 90-4, Univ. of Missouri-Rolla, Rolla, Missouri, 1993.

3. "The AASHO Road Test, Rpt. 5-Pavement Research," Hwy. Res. Bd. Spec. Rpt. 61-E, Hwy. Res. Bd., 1962, 352 p.

4. Gomez, M. and M.R. Thompson, "Structural Coefficients and Thickness Equivalency Ratios", Trans. Engrg. Series No. 38, Illinois Coop. Hwy. and Trans. Series No. 202, Univ. of Illinois, 1983, 48 p.

5. Transportation Engineering Handbook, Ch. 50, Pavement, U.S. Forest Service, 1974, p. 51.1-54.4-16.

6. Van Til, C.J., B.F. McCullough, B.A. Vallerga, and R.G. Hicks, "Evaluation of AASHO Interim Guides for Design of Pavement Structures, "NCHRP Rpt. 128, Hwy. Res. Bd., Washington, DC, 1972, 111 p.

7. Wang, M.C., T.D. Larson, and W. P. Kilareski, "Structural Coefficients of Bituminous Concrete and Aggregate Cement Base Materials by the Limiting Criteria Approach", Rpt. No. FHWA-PA-RD-75-2-4, Penn. State Univ., Univ. Park, Penn., 1977, 52 p.

8. Sowers, G.F. "Georgia Satellite Flexible Pavement Evaluation and Its Application to Design," Hwy. Res. Rec. 71, Hwy. Res. Bd., 1965, pp. 151-171.

9. Walters, R., "Implementation of the New AASHTO Design Practice", 31 st Annual UMR Asphalt Conference, Univ. of Missouri-Rolla, Rolla, Missouri, 1988.

10. Rada, G. and M.M. Witczak, "Material Layer Coefficients of Unbound Granular Materials from Resilient Modulus", Trans. Res. Rec. 852, 1982, pp. 15-21.

11. Jorenby, B.N. and R.G. Hicks, "Base Course Contamination Limits", Trans. Res. Rec. 1095, Trans. Res. Bd., 1986, pp. 86-101.

12. Richardson, D.N., J.K. Lambert, and P.A. Kremer, "Determination of AASHTO Layer Coefficients, Vol. I: Bituminous Materials", MCHRP Final Rpt. Study 90-5, Univ. of Missouri-Rolla, Rolla, Missouri, 1993, 237 p.

13. Barksdale, R.D., "Laboratory Evaluation of Rutting in Base Course Materials", Proc. 3rd Int'l. Conf. on the Structural Design of Asphalt Pavements, London, England, 1972, pp. 161-174.

14. Barksdale, R.D., S.Y. Itani, and T.E. Swor, "Evaluation of Recycled Concrete, Open-Graded Aggregate," Trans. Res. Bd. 71st Annual Meeting, Trans. Res. Bd., Washington, D.C., 1992, 25 p.

15. Jin, M., K.W. Lee, and W.D. Kovacs, "Field Instrumentation and Laboratory Study to Investigate Seasonal Variation of Resilient Modulus of Granular Soils," Trans. Res. Bd. 71st Annual Meeting, Trans. Res. Bd., Washington, DC., 1992, 30 p.

16. Kallas, B.F. and J.C. Riley, "Mechanical Properties of Asphalt Pavement

Materials," Proc. 2nd Int'l. Conf. on the Structural Design of Asphalt Pavements, Univ. of Michigan, 1967, pp. 931-952.

17 Thorn, N.H. and S.F. Brown, "The Effect of Moisture on the Structural Performance of a Crushed Limestone Road Base," Trans. Res. Bd. Annual Meeting, Trans. Res. Bd., Washington, D.C., 1987, 24 p.

18 Hicks, R.G. and C.L. Monismith, "Prediction of the Resilient Response of Pavements Containing Granular Layers Using Non-Linear Elastic Theory," Proc. 3rd Int'l. Conf. on the Structural Design of Asphalt Pavements, London, Vol. I, 1972, pp. 410-427.

19 Barker, W.R. and R.C. Gunkel, "Structural Evaluation of Open-Graded Bases for Highway Pavements," Misc. Paper GL-79-18, U.S. Corps of Engrs., WES, 1979, 82 p.

20 Thompson, M.R. and K.L. Smith, "Repeated Triaxial Characterization of Granular Bases," Trans. Res. Rec. 1278, Trans. Res. Bd., Washington, D.C., 1990, pp. 7-17.

21 Finn, F.N., C.L. Saraf, R. Kulkarni, K. Nair, W. Smith, and A. Abdullah, "Development of Pavement Structural Subsystems," NCHRP Rpt. 291, Hwy. Res. Bd., Washington, D.C., 1986, 59 p.

22 Rada, G. and M.W. Witczak, "Comprehensive Evaluation of Laboratory Resilient Moduli Results for Granular Material," Trans. Res. Rec. 810, Trans. Res. Bd., 1981, pp. 23-33.

23 Haynes, J.H. and E.J. Yoder, "Effects of Repeated Loading on Gravel and

Crushed Stone Base Course Materials Used in the AASHO Road Test," Hwy. Res. Rec. 39, Hwy. Res. Bd., Washington, D.C., pp. 82-96.

24 Kandhal, P.S., J.B. Motter, and M.A. Khatri, "Evaluation- of Particle Shape and Texture: Manufactured vs. Natural Sands," NCAT Rpt. No. 91-3, NACT, Auburn, Ala., 1991, 23 p.

25 "Test Method for Index of Aggregate Particle Shape and Texture," ASTM D3398-87, Annual Book of ASTM Standards, Vol. 05.03 ASTM, Philadelphia, PA, 1992, pp. 393-396.

26 "Standard Test Method for Particle Shape, Texture, and Uncompacted Void Content of Fine Aggregate," Draft, National Aggregate Assn., Silver Spring, MD, 1991, 12 p.

27 "Standard Test Method for Specific Gravity and Absorption of Coarse Aggregate, " AASHTO T-85 (1988), Standard Specifications for Transportation Materials and Methods of Sampling and Testing, 15th ed, Part II, Tests AASHTO, Washington, D.C., 1990, pp. 183-186.

28 "Standard Test Method for Specific Gravity and Absorption of Fine Aggregate," AASHTO T-84 (1988), Standard Specifications for Transportation Materials and Methods of Sampling and Testing, 15th ed, Part II, Tests, AASHTO, Washington, D.C., 1990, pp. 179-1 82.

29. "Standard Test Method for The Moisture-Density Relations of Soils Using a 5.5 lb Rammer and a 12 in. Drop," AASHTO T-99 (1990), Standard Specifications for Transportation Materials and Methods of Sampling and

Testing, 15th ed, Part II, Tests, AASHTO, Washington, D.C., 1990, pp. 226-230.

30. "Standard Test Method for Moisture-Density Relations of Soils Using a 10 lb Rammer and a 18 in. Drop," AASHTO T-180 (1990), Standard Specifications for Transportation Materials and Methods of Sampling and Testing, 15th ed, Part II, Tests, AASHTO, Washington, D.C., 1990, pp. 455-459.

31. "Standard Test Method for Maximum Index Density of Soils Using a Vibratory Table," ASTM D4253-83, Annual Book of ASTM Standards, Vol. 04.08, ASTM, Philadelphia, PA, 1990, pp 572-583.

32. "Standard Test Method for Minimum Index Density of Soils and Calculation of Relative Density," ASTM D4254-83, Annual Book of ASTM Standards, Vol. 04.08, ASTM, Philadelphia, PA 1990, pp. 584-590.

33. Interim Method of Test for Resilient Modulus of Subgrade Soils and Untreated Base/Subbase Materials, AASHTO T-XXXC-91, AASHTO, Washington, D.C., 1991, p. 1-35.

34. Resilient Modulus of Unbound Granular Base/Subbase Materials and Subgrade Soils, SHRP Protocol P46, S.H.R.P., Washington, DC., 1992.

35. Claros, G., W.R. Hudson, and K.H. Stokoe, II, "Modifications to the Resilient Modulus Testing Procedure and the Use of Synthetic Samples for Equipment Calibration," Trans. Res. Bd. 69th Annual Meeting, Trans. Res. Bd., Washington, D.C., 1990, 27 p.

36. SYSTAT, 1990, Systat, Inc., Evanston, Illinois.

37. Huang, Y.H., Pavement Analysis and Design, Prentice Hall, Englewood Cliffs, NJ, 1993, 805 p.

38 Witczak, M.W., and B.E. Smith, "Prediction of Equivalent Granular Base Moduli Incorporation Stress Dependent Behavior in Flexible Pavements," ASCE Trans. Journal, 1981.

39 Thompson, M.R. and Q.L. Robnett, "Resilient Properties of Subgrade Soils," ASCE Trans. Journal, TE1, 1979, pp. 71-89.

40 Kersten, M.S., "Progress Report of Special Project on Structural Design of Non-rigid Pavements; Subgrade Moisture Conditions Beneath Airport Pavements," Hwy. Res. Bd. 25th Annual Meeting, V. 25, Hwy. Res. Bd., Washington, D.C., 1945, pp. 450-463.

41 "Method for Determining the Potential Vertical Rise, PVR," Texas Hwy. Dept., Austin, Texas, 1972, 8 p.

42 Elliot, R.P., "Selection of Subgrade Modulus for AASHTO Flexible Pavement Design," Trans. Res. Bd. 71st Annual Meeting, 1992, 12 p.

43 Seed, H.B., C.K. Chan, and C.E. Lee, "Resilient Characteristics of Subgrade Soils and Their Relation to Fatigue Failures in Asphalt Pavements," Proc. International Conf. on the Structural Design of Asphalt Pavements, Univ. of Michigan, 1962, pp. 611-636.

44 Shook, J.F., and H.Y. Fang, "Cooperative Materials Testing Program at the AASHO Road Test," Hwy. Res. Bd. Spec. Rep. 66, Hwy. Res. Bd., 1961,

36. SYSTAT, 1990, Systat, Inc., Evanston, Illinois.

37. Huang, Y.H., Pavement Analysis and Design, Prentice Hall, Englewood Cliffs, NJ, 1993, 805 p.

38 Witczak, M.W., and B.E. Smith, "Prediction of Equivalent Granular Base Moduli Incorporation Stress Dependent Behavior in Flexible Pavements," ASCE Trans. Journal, 1981.

39 Thompson, M.R. and Q.L. Robnett, "Resilient Properties of Subgrade Soils," ASCE Trans. Journal, TE1, 1979, pp. 71-89.

40 Kersten, M.S., "Progress Report of Special Project on Structural Design of Non-rigid Pavements; Subgrade Moisture Conditions Beneath Airport Pavements," Hwy. Res. Bd. 25th Annual Meeting, V. 25, Hwy. Res. Bd., Washington, D.C., 1945, pp. 450-463.

41 "Method for Determining the Potential Vertical Rise, PVR," Texas Hwy. Dept., Austin, Texas, 1972, 8 p.

42 Elliot, R.P., "Selection of Subgrade Modulus for AASHTO Flexible Pavement Design," Trans. Res. Bd. 71st Annual Meeting, 1992, 12 p.

43 Seed, H.B., C.K. Chan, and C.E. Lee, "Resilient Characteristics of Subgrade Soils and Their Relation to Fatigue Failures in Asphalt Pavements," Proc. International Conf. on the Structural Design of Asphalt Pavements, Univ. of Michigan, 1962, pp. 611-636.

44 Shook, J.F., and H.Y. Fang, "Cooperative Materials Testing Program at the AASHO Road Test," Hwy. Res. Bd. Spec. Rep. 66, Hwy. Res. Bd., 1961,

Washington, D.C., 1990, pp. 12-15.

54. "Standard Test Method for Static Modulus of Elasticity and Poisson's Ratio of Concrete in Compression," ASTM C469-87a, Annual Book of ASTM Standards, Vol. 04.02, ASTM, Philadelphia, PA, 1989, pp. 236-239.

55. QUATTRO PRO, Borland International, Inc.

56. TABLECURVE, Jandel Scientific, Inc.

57. Murray, L.T., "Flexible Design and Experimentation in Missouri," Proc. of Assn. of Asphalt Paving Tech., Vol. 34, 1965, pp. 496-519.

58. Saville, V.B. and W.C. Davis, MHTC Geology and Soils Manual, Von Hoffman Press, Jefferson City, Missouri, 1962, 436 p.

APPENDIX A

DATA SET FOR RESILIENT MODULUS

REGRESSION EQUATION (Eq. 10)

Resilient Moduli for Granular Base Material (E_1 = 130,000 psi),

E_1 = 130,000 psi		E_g (filename/base/subgrade), psi						
		D_2 (in.)						
		4			12			
D_1 (in.)	E_{sg}	k_1 = 1800 k_2 = 0.776	k_1 = 3000 k_2 = 0.653	k_1 = 11,000 k_2 = 0.341	k_1 = 1800 k_2 = 0.776	k_1 = 3000 k_2 = 0.653	k_1 = 11,000 k_2 = 0.341	18 k_2 = 0.7
2	very soft 1000-5662				12vs121	12vs122	12vs123	12vs18
		*	*	*	21,840	24,800	33,670	22,46
					2820	2980	3383	3940
	medium 4716-12,342	12M41.DAT	12M42.00	12M45.DAT	12M121	12M122	12M123	12M18
		19,860	21,790	28,900	24,220	26730	34,350	23,16
		6725	6762	6863	7501	7545	7650	8856
	stiff 7605-17,002	12541	12542	12543	125121	125122	125123	12518
		23,610	25,560	32,380	25,060	27,440	34,820	23,45
		11,300	11,320	11,390	11,890	11,930	12,030	12,71
8	very soft 1000-5662	18vs541	18vs542	18vs543	18vs121	18vs122	18vs123	18vs18
		6850	7976	10,260	8761	10,990	20,520	9435
		3487	3457	3435	4227	4257	4503	4798
	medium 4716-12,342	18m41	18m42	18m43	18m121	18m122	18m123	18m18
		10,740	12,460	18,970	11,330	13,910	23,760	10,99
		8204	8132	8027	9786	9760	9896	10,71
	stiff 7605-17,002	18541	18542	18543	18121	185122	185123	18518
		12,850	14,890	22,390	12,300	15,050	25,070	11,59
		12,230	12,210	12,140	13,960	13,910	13,980	15,06
	very soft 1000-5662	115vs41	115vs42	115vs43	115vs121	115vs122	115vs123	115vs1
		6628	8255	14,450	6991	9076	17,960	7138
		5412	5346	5237	5662	5662	5662	5662

15	medium 4716-12,342	115m41	115m42	115m43	115m121	115m122	115m123	115m181	115m182	115m183
		8651	10,680	18,540	8298	10,680	20,320	8106	10,610	20,860
		11,200	11,070	10,810	11,950	11,830	11,650	12,260	12,170	12,050
	stiff 7605-17,002	115541	15542	115543	115121	1155122	1155123	1155181	1155182	1155183
		9645	11,850	20,370	8804	11,290	21,240	8444	11,010	21,560
		15,420	15,250	14,930	16,370	16,220	15,980	16,730	16,620	16,500

Note: E_g values based on °S = 10, 60%; D_3 = 0 in.; for multiple asphalt layers, use $E_{eq} = \left[\frac{D_{1a}(E_{1a})^{0.333} + D_{1b}(E_{1b})^{0.333}}{D_{1a} + D_{1b}}\right]^3$

- statistical outliers due to non-convergence in iterative process.

Resilient Moduli for Granular Base Material (E_1 = 500,000 psi).

E_1 = 500,000psi		E_a (filename/base/subgrade), psi								
		D_2(in.)								
		4			12			18		
D_1 (in.)	E_{sg}	k_1 = 1800 k_2 = 0.776	k_1 = 3000 k_2 = 0.653	k_1 = 11,000 k_2 = 0.341	k_1 = 1800 k_2 = 0.776	k_1 = 3000 k_2 = 0.653	k_1 = 11,000 k_2 = 0.341	k_1 = 1800 k_2 = 0.776	k_1 = 3000 k_2 = 0.653	k_1 = 11,000 k_2 = 0.341
2	very soft 1000-5662	22vs541			22vs121	22vs122	22vs123	22vs181	22vs182	22vs183
		5938	*	*	18,370	21,160	30,500	19,610	22,470	31,610
		1000			2820	2986	3447	3946	4107	4515
	medium 4716-12,342	22m41	22m42	22m43	22m121	22m122	22m123	22m181	22m182	22m183
		18,760	20,580	27,180	21,810	24,260	32,590	21,080	23,730	32,390
		6798	6876	6896	7505	7542	7873	8955	9121	9630
	stiff 7605-17,002	22541	22542	22543	225121	225123	225123	225181	225182	225183
		22,830	24,700	31,130	23,370	25,780	33,430	21,680	24,340	32,720
		11,270	11,290	11,290	11,960	12,000	12,090	12,870	13,040	13,510
	very soft 1000-5662	28vs541	28vs542	28vs43	28vs121	28vs122	28vs123	28vs181	28vs182	28vs183
		6933	8677	15,310	7162	9337	18,550	7245	9683	19,960
		5374	5312	5193	5577	5504	5459	5662	5662	5662
	medium 4716-12,342	28m41	28m42	28m43	28m121	28m122	28m123	28m181	28m182	28m183
		9363	11,510	19,700	8695	11,260	21,290	8353	11,030	21,750
		11,090	10,950	10,660	11,640	11,530	11,330	12,030	11,910	11,800
	stiff 7605-17,002	28541	28542	28543	285121	285122	285123	285181	285182	285183
		10,570	12,900	21,590	9346	12,060	22,350	8760	11,540	22,410
		15,290	15,110	14,720	16,060	15,920	15,620	16,540	16,390	16,190
	very soft 1000-5662	215vs41	215vs42	215vs43	215vs121	215vs122	215vs123	215vs181	215vs182	215vs183
		5714	7613	15,850	5916	7992	17,230	6093	8267	18,090
		5662	5662	5662	5662	5662	5662	5662	5662	5662

15	medium 4716-12,342	215m41	215m42	215m43	215m121	215m122	215m123	215m181	215m182	215m183
		6913	9111	18,320	6679	9033	18,980	6674	9078	19,340
		12,340	12,340	12,340	12,340	12,340	12,340	12,340	12,340	12,340
	stiff 7605-17,002	215541	215542	215543	2155121	2155122	2155123	2155181	2155182	2155183
		7506	9840	19,390	7022	9424	19,580	6932	9347	19,820
		17,002	17,002	17,002	17,002	17,002	17,002	17,002	17,002	17,002

Note: E_g values based on °S = 10, 60%; D_3 = 0 in.; for multiple asphalt layers, use $E_{eq} = \left[\frac{D_{1a}(E_{1a})^{0.333} + D_{1b}(E_{1b})^{0.333}}{D_{1a} + D_{1b}}\right]^3$

* statistical outliers due to non-convergence in iterative process

Resilient Moduli for Granular Base Material (E_1 -- 2,100,000 psi).

E_1 = 2,100,000 psi		E_a (filename/base/subgrade), psi								
		D_2 (in.) BASE (Granular)								
		4			12			18		
D_1 (in.)	E_{sg}	k_1 = 1800 k_2 = 0.776	k_1 = 3000 k_2 = 0.653	k_1 = 11,000 k_2 = 0.341	k_1 = 1800 k_2 = 0.776	k_1 = 3000 k_2 = 0.653	k_1 = 11,000 k_2 = 0.341	k_1 = 1800 k_2 = 0.776	k_1 = 3000 k_2 = 0.653	k_1 = 11,000 k_2 = 0.341
2	very soft 1000-5662	32vs41	32vs42	32vs43	32vs121	32vs122	32vs123	32vs181	32vs182	32vs183
		9219	10,570	15,220	14520	17450	27660	15,730	18,760	29,090
		2293	2294	2333	3176	3313	3732	4098	4243	4667
	medium 4716-12,342	32m41	32m42	32m43	32m121	32m122	32m123	32m181	32m182	32m183
		16,770	18800	26130	18110	20940	30260	17,550	20,490	30,270
		7341	7336	7340	4906	8031	8456	9397	9520	9958
	stiff 7605-17,002	32541	32542	32543	325121	325122	325123	325181	325182	325183
		20300	22430	29810	19690	22440	31310	18,190	21,180	30,760
		11770	11760	11760	12200	12220	12280	13,460	13,570	13,950
8	very soft 1000-5662	38vs41	38vs42	38vs43	38vs121	38vs122	38vs123	38vs181	38vs182	38vs183
		5184	7074	15,390	5257	7326	16710	5396	7535	18,460
		5662	5662	5662	5662	5662	5662	5662	5662	5662
	medium 4716-12,342	38m41	38m42	38m43	38m121	38m122	38m123	38m181	38m182	38m183
		6595	8821	18,250	6168	8552	18680	6056	8479	19,020
		12,340	12,340	12,340	12340	12340	12340	12,340	12,340	12,340
	stiff 7605-17,002	38541	38542	38543	385121	385122	385123	385181	385182	385183
		7264	9650	19,510	6520	9028	19540	6293	8826	19,590
		17,002	17,002	17,002	17002	170[redacted]02		17,002	17,002	17,002
	very soft 1000-5662	315vs41	315vs42	315vs43	315vs121	315vs[redacted]s123		315vs181	315vs182	315vs183
		4906	6868	16,160	5186	7248	16,930	5410	7534	17,430
		5562	5662	5662	5662	5662	5662	5662	5662	5662

15	medium 4716-12,342	315m41	315m42	315m42	315m121	315m122	315m123	315m181	315m182	315m183
		5455	7576	17,280	5568	7760	17,780	5717	7953	18,130
		12,340	12,340	12,340	12,340	12,340	12,340	12,340	12,340	12,340
	stiff 7605-17,002	318841	315542	315543	3155121	3155122	3155123	3155181	3155182	3155183
		5735	7933	17800	5742	7963	18,150	5827	8109	18,430
		17002	17002	17002	17,002	17,002	17,002	17,002	17,002	17,002

Note: E_g values based on ^oS = 10, 60%; D_3 = 0 in.; for multiple asphalt layers, use $E_{eq} = \left[\frac{D_{1a}(E_{1a})^{0.333} + D_{1b}(E_{1b})^{0.333}}{D_{1a} + D_{1b}}\right]^3$

15	medium 4716-12,342	315m41	315m42	315m42	315m121	315m122	315m123	315m181	315m182	315m183
		5455	7576	17,280	5568	7760	17,780	5717	7953	18,130
		12,340	12,340	12,340	12,340	12,340	12,340	12,340	12,340	12,340
	stiff 7605-17,002	318841	315542	315543	3155121	3155122	3155123	3155181	3155182	3155183
		5735	7933	17800	5742	7963	18,150	5827	8109	18,430
		17002	17002	17002	17,002	17,002	17,002	17,002	17,002	17,002

Note: E_g values based on ^oS = 10, 60%; D_3 = 0 in.; for multiple asphalt layers, use $E_{eq} = \left[\frac{D_{1a}(E_{1a})^{0.333} + D_{1b}(E_{1b})^{0.333}}{D_{1a} + D_{1b}}\right]^3$